THREE-DIMENSIONAL MODELING OF COMPLEX SALT WALL TERMINATIONS IN THE PARADOX BASIN: IMPLICATIONS FOR SALT STRUCTURE EVOLUTION, COMPARTMENTALIZING FAULT TRENDS AND PETROLEUM EXPLORATION

by

Katie Lehmann

A thesis submitted to the Faculty and Board of Trustees of the Colorado School of Mines in partial fulfillment of the requirements for the degree of Master of Science (Geology).

Golden, Colorado

Date _____

Signed: _____
Katie Lehmann

Signed: _____
Dr. Bruce D. Trudgill
Thesis Advisor

Golden, Colorado

Date _____

Signed: _____

Dr. Paul Santi

Professor and Interim Head of Department of

Geology and Geological Engineering

ABSTRACT

The Paradox Basin, located in southeastern Utah and southwestern Colorado, is a stunning geologic area for salt tectonics research. Characterized by the halite-rich Pennsylvanian Paradox Formation, this region provides pristine examples of the many structural and stratigraphic relationships associated with evolving salt structures. Formed during the Ancestral Rocky Mountain orogeny (ARM), the basin displays the complex development of the Colorado Plateau throughout the past ~320-300 million years. Unlike other ARM basins, the Paradox Basin was substantially influenced by the dynamic evolution of the Paradox Formation.

The northwest-southeast-striking salt structures in the Paradox Basin exhibit unusual morphologies, which has been attributed to compartmentalization of the basin by northeast-southwest-trending Precambrian basement structures. This has resulted in the abrupt or abnormal terminations of these salt structures observed in the basin today. Previously, minimal research was conducted on these salt wall terminations, perhaps due to their complex, three-dimensional geometries. However, study of these salt wall terminations is essential to understanding the evolution of the salt walls and the adjacent stratigraphy. Three-dimensional modeling of the Castle Valley and Gypsum Valley salt wall terminations reveals: (1) pre-existing Precambrian basement structures directly influenced the flow of the Paradox salt, generating the unusual salt wall terminations in the Paradox Basin; (2) asymmetry across the salt wall flanks, resulting in different amounts of accommodation and stratigraphic thicknesses; (3) the important relationship between eolian deposition of the White Rim Sandstone and the timing of the rise of the Castle Valley salt wall; (4) the amount of faulting along salt wall terminations and the resulting compartmentalization; (5) the development of multiple halokinetic sequences in response to passive diapirism of the Gypsum Valley salt wall; (6) growth faulting at Klondike Ridge associated with failure of the stratigraphy to imitate the salt wall termination; (7) the potential to better predict White Rim Sandstone petroleum reservoirs throughout the basin; (8) the possibility of new petroleum plays along the southern flank of the Gypsum Valley salt wall termination.

The results of this study indicate that modeling of salt wall terminations is essential to

understanding the complexity associated with salt structures. Furthermore, these models provide insight into other systems and may help with improved petroleum exploration and production. In areas such as the Gulf of Mexico, diapiric Jurassic Louann Salt produces irregularly shaped salt structures. The study of the salt wall terminations would be more applicable in these instances than the study of the central, linear parts of the salt walls. Therefore, this study illustrates the significance of three-dimensional models in developing a better understanding of the Paradox Basin and other salt systems.

TABLE OF CONTENTS

LIST OF FIGURES

LIST OF TABLES

ACKNOWLEDGEMENTS

The success and completion of this project would not have been possible without the endless support and encouragement from my colleagues, peers, friends, and family. First, I would like to thank my advisor Dr. Bruce Trudgill for granting me the opportunity and the means to research this exciting topic in the breathtaking environments found in the Paradox Basin. His assistance and expertise in the field as well as his unfailing patience and guidance throughout the completion of my project were pivotal to my success, and I cannot thank him enough for all of his help throughout the duration of this research project. I am also indebted to my colleagues Carter Timbel, Lily Horne, and Travis Wokasch, who generously acted as field assistants and always added fresh and insightful perspective pertaining to my research. I would also like to thank Dr. Mary Carr and Dr. Rick Sarg, who rounded out an incredible thesis committee, challenging me to think creatively and providing the encouragement I needed to complete this project.

Additionally, I would like to thank the Colorado School of Mines Department of Geology and Geological Engineering for accepting me into this rigorous and rewarding graduate program. I was fortunate enough to be granted research funds by my advisor, allowing me to complete my data collection and fully address my research goals.

Finally, I would like to recognize my family and friends for their constant support, I truly would not be where I am today without their love and reassurance. Their confidence in my abilities both as a student and a scientist were essential to my success at the Colorado School of Mines, and for that I am incredibly grateful.

CHAPTER 1

INTRODUCTION

The Paradox Basin represents a geologically unique and economically significant petroleum system in the western United States. Located in the Four Corners Region (Figure 1.1), the Paradox Basin covers an area approximately 265 km x 190 km in size (~50,000 km^2). This basin is characterized predominantly by the presence and dynamic nature of the immense salt structures, some of which are cored by over four kilometers of primarily halite (NaCl). Decades of research have revealed a great deal about the behavior of the Paradox salt throughout the tectonic history of this basin, which in turn provides valuable insight into similar basins around the globe (e.g., the Gulf of Mexico). Within the Paradox Basin, evacuation and diapirism of the Paradox Formation salt has substantially influenced sedimentation and the resulting stratigraphy (Kluth & DuChene, 2009; Trudgill, 2011). This process has profound implications for the presence, location, and geometry of petroleum and potash deposits. Although a significant amount of research has been conducted in the north-western portion of structural foredeep (located in the Paradox Basin), the database for the southeastern part of the foredeep in Colorado is much less extensive in comparison.

While the stratigraphic and structural framework has been studied in detail along the flanks of many of the salt structures in the Paradox Basin (Cater, 1970; Trudgill & Paz, 2009; Venus et al., 2013; Deatrick et al., 2014), the nature of the structurally complex terminations of these structures has remained elusive. From both a scientific and economic standpoint, the resolution of these terminations will reveal the extent of structural deformation and the potential for renewed petroleum exploration (Amador et al., 2009; DuChene et al., 2009). Therefore, the goal of this study is to combine existing field, map, and subsurface data with new field data to generate integrated models for the Castle Valley and Gypsum Valley salt wall terminations. These models will help resolve some of the structural complexity and allow for more accurate interpretation of potential petroleum systems in similar basins.

In order to address the goal characterizing salt wall terminations, several objectives were established: (1) collect key field measurements (i.e., strike/dip measurements of bedding, faults, folds, lineations, and slickenlines) within the complex structural zones located at the terminations of the Castle Valley and Gypsum Valley salt structures; (2) generate detailed field maps for these fields areas; 3) generate and annotate photomosaics of key outcrops; (4) aid in the construction of a comprehensive digital database and incorporate the collected field data with existing field, well, and seismic data (where available); (5) create and/or revise 2D and 3D structural models for this region; (6) provide insight into similar structural trends in the basin and suggest possible implications of these results for other salt-dominated systems; (7) utilize the results of this project to provide interpretations of possible petroleum systems along the terminations of these salt structures.

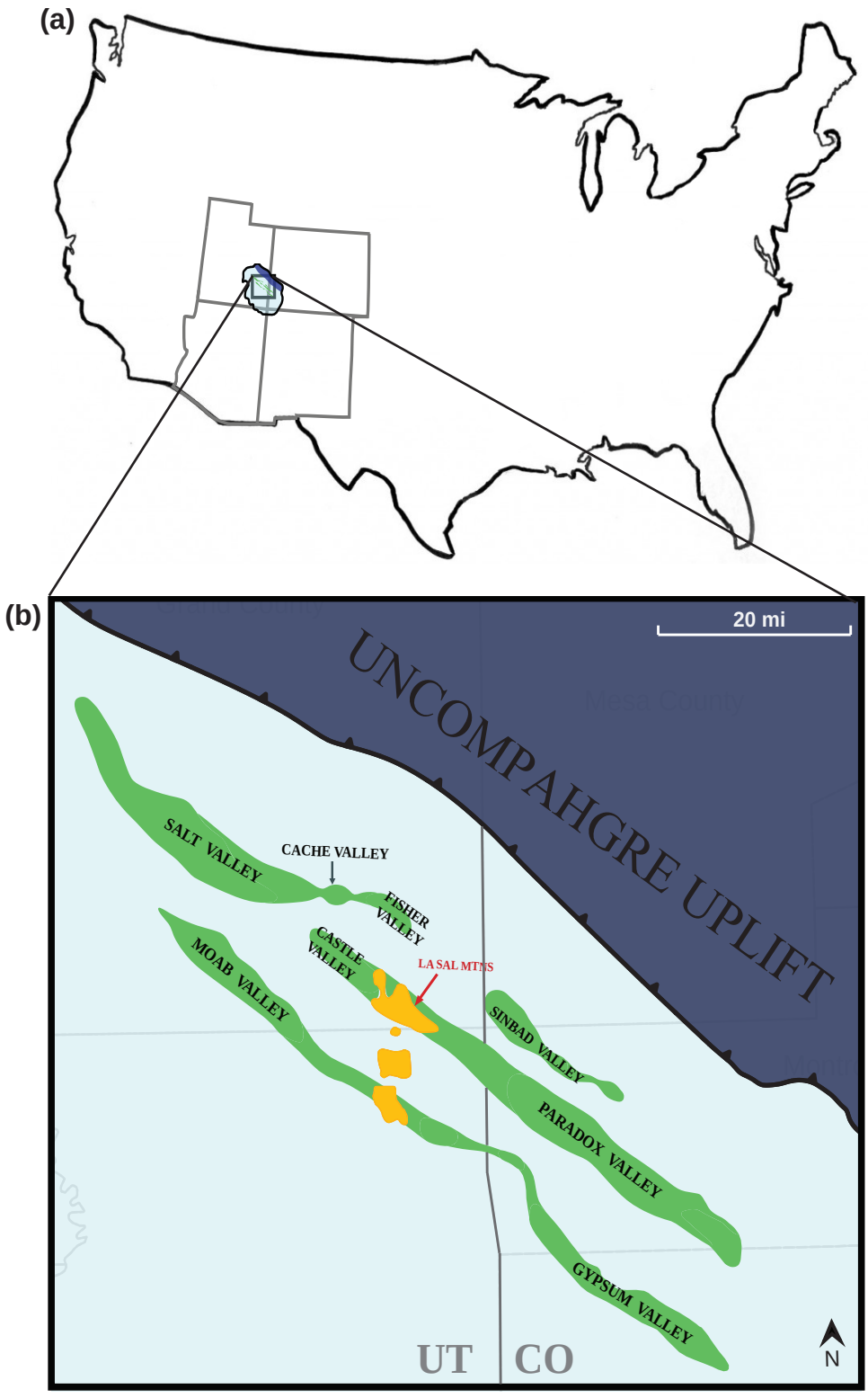

Figure 1.1 Location maps for the Paradox Basin. (a) Outline of the United States, with the Four Corners region and Paradox Basin highlighted. (b) Focused view of the Salt Anticline Region of the Paradox Basin.

CHAPTER 2

GEOLOGICAL BACKGROUND AND PREVIOUS WORK

2.1 The Paradox Basin

The Paradox Basin, located in the center of the Colorado Plateau, is a large (265 km x 190 km) asymmetric basin that developed during the Ancestral Rocky Mountain (ARM) orogeny (Figure 2.1). The adjacent Uncompahgre Uplift is a NW-SE-trending arch, 50-km wide and bounded by 200-300 km long fault zones to the southwest and northeast. The Uncompahgre fault bounding the uplift to the southwest dips moderately to the northeast and exhibits top-to-the-southwest relative displacement, generating approximately 10 km of shortening (Barbeau, 2003). Much like the other ARM associated basins found across the western United States, the Paradox Basin contains thick successions of coarse-grained synorogenic sediments, shed from the Uncompahgre Uplift during the Late Pennsylvanian – Early Permian (Trudgill & Paz, 2009).

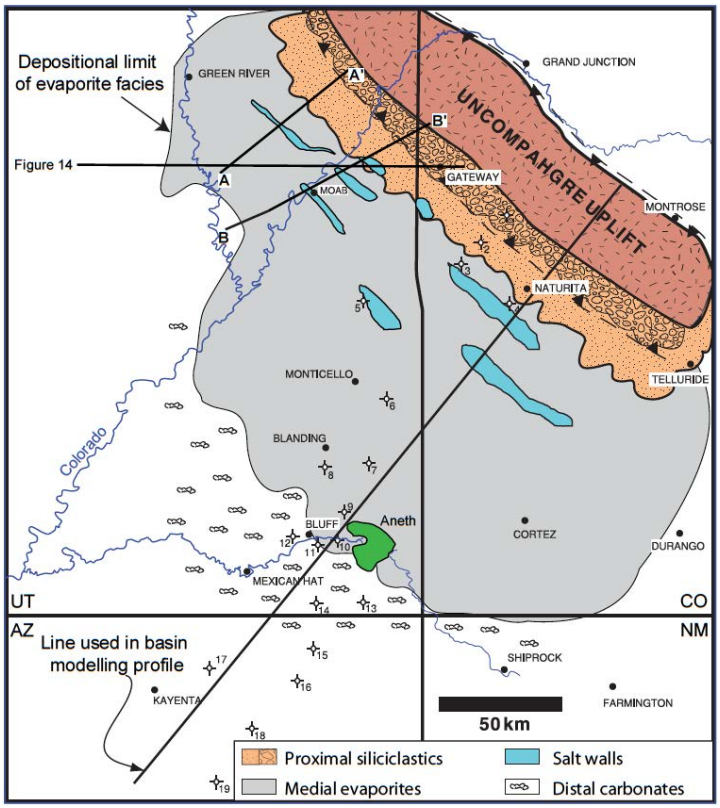

Figure 2.1 Regional map of the Paradox Basin and the Uncompahgre Uplift, highlighting prominent intrabasinal salt structures and overall extent of the basin, as defined by the limit of evaporite facies (Trudgill & Paz, 2009; after Barbeau, 2003).

Although its relation to the ARM orogeny is generally undisputed, the geometry and orientation of the Paradox Basin has elicited numerous hypotheses concerning the tectonic setting responsible for the structural evolution of the basin. Stone (1977) attributed the "anomalous orientation" of the Uncompahgre Uplift to ancestral oblique slip that resulted from left-lateral regional movement along several ancient Precambrian fault zones. However, he recognized that the dominant vertical component of the Uncompahgre fault would render the overall region as a reverse fault zone. Kluth and Coney (1981) ascribed the ARM uplifts to an escape tectonic regime during the collision of the South American-African plates with the North American plate, comparing this event to the present-day collision of India and Asia. Stevenson and Baars (1986) concluded that the uplift of the Uncompahgre range was the result of regional strike-slip tectonics, thereby classifying the Paradox Basin as a pull-apart basin. According to their model, subsidence in the basin was generated via strike-slip offset along a releasing bend adjacent to the southwestern margin of the Uncompahgre front. Although the tectonic regime in this area during the ARM orogeny is poorly constrained, the flexural foreland basin model proposed by Barbeau (2003) appears to best satisfy the numerous trends and observations made regarding the Uncompahgre Uplift and Paradox Basin (Figure 2.2). In this model, Barbeau argued that the model proposed by Kluth and Coney (1981) is unlikely, as the extensive strike-slip offset observed in central Asia (attributed to an escape tectonic setting) is not detected in vicinity of the Paradox Basin and Uncompahgre front. Likewise, Barbeau contended that the Paradox Basin is both larger and wider than any modern or ancient pull-apart basins documented to date, rendering the scenario put forth by Stevenson and Baars (1986) unlikely. Furthermore, Barbeau argued that movement along thrust-bounding faults was predominantly reverse dip-slip, lacking the significant strike-slip movement proposed by Stone (1977). This is further supported by observations made by Mack and Rasmussen (1984), who recognized a unique quartz monzonite in the Uncompahgre Uplift in outcrop as well as in erosional remnants found in the sedimentary basin fill (Cutler Group). Accordingly, the Barbeau (2003) flexural foreland basin model most successfully encompasses the basin/uplift geometries, structural framework and

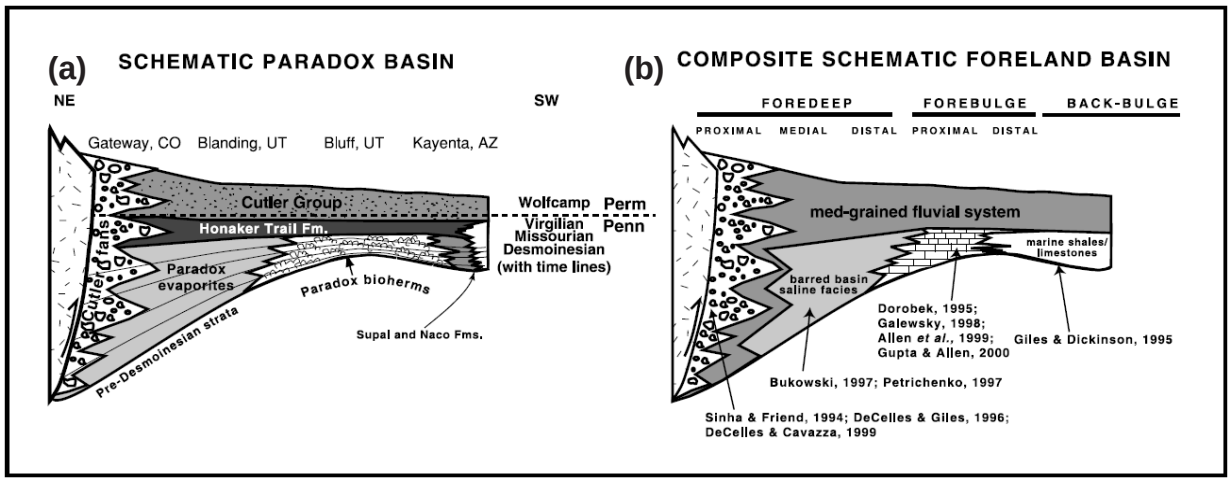

Figure 2.2 (a) Schematic facies model of the Paradox Basin, illustrating the location and architecture of key facies. (b) Schematic facies model of a composite restricted-marine isolated flexural basin. Note the similarities between the Paradox Basin architecture and that of a flexural foreland basin (Barbeau, 2003).

subsidence trends observed in the Paradox Basin - Uncompahgre Uplift tectonic setting.

The Middle to Late Pennsylvanian stratigraphy in the Paradox Basin illustrates the intricate interplay of eustatic sea level change, tectonic uplift, and the morphology of the basin at the time of deposition (Figure 2.3). The Hermosa Group contains the Molas/Pinkerton Trail Formations (Atokan), the Paradox Formation (Atokan – Desmoinesian), and the Honaker Trail Formation (Missourian – Virgilian). The Paradox Formation and time equivalent strata vary considerably across the basin and signal the beginning of subsidence along the northeast side of the basin (Fillmore, 2011). Composed of dolostone, black shale, anhydrite, halite, and other salts, the Paradox Formation was deposited during numerous cycles of repeated flooding and desiccation of the basin caused by glacio-eustatic fluctuations in sea level (Figure 2.3; Nuccio & Condon, 1996). In the deepest portion of the basin, most proximal to the Uncompahgre Uplift, the Paradox Formation is difficult to distinguish from the coarse clastic material and/or carbonate shelf of the undivided Cutler Formation, shed from the rising Uncompahgre Mountains. In the central part of the basin, the Paradox Formation consists of evaporite-dominated deposits reaching thicknesses of 2,000-2,500 meters and upwards of 4,300 meters in some of the prominent salt diapirs (Trudgill, 2011). This significant evaporite succession, predominantly composed of halite, may contain the largest aggregate thickness of rock salt in any single formation in North America

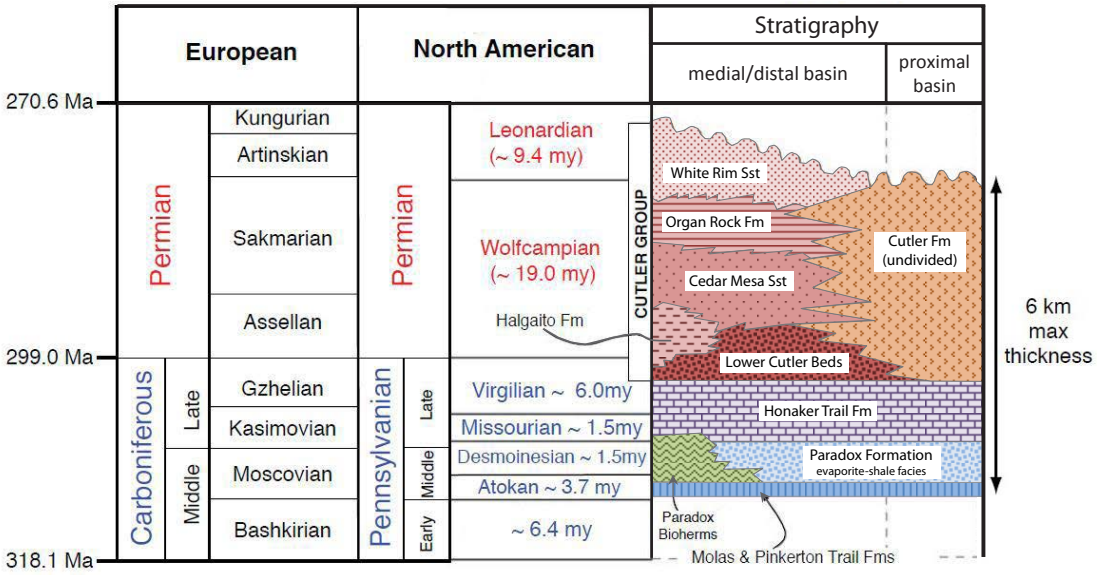

Figure 2.3 Stratigraphic column of Pennsylvanian and Permian units in the Paradox Basin (modified from Trudgill & Paz, 2009).

(Hite, 1960). To the southwest, evaporite sequences transition gradually into shelf carbonates and biohermal carbonate mounds, the latter have proven to be prolific petroleum reservoirs along the basin margin (Figure 2.4; Sarg et al., 1999).

Most notably, organic-rich units defined as black laminated mudstones (BLM's) by Goldhammer et al. (1991), are recognizable, chronostratigraphic surfaces in the Paradox Basin. These surfaces are interpreted to represent highstand conditions, during which the basin and shelf were flooded and sedimentation of organic-rich material was favored. Sea level fall and subsequent sea level rise resulted in the deposition of limestone and carbonate mudstone on the shelf, capped

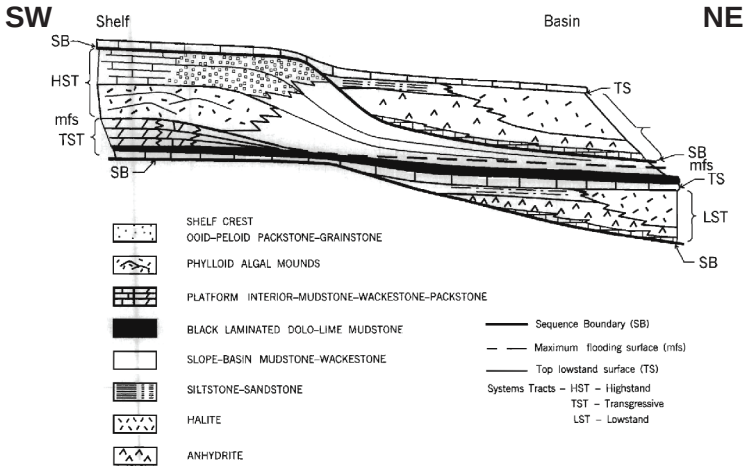

Figure 2.4 Depositional sequence model for the Desmoinesian period in the Paradox Basin (Sarg et al., 1999).

by algal mounds. This was followed by the deposition of dolomite and precipitation of anhydrite, gypsum, halite and locally potash within the basin as the sea level fell and the basin became more restricted and hypersaline (Hite & Gere, 1958).

The Honaker Trail Formation conformably overlies the Paradox Formation and displays the same cyclic stratigraphic pattern observed throughout the Paradox. Unlike the underlying Paradox Formation, the Honaker Trail contains no evaporite beds; instead, the Honaker Trail Formation is composed of alternating marine carbonate during highstands and shale with fluvial and eolian sandstone during lowstands (Sarg et al., 1999). This repeating, cyclic sedimentation during the Middle to Late Pennsylvanian has allowed for local and regional stratigraphic correlation in the Paradox Basin. Figure 2.5 illustrates idealized evaporite and carbonate cycles as well

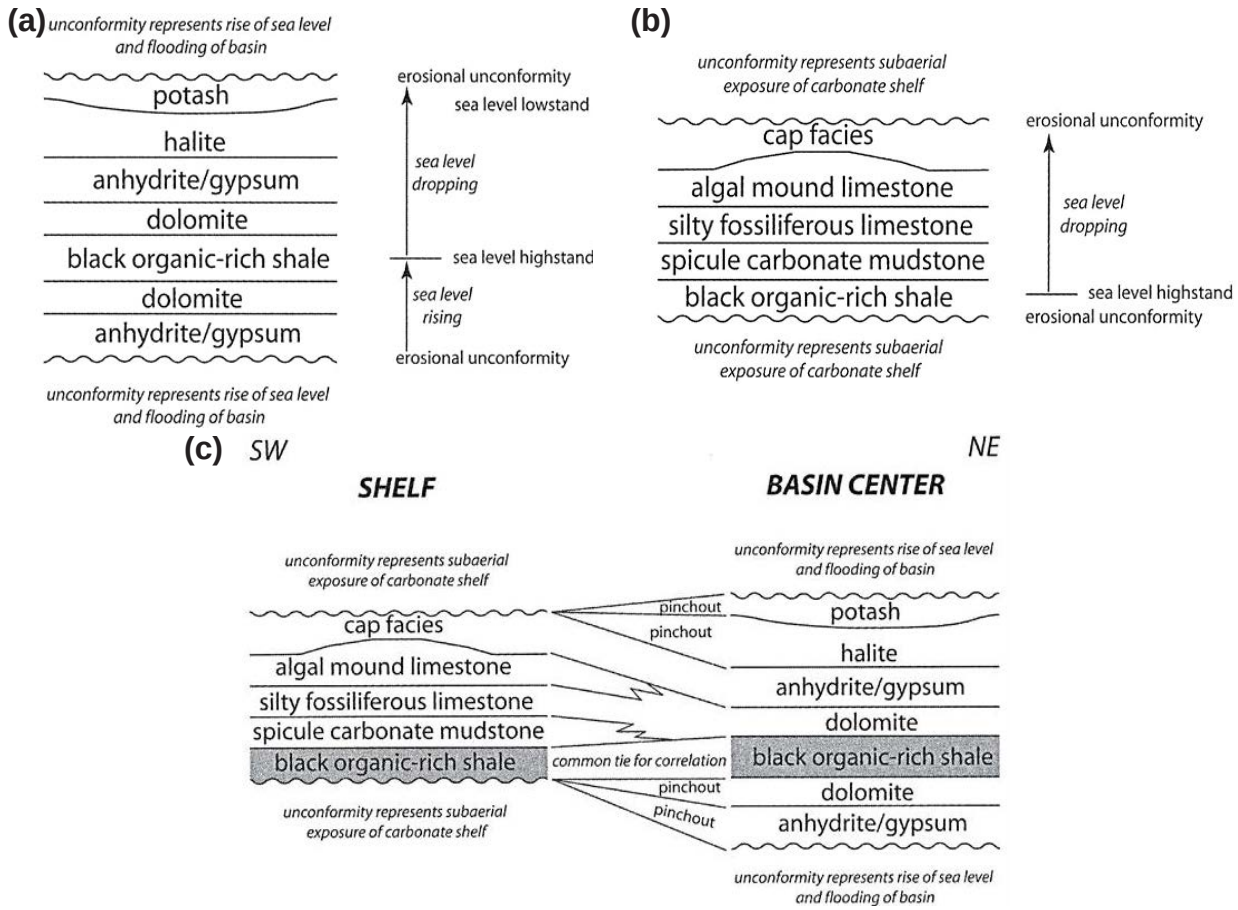

Figure 2.5 (a) Idealized evaporite cycles from the center of the Paradox Basin, illustrating the typical vertical sequence of expected lithologies and unconformities; (b) Idealized carbonate cycle from the shallow shelf setting on the southwest margin of the Paradox Basin, illustrating the carbonate facies and unconformities present; (c) Correlation of evaporite and carbonate cycles observed in the Paradox Basin. Note that these depositional events occur via different processes and at different times (Fillmore, 2011).

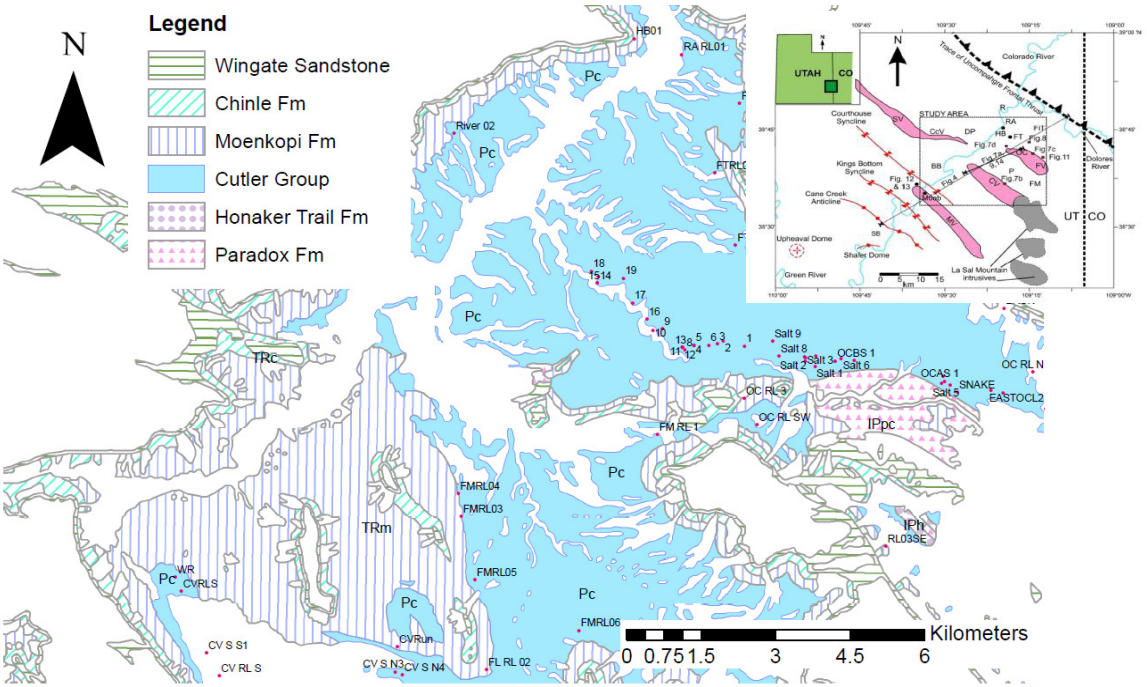

Figure 2.6 Map illustrating the location and extent of key stratigraphic units within this study area (see index map for location), Pennsylvanian through Lower Jurassic in age. Note the significant distribution of the Permian Cutler Group, highlighted in light blue (Venus et al., 2013).

as the continuity of certain facies throughout the basin.

The overlying Cutler Group (Virgilian?-Wolfcampian) is a heterogeneous unit deposited during the most significant phase of uplift of the Uncompahgre range. The Cutler Group displays the greatest thickness (0-2450 m) and facies variations of all post-salt strata, comprised of sediments deposited via fluvial, eolian, and marine processes (Figure 2.3). Proximal to the Uncompahgre front, deposition likely occurred as a series of alluvial fans and debris flows. Further to the west, marine-influenced lower Cutler beds are overlain by eolian and fluvial deposits (Cedar Mesa Sandstone, Organ Rock Formation, and White Rim Sandstone). Figure 2.6 shows the considerable extent of the Cutler Group in the northern part of the basin. However, the marine, eolian, and fluvial facies found to the west are likely not correlative with the arkosic conglomerates and sandstones located proximal to the thrust front (Venus et al., 2013; Trudgill, 2011). This is likely due to the “heel-toe” method of mini-basin fill (Kluth & DuChene, 2009), which would indicate that sediments become progressively younger with increasing distance from the Uncompahgre Front.

Locally, the White Rim Sandstone, which constitutes the uppermost member of the Cutler Group, is a prominent and important unit, particularly when considering the evolution of the salt structures during the Permian. The White Rim Sandstone is characterized as a coastal dune environment, within which large-scale dune complexes were periodically flooded by marine waters. In general, this unit is confined to a region west of the Colorado River reaching a maximum thickness of approximately 244 meters in the subsurface and 60-122 meters in outcrop (Kamola & Chan, 1988). While the White Rim Sandstone is absent throughout much of the Paradox Basin, it is anomalously thick along the northwestern termination of the Castle Valley salt structure, tapering out to the southeast over a relatively short distance at the surface. Furthermore, it lies just west and southwest of the two salt welds described by Lawton and Buck (2006). The northwesterly strike of the Castle Valley salt wall appears to change abruptly and welds out to the north. This change in strike appears to coincide with the location of the thick White Rim Sandstone as well as the location of the Colorado River.

Deposition of the thick, clastic Cutler Group wedge throughout the Permian led to differential loading of the Paradox Formation, subsequently resulting in the predominantly southwestward withdrawal and migration of the salt. Northwest-southeast-trending faults present in the underlying Cambrian – Mississippian strata likely acted as buttresses to salt flow and allowed for the significant relief achieved by the salt walls and diapirs (Baars, 1966; Baars & Stevenson, 1981; Doelling, 2001). The orientation and location of these major Mississippian-level faults appears therefore to have influenced the evolution of the salt structures found in the northern Paradox Basin (Trudgill, 2011; Figure 2.7). Prominent salt movement continued in the region through Triassic time for many of the salt walls in Utah but continued until the Middle Jurassic for most of the structures in Colorado. Following deposition of the Triassic Chinle Formation and Jurassic Salt Wash Member (in Utah and Colorado, respectively), the rise of salt structures attenuated sufficiently for overlying strata to cover the crests of the salt structures (Trudgill, 2011). Tectonic quiescence ensued until the Paleogene, during which Laramide folding and faulting generated new walls and intervening synclines whose axes were concurrent with the Permian

salt-cored structures. Uplift of the Colorado Plateau in the Neogene generated extension in the Paradox Basin, resulting in the collapse of the anticlinal crests and dissolution of the underlying salt (Randles, 2012).

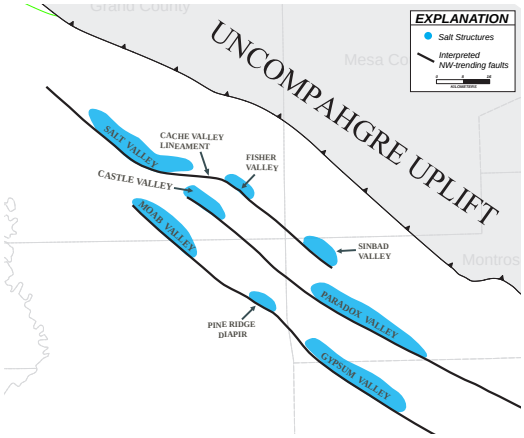

Figure 2.7 Regional map showing the locations of major salt structures (features in black), adjacent to interpreted northwest-trending basement faults (modified from Baars, 1966).

2.2 The Salt Anticline/Salt Wall Region

The Salt Anticline Region of the Paradox Basin comprises a sequence of northwest-trending salt walls coincident with the deepest part of the basin (Figure 2.7; Cater, 1970). Classifying this area as the Salt Wall Region may therefore resolve any confusion regarding the nature of the salt structures. These salt walls roughly parallel the Uncompahgre thrust front, with individual structures ranging from circular plugs to linear salt walls 60 km long (Jones, 1959). The Salt Valley, Cache Valley, Fisher Valley, Castle Valley, and Moab Valley salt walls are located in Utah (Figure 2.8); their counterparts, located in CO, are the Sinbad Valley, Paradox Valley, Gypsum Valley, and Lisbon Valley salt walls. The intrusion of the igneous La Sal Mountains laccoliths (Figure 1.1b) during the Oligocene (~29-25 Ma) geographically separated the Utah and Colorado salt walls, and Hunt (1958) further proposes that these intrusive bodies segmented the long salt features that once connected these structures along strike. Most of the salt walls are relatively asymmetrical, with the northeastern flanks having steeper dips and their associated synclinal troughs displaced to the southwest of their geographical central axis (Cater, 1970).

The salt walls of the Salt Wall Region in the Paradox Basin formed as a result of the differential loading of the Paradox salt through the process of “downbuilding”, during which salt

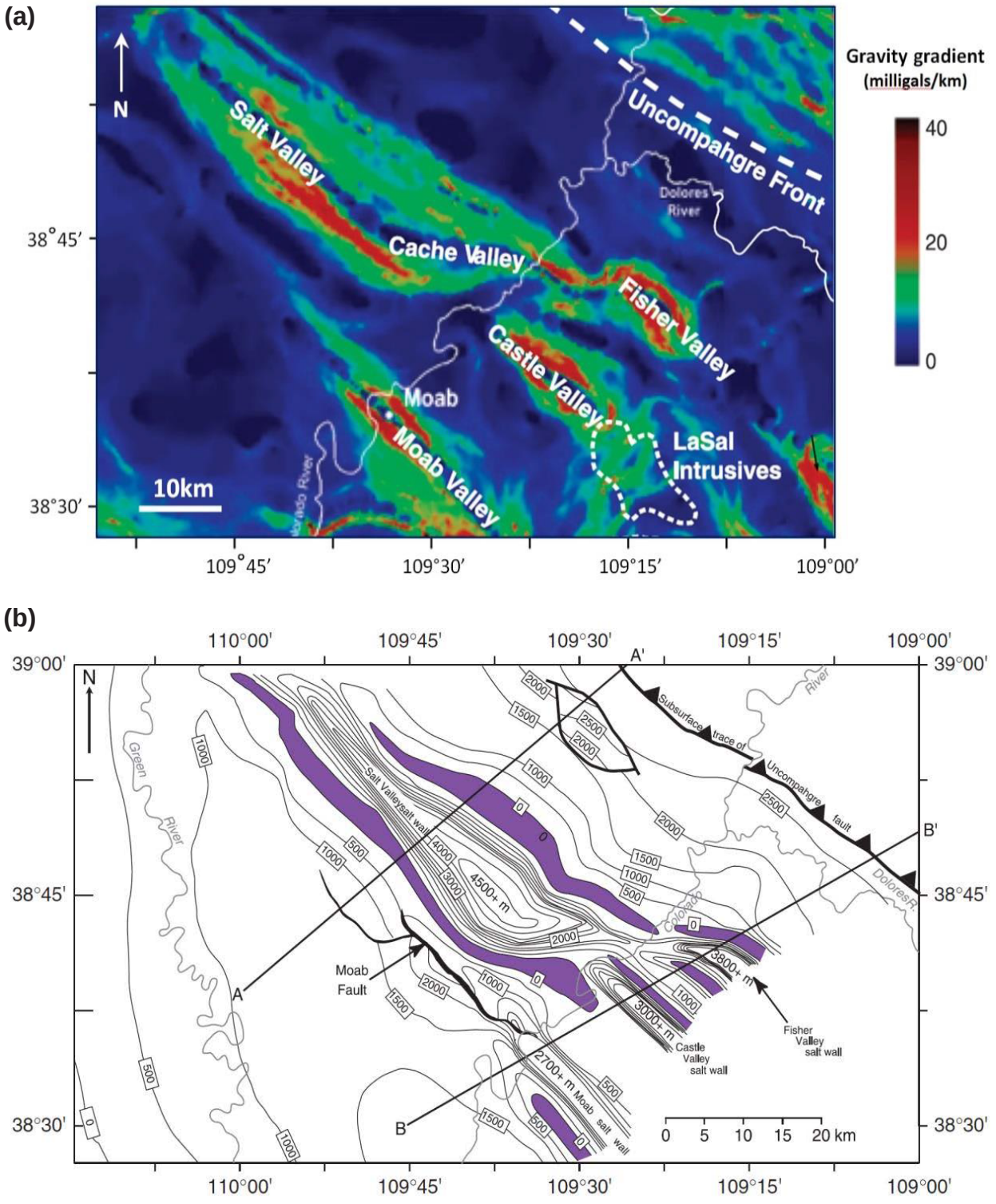

Figure 2.8 (a) Gravity gradient map of the northwestern portion of the salt wall region from Trudgill (2011), where warmer colors indicate steeper salt flanks; (b) Present-day isopach (contour interval of 500m) of the Paradox Formation, with maximum salt thickness highlighted for the Salt Valley, Castle Valley, Fisher Valley, and Moab salt walls (Trudgill, 2011).

was likely continually present at or close to the surface (Kluth & DuChene, 2009). Downbuilding often leads to “heel-toe” geometry (Figure 2.9) in the sedimentary infill of the mini-basin; the mechanism by which the salt walls developed systematically in a southwesterly direction. This style of evolution, also shown by structural restorations (Paz, 2006; Trudgill & Paz, 2009), indicates the oldest salt walls are those proximal to the Uncompahgre thrust front and the salt structures furthest from the uplift are the youngest. Diapirism of the salt led to the creation of accommodation in the form of mini-basins, which, filled by sediment, continued the process of downbuilding. The development of this accommodation ceased once the salt had been evacuated and post-salt strata had come to rest unconformably on top of pre-salt sections. Continued sedimentation, predominantly sourced from the rising Uncompahgre Uplift to the northeast, began to load the salt further to the southwest, generating a new salt wall and accompanying mini-basin

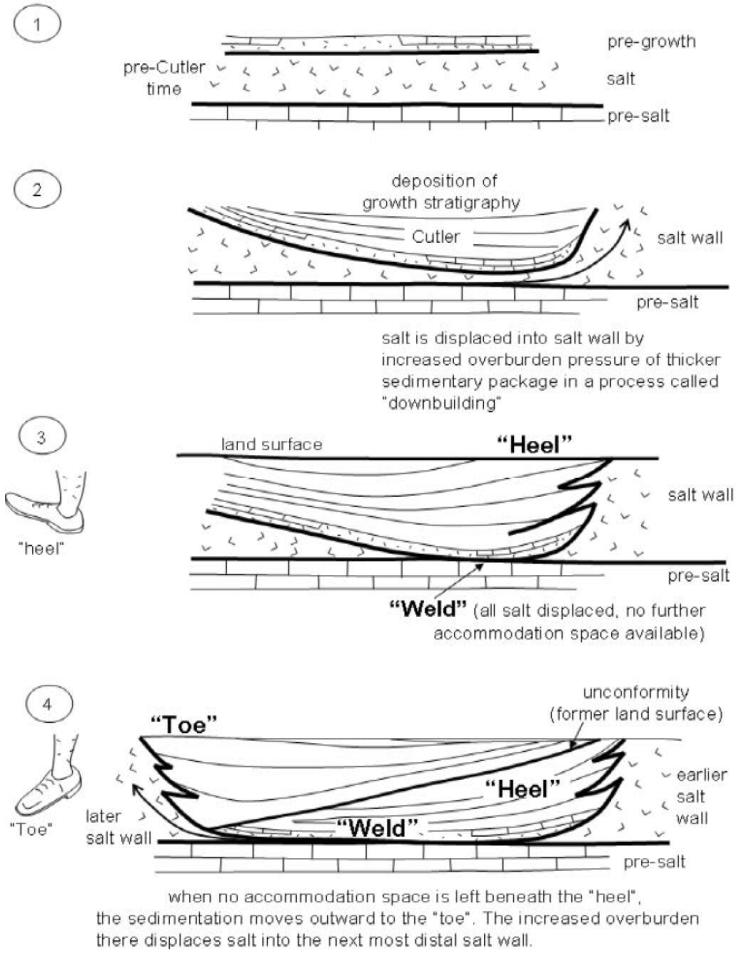

Figure 2.9 Cartoon illustration of the development of “heel-toe” structures, generated during the process of downbuilding and successive filling of accommodation (Kluth & DuChene, 2009).

(Kluth & DuChene, 2009). This process continued throughout the Permian, Triassic, and early Jurassic, ultimately forming the en echelon salt walls seen today. The timing and three-dimensional evolution of structures as well as the geometry and thickness of the associated mini-basin sedimentary strata have important implications for the location and character of petroleum system elements, most notably potential reservoir intervals and organic-rich source rocks. Furthermore, the development of these salt walls undoubtedly affected the distribution of the potassium-bearing sylvite salts, from which the economically significant potash mineral is produced.

2.3 Hypotheses regarding preexisting regional trends

Constraining the paleogeography and structural history of the Paradox Basin has presented a number of challenges to geoscientists, most notably regarding the location and lateral extent of the halite salt and the peculiar structural trends observed within the Salt Wall Region. Earlier publications suggested the Paradox Basin was the down faulted block in a pull-apart basin resulting from uplift of the Uncompahgre Front during the ARM Orogeny (Stevenson & Baars, 1988; Cater, 1970). More recently, the hypothesis proposing the Uncompahgre Uplift is the hangingwall block in a regional thrust system has gained widespread support (Barbeau, 2003; Figure 2.10). Kluth and DuChene (2009) advocated that the Paradox salts and the evaporites

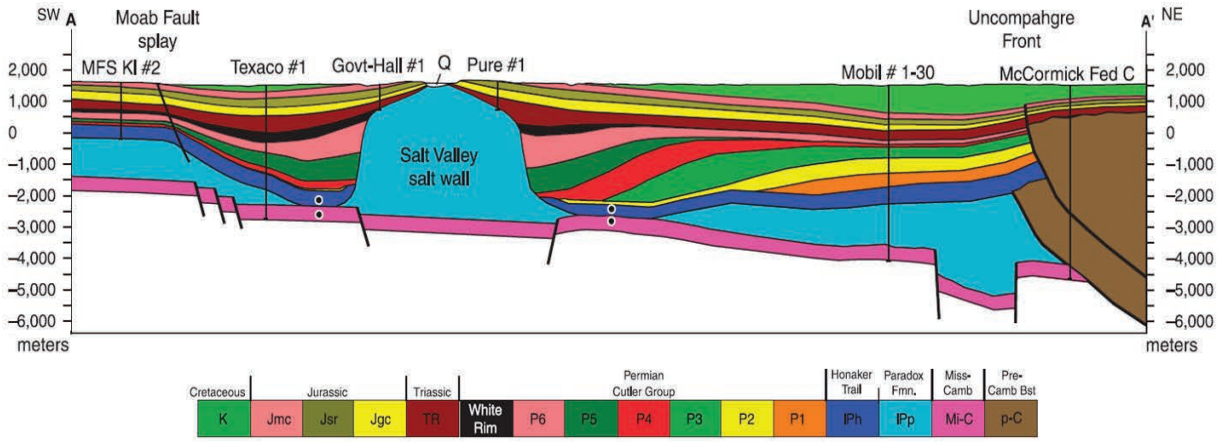

Figure 2.10 Structural cross-section A-A' based on the original sections produced by Doelling (2001), significantly modified by Trudgill (2011) to include new well, gravity and seismic data (no vertical exaggeration). Note "McCormick Fed C" well penetrating through Precambrian basement rocks in the Uncompahgre highlands and the underlying Mississippian-Cambrian pre-salt strata. (Trudgill, 2011).

located in the Eagle Valley to the northeast were originally deposited in a continuous basin, prior to the rise of the Uncompahgre and geographical separation of these basins. It has been generally accepted that the Uncompahgre Uplift resulted from thick-skinned tectonism (Kluth & DuChene, 2009; Barbeau, 2003) which superimposed Precambrian crystalline basement on the proximal Paradox Basin sedimentary fill (Trudgill, 2011). This hypothesis has been supported by well data (e.g., “McCormick Fed C” well) that exhibits crystalline basement above pre-salt formations, Mississippian to Cambrian in age (Figure 2.10).

The structural trends observed in the Salt Wall Region have been scrutinized for decades, generating numerous hypotheses on the origin and evolution of the vast salt structures observed in the Paradox Basin (e.g., Cater, 1970; Stone, 1977; Kluth & Coney 1981; Stevenson & Baars, 1986; Barbeau, 2003; Kluth & DuChene, 2009). Generally, these have focused on the overall structural setting of the Paradox Basin as well as northwest-southeast-striking pre-salt structures that may have influenced the diapirism and subsequent formation of the Paradox salt walls.

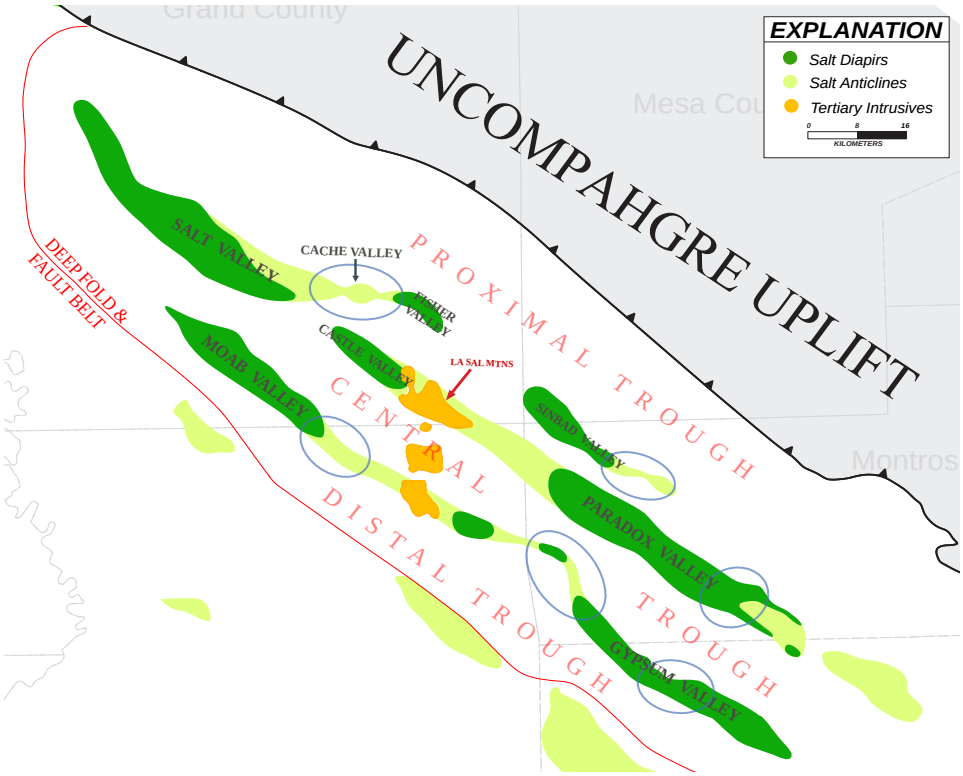

Figure 2.11 Map view of the Paradox Deep Fold and Fault Belt (DFFB), with salt diapirs and walls highlighted to show lateral variability and extent. Note areas of unusual terminations or deviations in the predominant strike of the region, highlighted within the blue ellipses (modified from Rasmussen & Rasmussen, 2009).

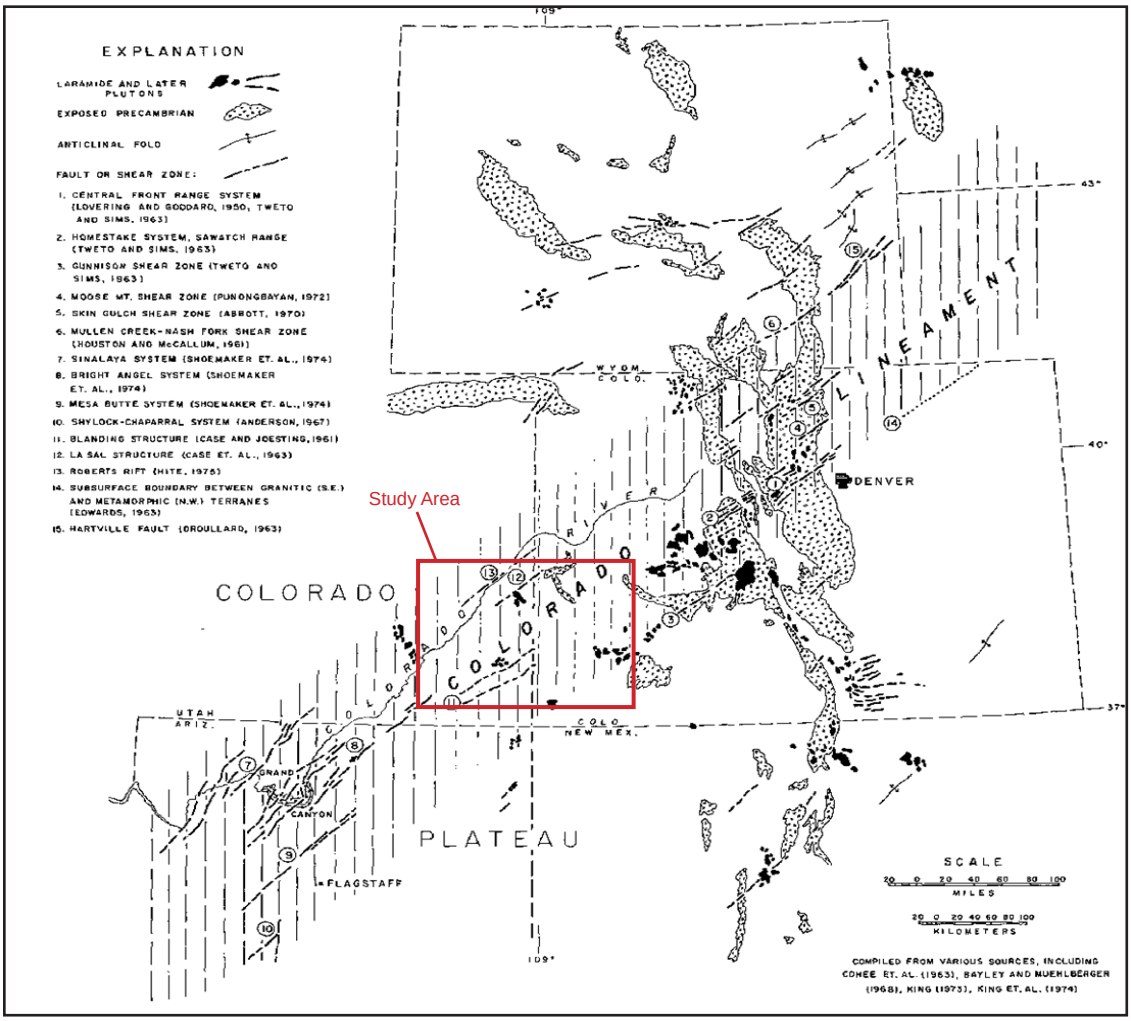

Figure 2.12 Tectonic map of the Rocky Mountain region and Colorado Lineament, with the study area highlighted (Warner, 1978).

However, a detailed study of some of these peculiar three-dimensional trends has not been entirely accomplished to date. In an idealized setting, one would expect these massive linear salt walls to laterally taper out gradually, as salt supply toward the basin margins thins and/or the effect of tectonism wanes. Yet, the salt walls observed in the Salt Wall Region deviate considerably from this model, displaying in places abrupt terminations of salt structures (e.g., Castle Valley, Figure 2.11) or significant changes in strike over relatively small distances (e.g., Salt Valley-Fisher Valley, Paradox Valley, Gypsum Valley). Figure 2.11 shows the lateral trends of the salt structures, illustrating the anomalous terminations, or apparent deflection of the anticlinal structures.

Several hypotheses have surfaced with respect to the unusual morphology of the salt

structures and are important to consider when generating more accurate structural restorations. Recognition of NE-SW-trending Precambrian shear zones, wrench faults, and lineaments have been extensively documented, most of which are attributed to the regional Colorado Lineament, coincident with the Colorado Mineral Belt (Figure 2.12; Warner, 1978). Warner (1978) suggested the La Sal uplift and the Blanding basin confirm the presence of northeast-trending basement structures. He interprets a series of northeasterly linear magnetic trends located west and north- west of the La Sal Mountains as evidence for an underlying structural discontinuity in the basement (Figure 2.13). He speculates a fault zone most likely underlies this area, and within this zone some of these Precambrian faults breach the overlying Mesozoic cover. Movement along these faults likely occurred during Laramide time, similar to the Bright Angel and Mesa Butte fault systems in Arizona (Figure 2.12; Warner, 1978). Further evidence may lie in the Roberts Rift region according to Hite (1975), which is located northwest of the town of Moab (Figure 2.13). Throughout the extent of the Roberts Rift (up to 34 km in length) this fracture zone appears to cut several Triassic to Jurassic age formations, including the Triassic Chinle Formation, the Jurassic Glen Canyon Group (Wingate Sandstone, Kayenta Formation, and Navajo Sandstone), and the Jurassic San Rafael Group (Dewey Bridge Formation and Entrada

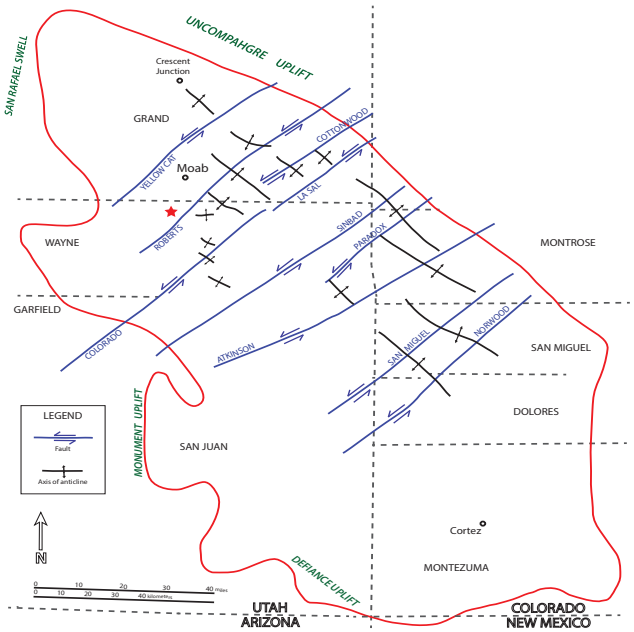

Figure 2.13 Northeast-trending features in the Paradox Basin that Warner (1978) and Hite (1975) suggest are related to a structural network in the basement (modified from Hite, 1975).

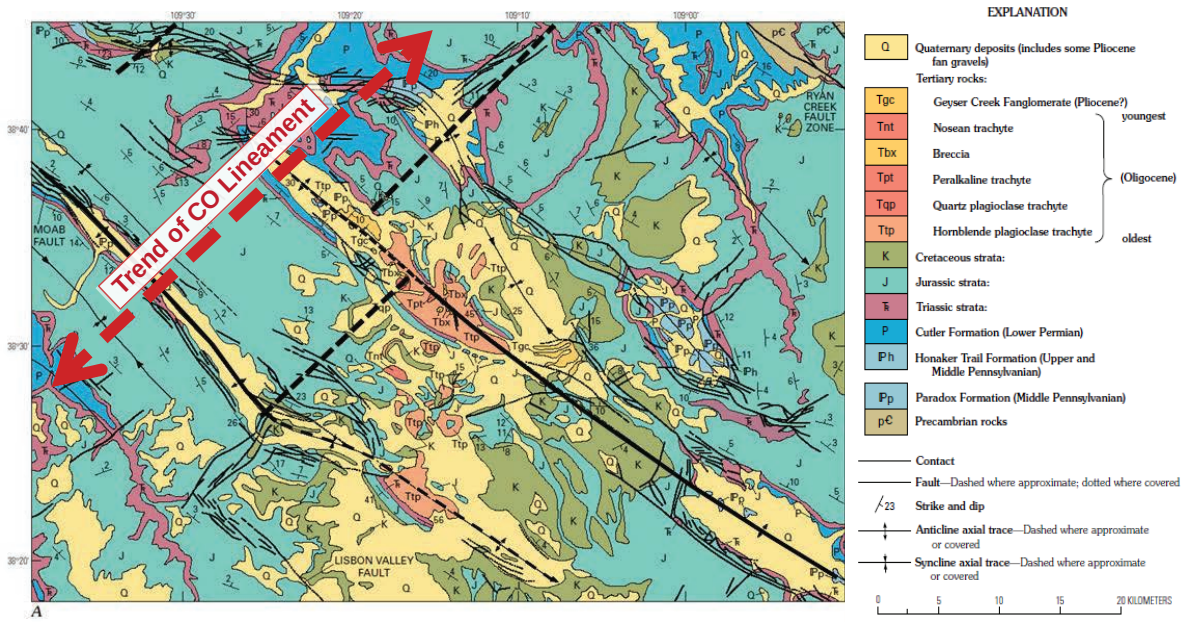

Figure 2.14 Geologic map of the La Sal Mountains and surrounding region. Red dashed double-arrow illustrates the approximate regional strike of the Colorado Lineament. Dashed black lines show interpreted network of subsurface faults, along which the La Sal Range intruded into a local zone of weakness (Ross, 1998).

Sandstone). Hite (1975) also recognized the unusual behavior of the southeastern end of the Salt Valley-Cache Valley structural trend (Figure 2.11), noting that the strike of the salt structure shifts abruptly from northwest to east-northeast. This observation is supported by a similar change in strike of a nearby joint system, in particular within the Jurassic Entrada Sandstone. Further evidence, located in the Bull Canyon area (approximate location indicated by red star in Figure 2.13), includes fractures filled with coarse breccia as well as local bleaching and and mineralization within fractures in the Wingate Sandstone (Hite, 1975). Kelley and Clinton (1960) suggested the attitude of the Salt Valley-Cache Valley salt wall trend illustrates drag along a reactivated Precambrian strike-slip shear zone extending from the San Rafael Swell. Accordingly, this lineament was termed the Cache Valley Lineament (Figure 2.11), and was hypothesized to extend to the magnetic highs that underlie Upheaval Dome northwest of the shear zone and Grays Pasture, located to the southeast of the fault (Kelley & Clinton, 1960). Joesting and Case (1962) recognized apparent left-lateral offset of basement rocks along the Uncompahgre Front oriented with the projected trace of the regional Precambrian shear zone. Ross (1998) suggested

that these northeast-striking fractures acted primarily as connecting structures for the more prominent northwest-striking faults, allowing for the compartmentalization of the Salt Wall Region (Figure 2.14). Additionally, this fault network forms a structural boundary between shallower pre-salt rocks to the south and the deeper pre-salt rocks to the north. Ross (1998) proposes that the location of the La Sal intrusive complex lies along a kink in this structural boundary, where ascending magmas exploited this local zone of weakness during the Paleogene (Figure 2.14). This study may have implications for other Tertiary lacco-lith centers in the Paradox Basin and the location of analogous fault junctions. Although the subsurface fault geometry for these northeast-trending structures is still uncertain, it is apparent that there may be convincing evidence at the surface to suggest that an additional structural regime, oriented roughly perpendicular to the dominant northwest-southeast trend, must be considered when constructing structural restoration models (Figure 2.15).

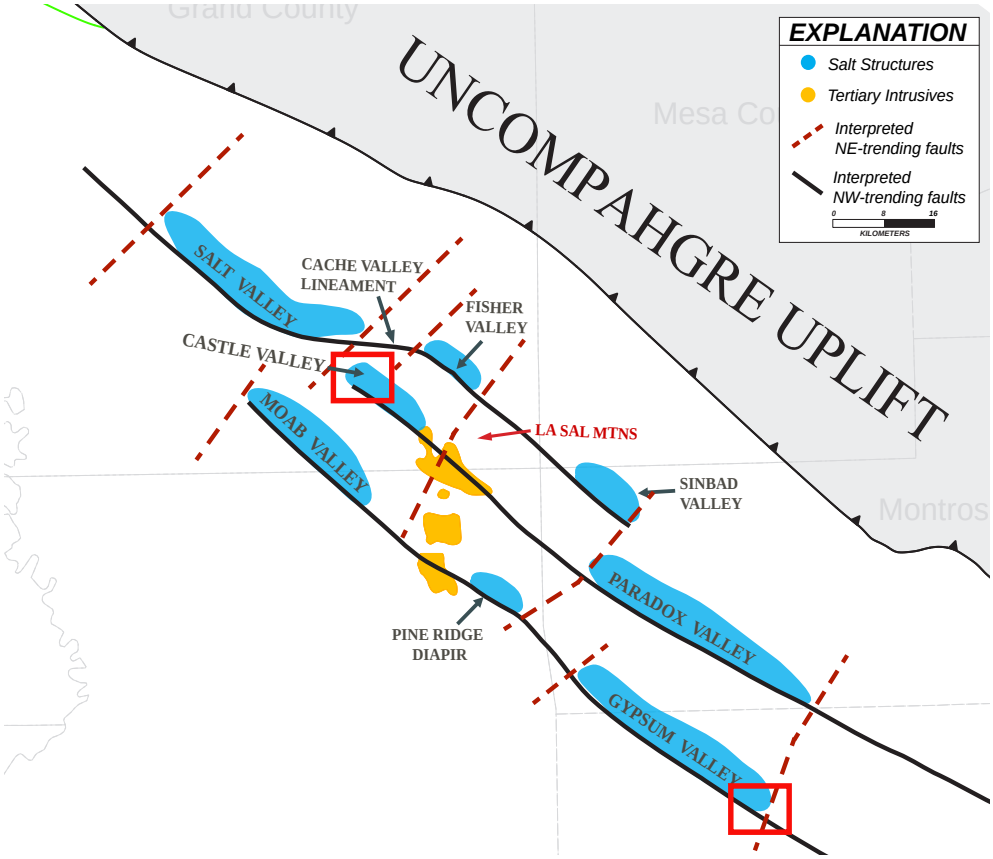

Figure 2.15 Comprehensive map illustrating the NW-trending and NE-trending CO-lineament basement structures compartmentalizing the basin, as well as the relationship between the location of the salt structures and laccoliths with these structures (modified from Rasmussen & Rasmussen, 2009). Red rectangles indicate study areas in the basin.

2.4 Petroleum and potash systems in the Paradox Basin

The Paradox Basin is one of many producing basins in which petroleum resources are directly associated with evaporites. Evaporites likely play a direct role in the creation and accumulation of petroleum, both in trapping and accelerating the generation of hydrocarbons (Peterson & Hite, 1969). Petroleum production occurs predominantly along the southwestern margin of the basin, primarily within the Aneth field (discovered in 1956; Figure 2.16). The prominent producing units in this portion of the basin are the Middle Pennsylvanian carbonates of the Ismay and Desert Creek intervals (Figure 2.17), with cumulative production of 450 MMBO and over 370 BCFG at Aneth Field (Stevenson & Wray, 2009). The most prolific reservoir facies on the Aneth Platform consists of biohermal mound deposits, resulting from the growth and colonization of phylloid algae during the Pennsylvanian. Primary interparticle and secondary dissolution porosity collectively create porosity values between approximately 5-18% (Weber et al., 1995). Despite the presence of these algal mound reservoirs throughout the south-western portion of the Paradox Basin, lateral variability with regards to the location of these reservoirs is high, especially within the Ismay interval, making exploration a more challenging endeavor. Production is

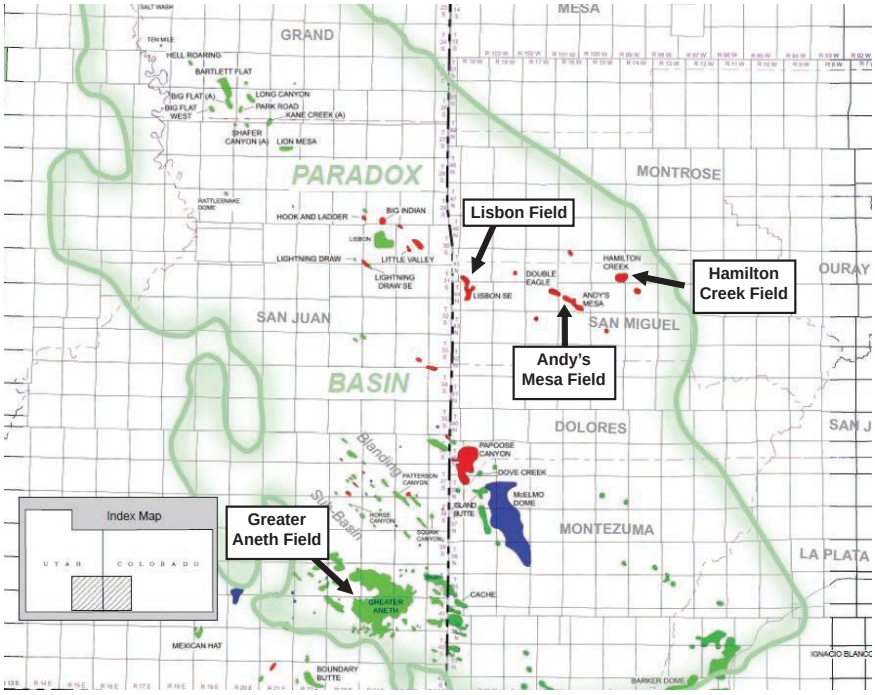

Figure 2.16 Field map of the Paradox Basin, highlighting the location and size of discovered petroleum fields (Stevenson & Wray, 2009).

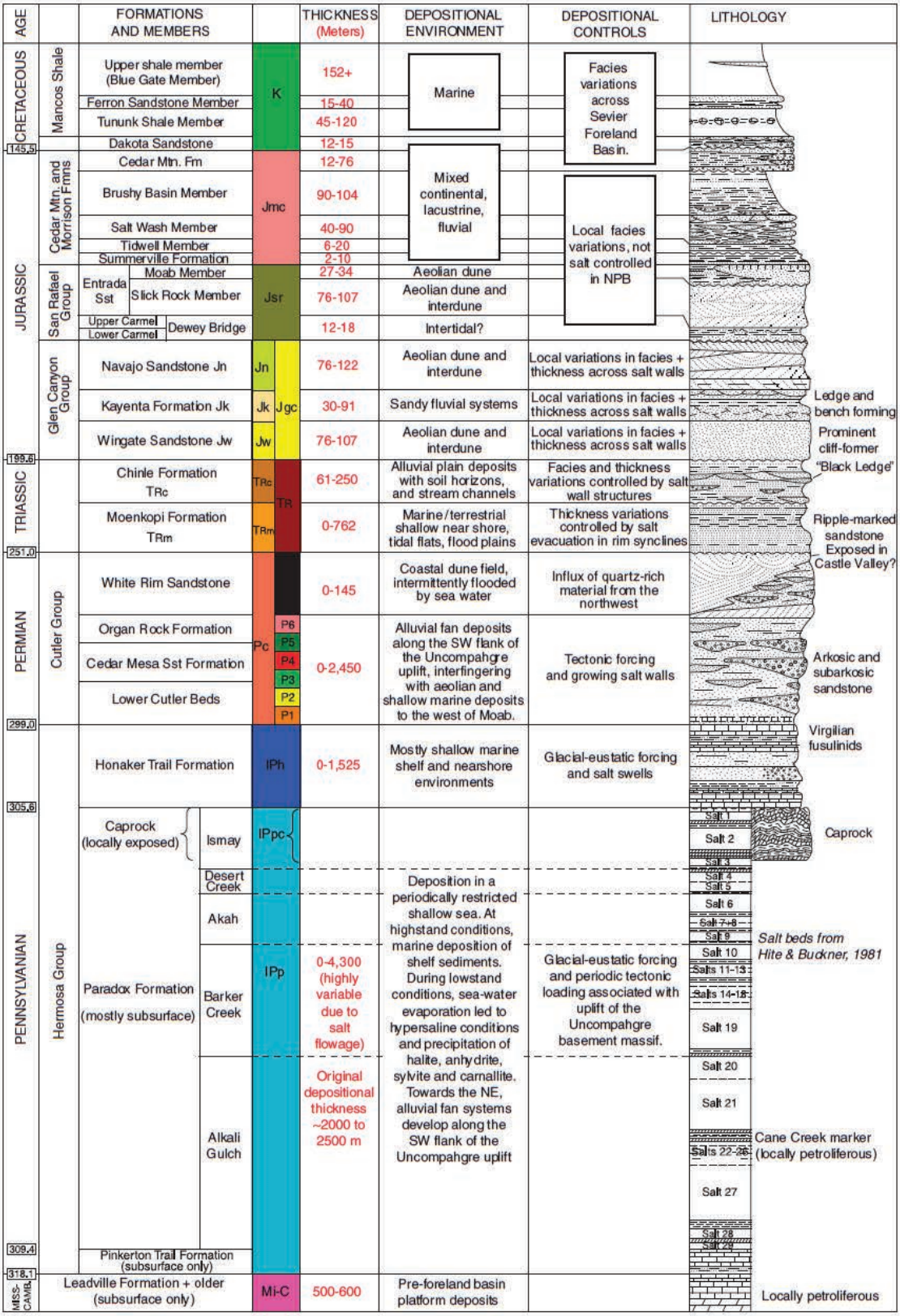

Figure 2.17 Generalized stratigraphic column for the Paradox Basin, with key petroleum intervals highlighted (Trudgill, 2011).

primarily from the Desert Creek interval, which lies between two organic-rich intervals: the basal Chimney Rock shale and overlying Gothic shale (Peterson, 1992; Hite et al., 1984). With regards to sequence stratigraphy, the Chimney Rock and Gothic shales are related to major transgressive phases within the Desert Creek and Ismay intervals (Sarg et al., 1999), with reported total organic carbon (TOC) values between 5-15% (Hite, 1970). Production in Lisbon Field (Figure 2.16), discovered in 1960, is from Devonian and Mississippian (Leadville Formation) intervals, located beneath the thick Paradox evaporite wedge. Like the Aneth Field, the Lisbon Field has exceeded its original estimated ultimate recovery (EUR), with cumulative production of 50 MMBO and 855 BCFG (Stevenson & Wray, 2009). Andy's Mesa Field (Figure 2.16), discovered in 1967, signaled a shift in exploration targets to include clastic sandstone reservoirs within the Pennsylvanian Honaker Trail and Permian Cutler formations. Until 1998, only 7 wells produced at Andy's Mesa; however, with the acquisition of the first 3D seismic survey of the field by UNOCAL, 35 additional infill wells were drilled in structural and stratigraphic reservoirs (Stevenson & Wray, 2009). The Cutler fluvial and eolian sands that produce at Andy's Mesa Field are located and developed intermittently throughout the Salt Wall Region, with average porosities of 15% and permeabilities exceeding 50 md (DuChene et al., 2009). In the Hamilton Creek Field (Figure 2.16), discovered in 1983, 3D seismic data confirmed Hermosa and Cutler 3-way fault-bound traps. As of August 2007, 42 producing wells were active in the Hamilton Creek Field (Stevenson & Wray, 2009). Current petroleum exploration targets are both conventional and unconventional reservoirs flanking the salt walls within the Salt Wall Region. The Paradox Basin, with its numerous trapping geometries, source rocks, and sealing mechanisms, is an intricate petroleum system, which will require continual research and data acquisition to understand, explore, and develop effectively. The complex fault zones located at the terminations of many of the salt walls may provide further insight into trap geometry, migration pathways, and seal integrity in the petroleum systems proximal to the salt structures.

Another important economic resource in the Paradox Basin is the potassium-bearing mineral potash (in particular, sylvite, KCl) that corresponds to hypersaline conditions within

evaporite environments. Potash was discovered in the basin in 1924 by Crescent Eagle Oil Co., whose petroleum exploration well encountered deposits of sylvite and carnallite (Hite & Gere, 1958). Currently, large-scale mining of potash in the Paradox Basin is limited to the Cane Creek anticline area, and exploration along the Salt Valley salt wall, despite its widespread distribution throughout the basin. Since potash is deposited under hypersaline conditions (in which 98% of original seawater has evaporated), it generally is the last salt to precipitate within a given cyclothem and is only present in eighteen of the twenty-nine evaporite cycles identified by Hite (1960). Goldsmith (1969) contends that the Paradox Basin likely had uniform geologic and environmental conditions during the Pennsylvanian, thereby allowing for relatively uniform deposition of potash in the deeper, central part of the basin. The mineralogy of the potash deposits in the Paradox Basin is relatively simple (when compared with the deposits mined in New Mexico and Germany), seemingly composed only of sylvite and carnallite (Hite & Gere, 1958). Hite et al. (1984) recognized an interesting and potentially significant relationship when studying the Alviso salt ponds near San Francisco Bay. They noticed that there seemed to exist a positive correlation between the higher saturation point of potash and higher levels of organic productivity (and therefore more enriched source rocks). Table 2.1 shows the results of their analyses, where the relationship between the hypersaline conditions for potash precipitation and the level of

Table 2.1 Results from the study of three brine samples collected from the Alviso salt ponds in San Francisco, CA (Hite et al., 1984).

Sp. gr.	Saturation field	Organic Carbon (ppm)
1.16	Gypsum	223
1.21	Halite	249
1.30	Close to potash	2,417

organic carbon is evident. Hite et al. (1984) suggest the organic productivity is directly related to level of saturation in the water: the higher the salinity of the water, the greater the abundance of halophillic bacteria, which are the primary producers in this type of environment. Additionally, they note that much of the observed organic material under these conditions is also in solution, thus supporting similar observations made by Peterson and Hite (1969).

CHAPTER 3

METHODS

Structural and stratigraphic data were collected in three field areas within the Paradox Basin in order to address the goals outlined for this project. Fieldwork was conducted in the Fall of 2014, totaling approximately ten days. Field mapping was completed using Google Earth aerial images at a variety of scales, to allow for collection of structural data at varying levels of detail. Structural measurements, including the strike and dip of bedding and fault surfaces, were collected using *Midland Valley's FieldMove Clino* application. Previously published maps (Cater, 1955; Vogel, 1960; Doelling & Ross, 1998; Doelling, 2002; Lawton & Buck, 2006) were also consulted while mapping and collecting data in the field. Final maps of the Castle Valley and Gypsum Valley salt wall terminations were drafted using Global Mapper 15, Adobe Illustrator CS6, and previous interpretations of these areas (Cater, 1955; Vogel, 1960; Lawton & Buck, 2006). In addition to geologic maps, several photomosaics were generated and interpreted using Adobe Illustrator CS6. These photomosaics illustrated the relationships between units where data was unattainable (i.e., on steep slopes and inaccessible cliffs), most notably the growth strata flanking the salt structures.

Development of the 3D models of the Castle Valley and Gypsum Valley salt wall terminations involved several steps of data compilation and organization. This included importing the data, generating surfaces from field and well data, and ultimately creating master surfaces from these preliminary surfaces. The collected field data were exported from *Midland Valley's FieldMove Clino* application to the *Midland Valley Move* software package. Additionally, published field data (Vogel, 1960; Lawton & Buck, 2006) were digitized and imported into the project to complement the field measurements. These data were then used to generate individual surfaces within *3D Move*, where each surface was created using the structural orientation of its assigned point datum (e.g., the strike and dip of a bedding plane or fault surface). Once generated, these surfaces were grouped within a regional Paradox Basin Petrel project according

to their specific horizon or type of structural data (e.g., fault, lineation, etc.). The stratigraphic horizons for which surfaces were generated include the following, from oldest to youngest: the Paradox and Honaker Trail Formations of the Pennsylvanian Hermosa Group, the Permian Cutler Formation, the Triassic Moenkopi Formation, the Triassic Chinle Formation, the Triassic/Jurassic Wingate Sandstone and Jurassic Kayenta Formation of the Glen Canyon Group, and the Salt Wash and Brushy Basin Members of the Jurassic Morrison Formation.

Following the generation of these field surfaces, well data for the Paradox Basin were incorporated to create surfaces at depth, according to the formation tops designated in each well. These well data were acquired from the online IHS database and from a Paradox Basin Petra project created by the Rocky Mountain Association of Geologists in 2009. Surfaces were then generated for each formation using the corresponding well tops within Petrel. Several gridding algorithms within Petrel were tested in order to ensure the most realistic geologic formations were created. These surfaces were then transferred to the *3D Move* project to be incorporated into the working three-dimensional model.

New surfaces linking the field and well data were then interpreted in *2D Move* (Figure 3.1, 3.2; Appendices A and B). It was necessary to interpret these surfaces to ensure that the final surfaces used in the 3D model would realistically reflect the geologic formations at depth. It is important to note, however, that these surfaces linking the surface and well data are highly interpretive. They are projected from the available data and also include general knowledge on the behavior of salt and overlying stratigraphy in the subsurface. If seismic data can be acquired for these areas, then these interpretations can be improved upon and refined to more accurately reflect the geology. Once several 2D sections were interpreted, master surfaces were created for each stratigraphic horizon by combining the field, well, and interpreted surfaces.

Following the creation of stratigraphic master surfaces, structural data (including faults, lineations, etc.) were incorporated into the 3D model to complete the interpretation. These structural data included the measurements collected in the field as well as digitized structural data published in literature (Cater, 1955; Vogel, 1960; Doelling & Ross, 1998; Doelling, 2002;

Lawton & Buck, 2006). Stratigraphic and structural relationships were analyzed and edited where necessary. Finally, the surfaces were refined in order to generate an accurate and visually impactful final product (Figures 3.3a, b ; Appendices A and B).

Throughout the modeling process, figures and the models were frequently updated to maintain consistency between these different types of data. Difficulty in locating existing seismic data and obtaining permission to use these seismic surveys prevented use of this type of subsurface data in the creation of these 3D models. The field data provided the greatest data control at the surface, whereas surfaces generated from well top data were the main subsurface control. Figures 3.1-3.3 exemplify the new 2D and 3D interpretations for the Castle Valley and Gypsum Valley salt wall terminations.

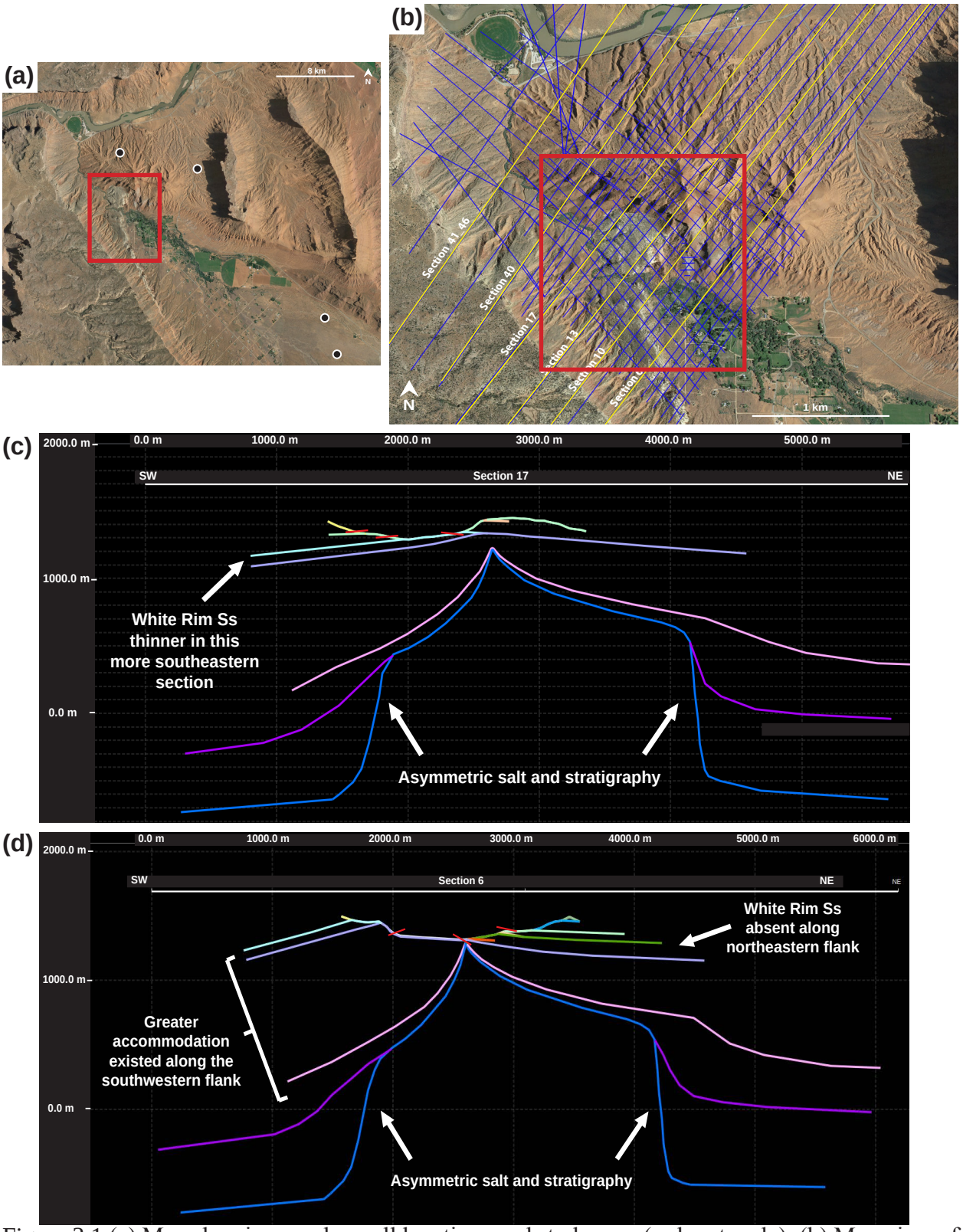

Figure 3.1 (a) Map showing nearby well locations and study area (red rectangle); (b) Map view of 2D section lines interpreted from field and well data at Castle Valley (study area in red rectangle); Representative section line 17 (c) and section line 6 (d), showing horizon lines that were used to construct 3D surfaces (red lines show bedding dip measurements in the field).

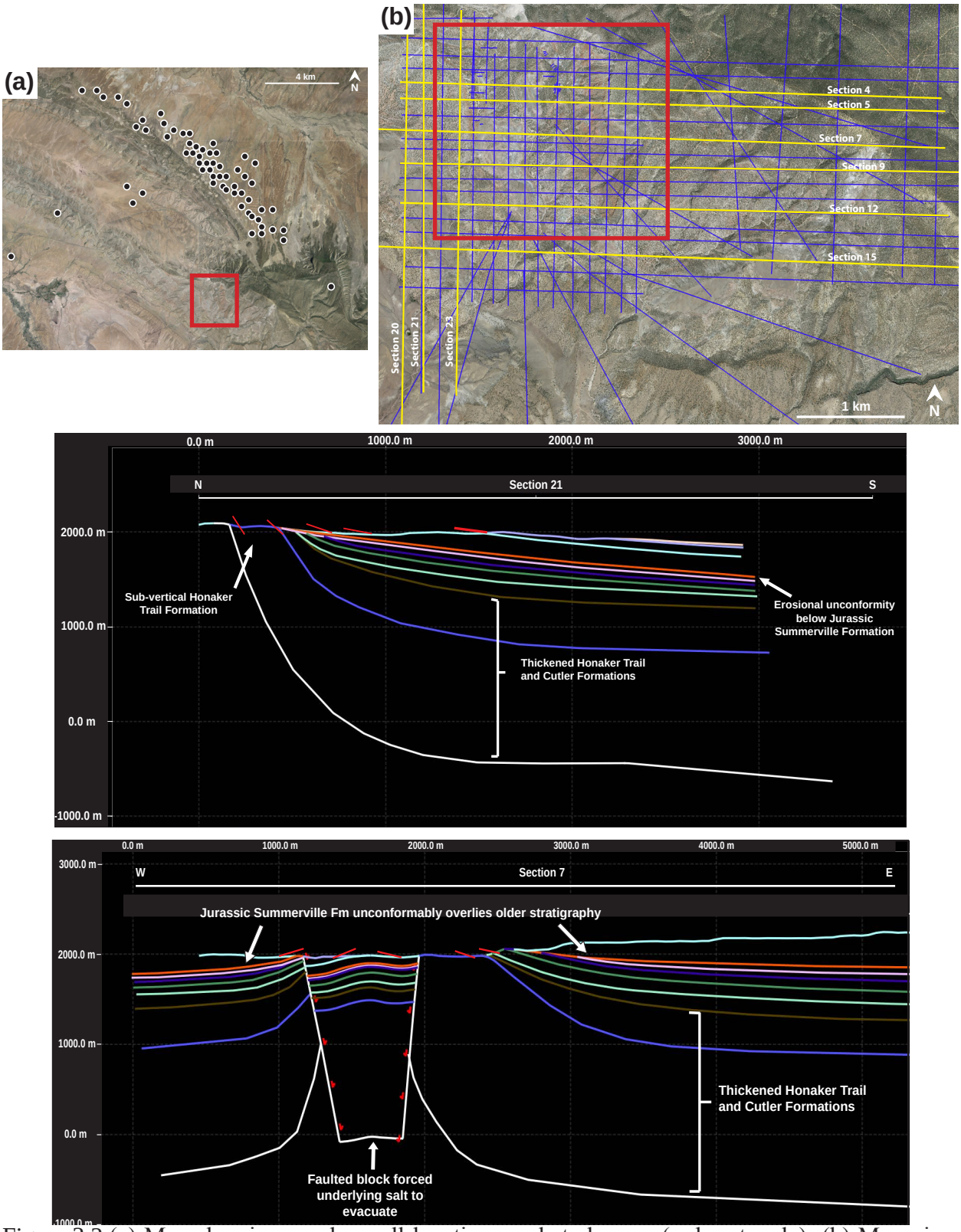

Figure 3.2 (a) Map showing nearby well locations and study area (red rectangle); (b) Map view of 2D section lines interpreted from field and well data at Gypsum Valley (study area in red rectangle); Representative section line 21(c) and section line 7 (d), showing horizon lines that were used to construct 3D surfaces (red lines show bedding dip measurements in the field).

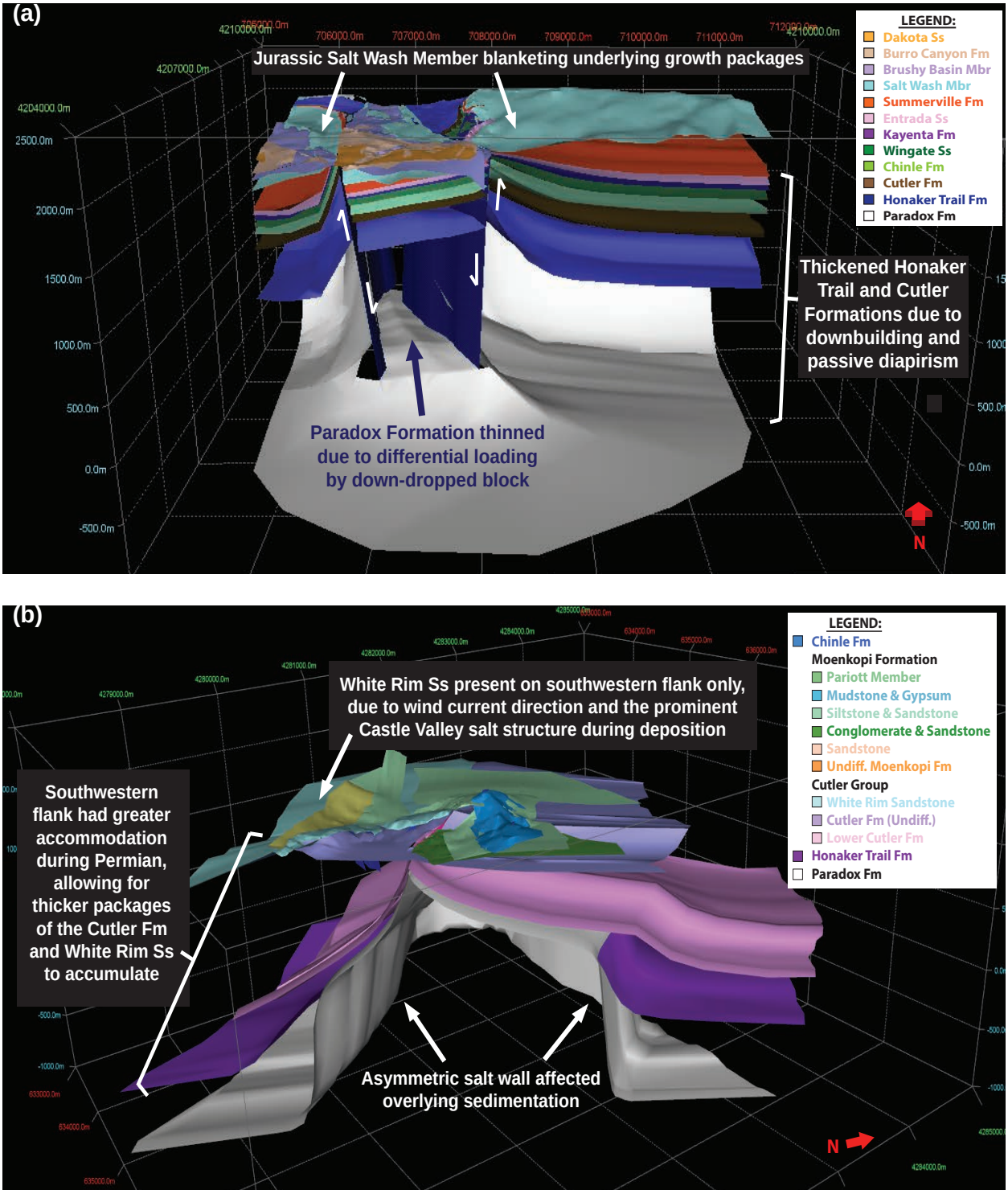

Figure 3.3 (a) Overview of completed 3D model of the Gypsum Valley salt wall termination; (b) Overview of completed 3D model of the Castle Valley salt wall termination (Klondike Ridge).

CHAPTER 4

CASTLE VALLEY SALT WALL TERMINATION

4.1 General Characteristics

The Castle Valley salt wall is located northeast of the town of Moab and southeast of the Colorado River (Figure 4.1). The Castle Valley salt wall trends northwest from the Oligocene La Sal intrusive complex in the southeast, to its apparent abrupt termination at the Colorado River to the northwest. The primary study area (Study Area #1, Figure 4.1) is characterized by outcrops of caprock associated with the Paradox Formation, as wells as two salt welds present at the surface (Lawton & Buck, 2006). The presence of surficial welds and caprock facies (i.e., gypsum, dolostone, and black shale) imply that salt was at or near the surface during the development of this structure. More specifically, the mounds of Paradox Formation caprock indicate the salt structure was breached during its final stages of development. Crestal faulting atop the salt wall provided pathways for groundwater to infiltrate and dissolve the upper portion of the salt wall, ultimately resulting in collapse, and the flat-floored valley present today. A detailed stratigraphic column was compiled for this study area (Figure 4.2), incorporating lithologic characterization from

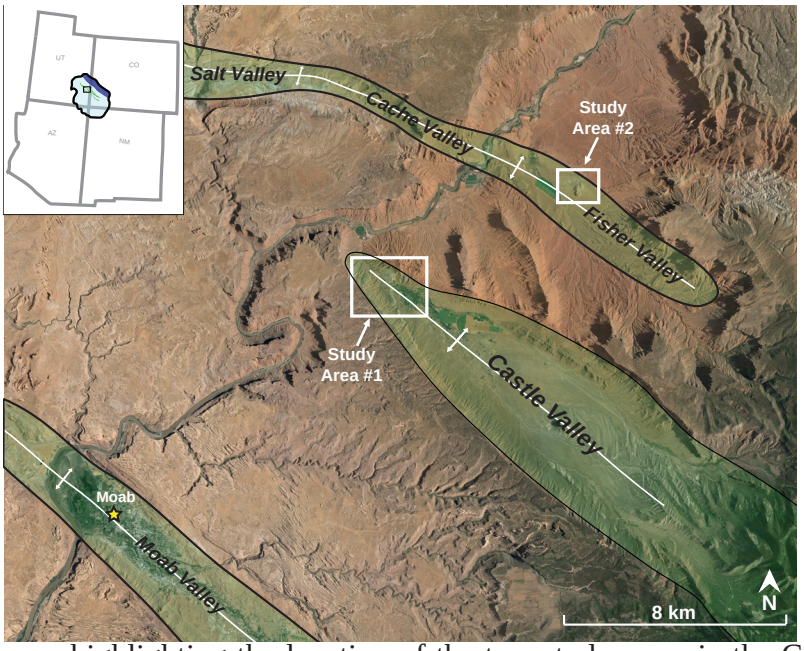

Figure 4.1 Aerial map highlighting the location of the two study areas in the Castle Valley area. Inset of regional map indicates location of aerial map in the basin.

several publications (Lawton & Buck, 2006; Trudgill, 2011). Although the Castle Valley salt wall is morphologically similar to other salt structures in the basin, the unique qualities of this salt wall made it an ideal candidate for study. Its northwestern plunge and the anomalously thick White Rim Sandstone unit adjacent to this northwestern termination invite much speculation with respect to its evolution. This relationship between structure and stratigraphy appears to be central to the formation of the Castle Valley structure. Therefore, detailed field study and 3D modeling of the northwestern termination of the Castle Valley salt wall were necessary to better understand the local development of this salt structure.

4.2 Stratigraphy

Within the study area, the stratigraphic units range from Pennsylvanian to Triassic in age, including, from oldest to youngest: the Pennsylvanian Paradox Formation, the undivided Cutler Formation and White Rim Sandstone of the Permian Cutler Group, the Triassic Moenkopi Formation, and the Triassic Chinle Formation. These units have been characterized in Figure 4.2,

AGE	FORMATIONS & MEMBERS		MAP SYMBOL	THICKNESS (Meters)	DESCRIPTION
TRIASSIC	Chinle Formation		Trc	**61-250**	Fluvial and alluvial plain deposits with soil horizons and stream channels.
	Moenkopi Formation	Pariott Member	Trmp	**0-762**	Marine and terrestrial shallow near shore, tidal flat, and floodplain deposits. Slope-forming deposits are reddish-brown to tan in color.
		Mudstone and Gypsum	Trmg		
		Heterolithic Siltstone and Sandstone	Trmh		
		Conglomerate and Sandstone	Trmc		
		Sandstone (numbered from oldest to youngest)	$Trms_x$		
		Undifferentiated Moenkopi Formation	Trmu		
PERMIAN	White Rim Sandstone		Pcw	**0-145**	Cliff-forming eolian sandstone. Highly variable thickness within the basin.
	Undifferentiated Cutler Arkose		Pcu	**0-2,450**	Alluvial fan deposits along the SW flank of the Uncompahgre uplift. Eolian and shallow marine deposits locally present.
	"Lower Cutler Beds"		PIPc		
PENNSYL-VANIAN	Paradox Formation		Php	**2,000+** (depositional) **4,300** (diapirs)	Consists of drab gray gypsum with minor beds of black shale, sandstone, and limestone. Thickness highly variable due to salt flowage.

Figure 4.2 Stratigraphic column of units in the Castle Valley study area showing colors, thickness variations, and general characteristics (after Lawton & Buck, 2006; Trudgill, 2011).

which combines previous and current interpretations of the geologic units (most notably, Lawton & Buck, 2006, and Trudgill, 2011). Of particular note in the Castle Valley area is the anomalously thick outcrop of the Permian White Rim Sandstone. Unlike many of the other stratigraphic units in the basin, deposits of the White Rim Sandstone are found sporadically, both at outcrop and the subsurface. The northwestern termination of the Castle Valley salt wall is characterized by one of these isolated deposits, which is quite thick (~105 m) towards the nose of the structure but rapidly pinches out to 0m within 3 km along the southwestern flank. Additionally, the White Rim Sandstone was recognized in Study Area #2 (here identified as "Professor Valley") approximately 8 km to the northeast (Figure 4.1), where it also blankets the northwestern side of the outcrop. Consideration of this impressive eolian sandstone was central to understanding the evolution of the Castle Valley structure.

4.3 Mapping Results

Field mapping was an essential first step in evaluating the northwestern termination of Castle Valley. Stratigraphic and structural data were collected and compiled into a comprehensive geologic map (Figure 4.3). In addition to these collected data, key publications (i.e., Lawton & Buck, 2006) and aerial imagery allowed for complete mapping of stratigraphic units, including those that were inaccessible in the field. Most notably, this study added structural and stratigraphic data to the modified geologic map, including different interpretations of the field relationships present in the area.

4.3.1 Castle Valley

The geologic map in Figure 4.3 illuminates several key aspects of the Castle Valley field area that are important to recognize. First, as discussed previously, the White Rim Sandstone is a dominant cliff-forming unit that thins drastically towards the southeast (Figure 4.4a). The thick White Rim Sandstone overlies the faulted Cutler Group (Figure 4.4b). Faults display predominantly down-to-the-west normal slip sense on the northern flank and down-to-the-north slip sense on the southern flank. Second, the dips of the overlying beds decrease rapidly away from the salt welds, indicating that the salt once supported the strata but its dissolution resulted in the collapse

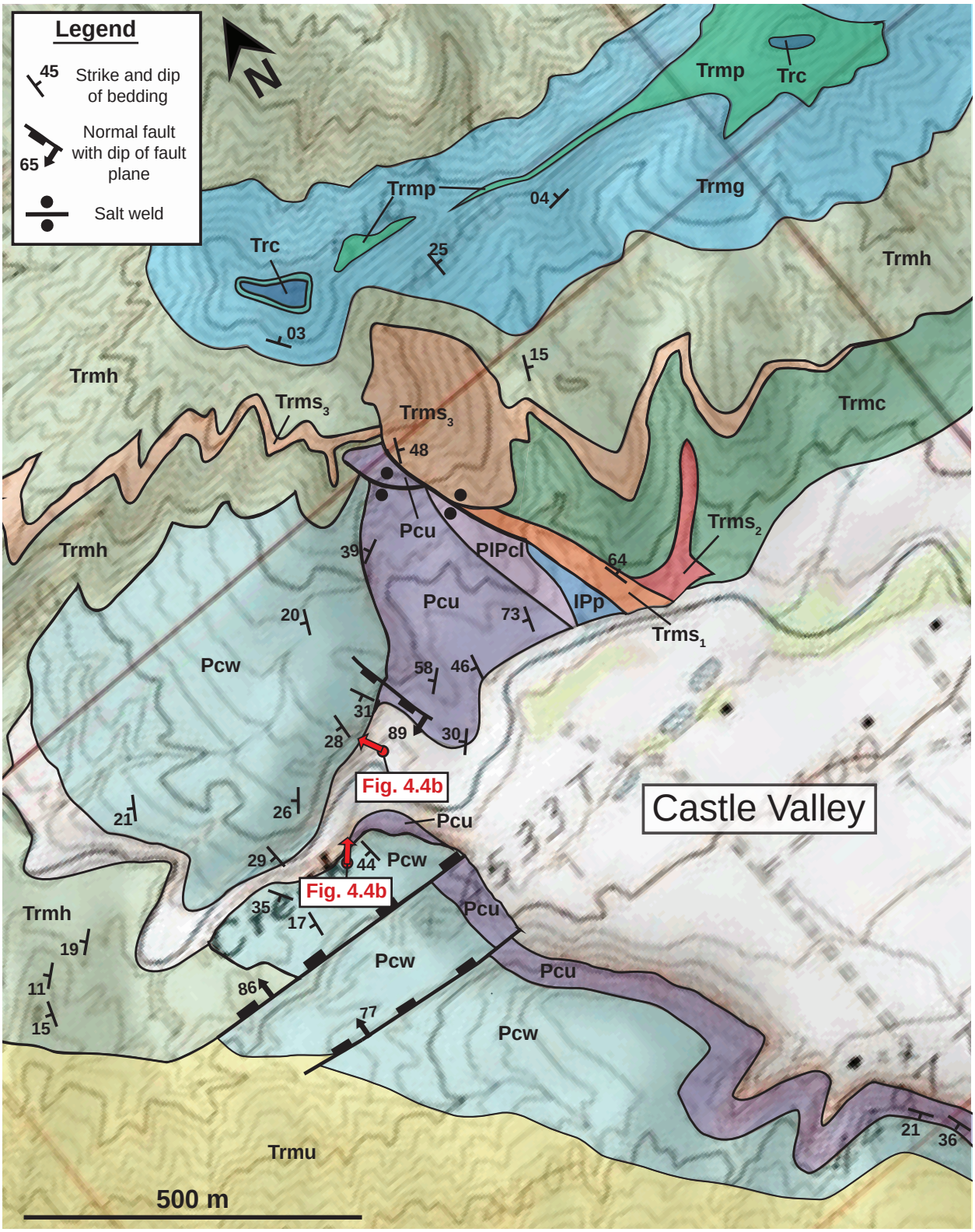

Figure 4.3 Geologic map of the Castle Valley salt wall termination (modified from Lawton & Buck, 2006). Geologic units correspond to those described in Figure 4.2. Locations and orientations of Figures 4.4a and 4.4b are designated on the map, and an explanation of symbols is provided. It is important to note the direction of the north arrow in this figure.

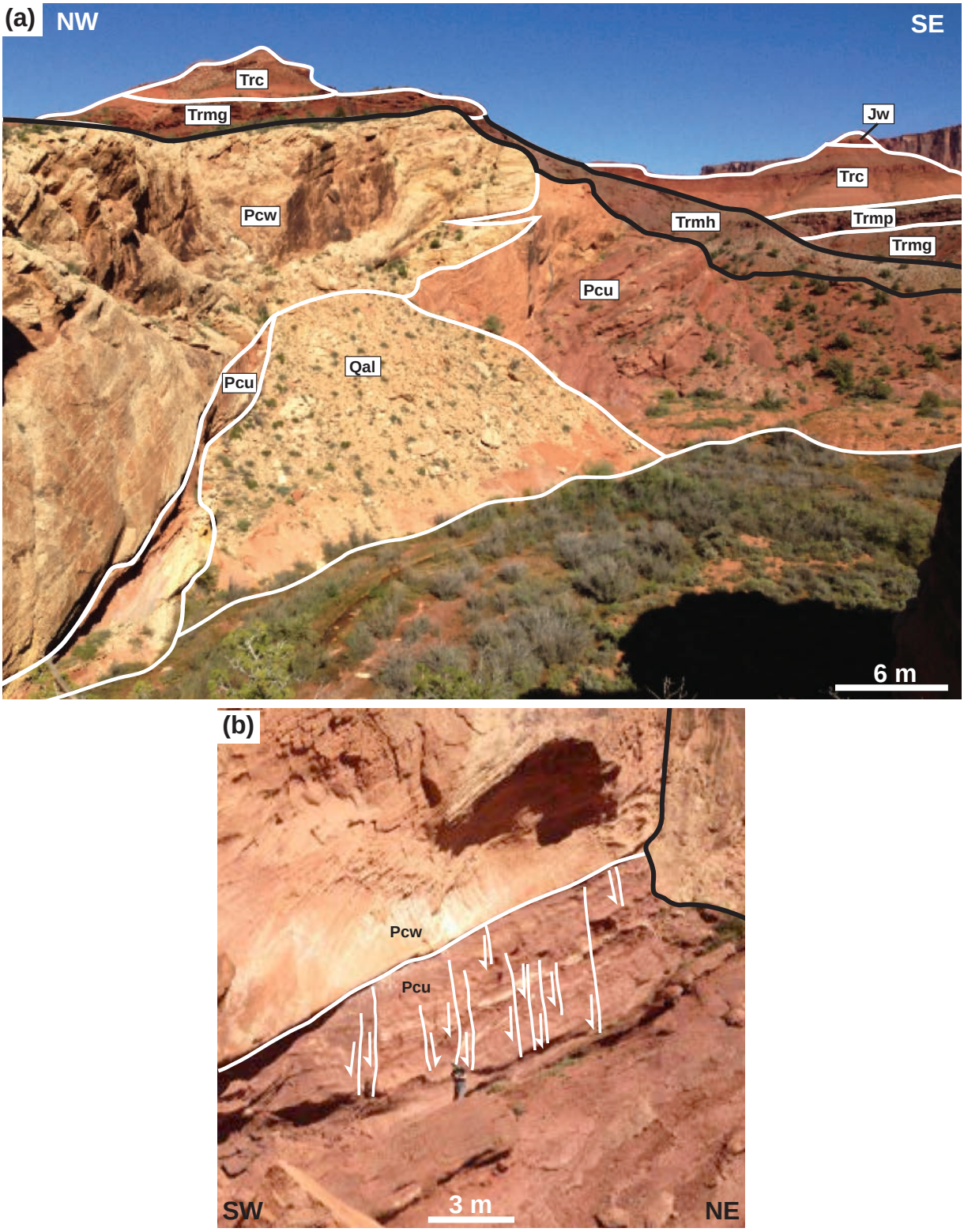

Figure 4.4 (a) View of outcrop, showing anomalously thick White Rim section atop the underlying Cutler Group. White lines are stratigraphic contacts, black lines indicate edges of the outcrop; (b) Close-up of contact between the Cutler Group and White Rim Sandstone, showing large eolian cross-bedding above and predominantly down-to-the-W/SW faulting below. White lines are faults, black lines indicate edges of the outcrop.

of the overlying beds. Third, a caprock sequence of the Paradox Formation is present at the surface, located just below the welds interpreted by Lawton and Buck (2006). This supports the notion that salt was close to or at the surface throughout much of its evolution. These observations collectively touch upon the important and dynamic relationship between the mobile salt in the Paradox Formation and concurrent sedimentation.

4.3.2 Professor Valley

The Professor Valley field area yielded surprising and encouraging results. Previous publications mapped several Jurassic eolian units in the outcrop, which required significant faulting and structural complexity in order to justify the mapped relationships (Figure 4.5; Doelling, 2002). However, detailed mapping of the field area (Figure 4.6) revealed that the units were similar to those found in Castle Valley (Figure 4.3). This study suggests that the eolian unit is the Permian White Rim Sandstone and not the Jurassic Wingate Sandstone as previously mapped. This area similarly exhibits the White Rim Sandstone blanketing the underlying Cutler Formation along the northwestern side of the outcrop (Figure 4.6). An interesting implication of this finding is that the White Rim Sandstone may have been an influential factor not only at Castle Valley but along the Salt Valley-Professor Valley-Cache Valley salt wall trend as well. By instead mapping this small area as White Rim Sandstone, it places the development of this feature within the regional framework of the surrounding salt structures. Furthermore, this mapping simplifies the structural framework of this local feature, eliminating the need for structural complexity to explain the observed stratigraphy. The preservation of the White Rim Sandstone in these two locations suggests that the topography in these areas was low during the time of deposition, which might be expected in an area with active salt growth and concurrent minibasin subsidence.

4.4 Modeling Results

The model generated using *3D Move* revealed interesting surface and subsurface trends present at the northwestern termination of the Castle Valley salt wall. Synthesis of field and well data allowed for interpretation of structural and stratigraphic relationships, which in turn has enabled a better understanding of the subsurface architecture of the area. Difficulty in acquiring

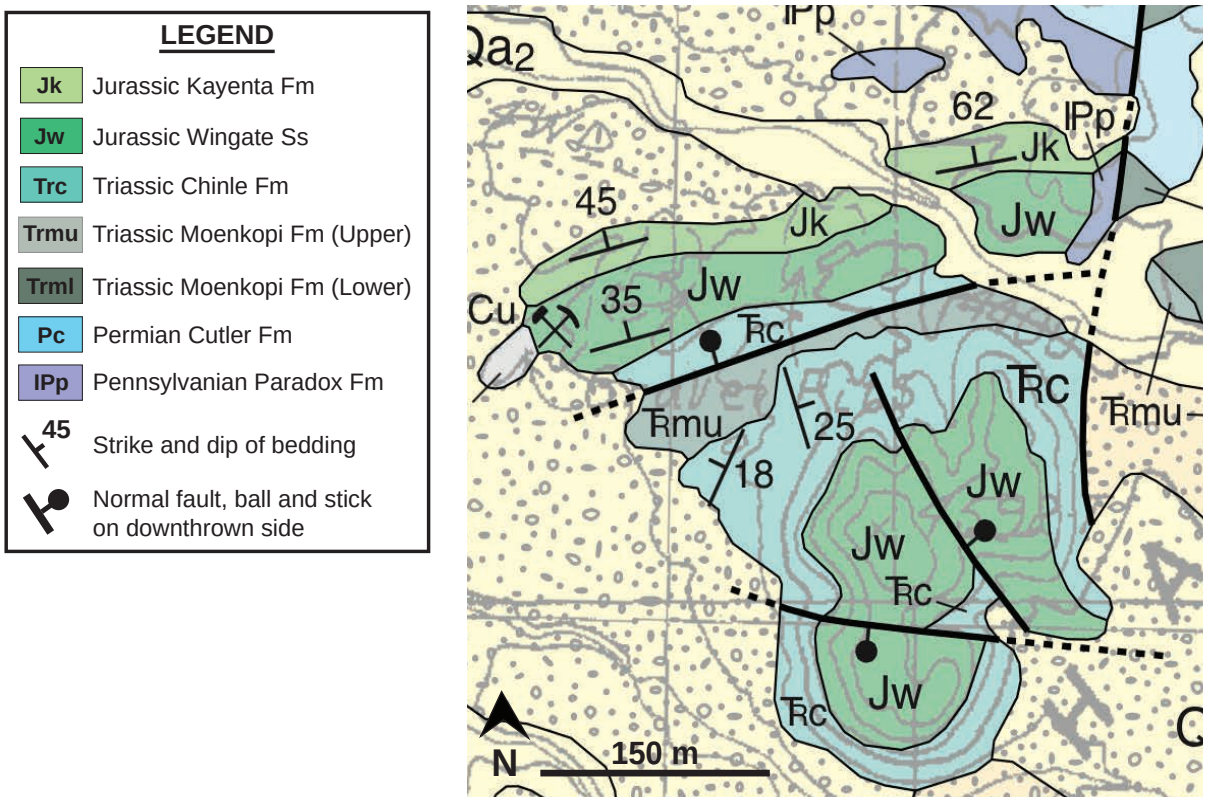

Figure 4.5 Published geologic map of the Professor Valley field area (Doelling, 2002). Note the structural complexity required to justify this interpretation of the stratigraphic units present.

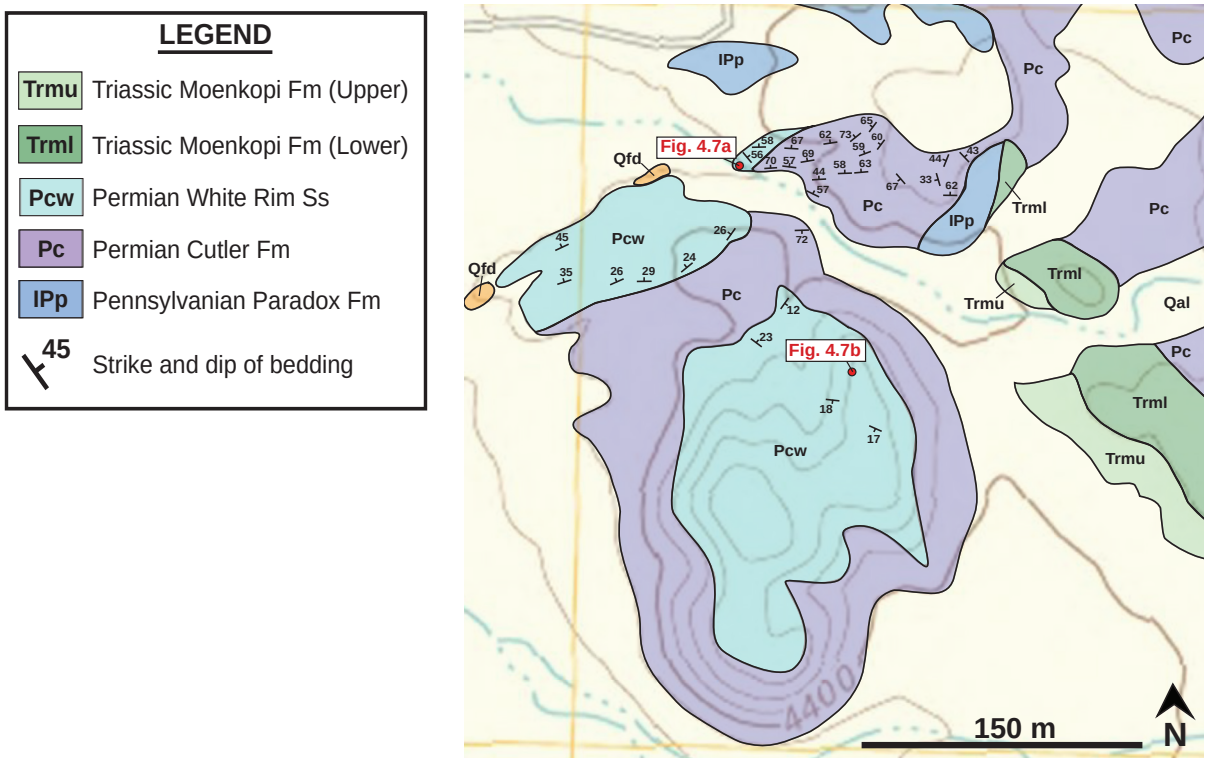

Figure 4.6 Revised geologic map for the Professor Valley field area. Note the presence of the White Rim Sandstone draping the underlying Cutler Formation from the northwest.

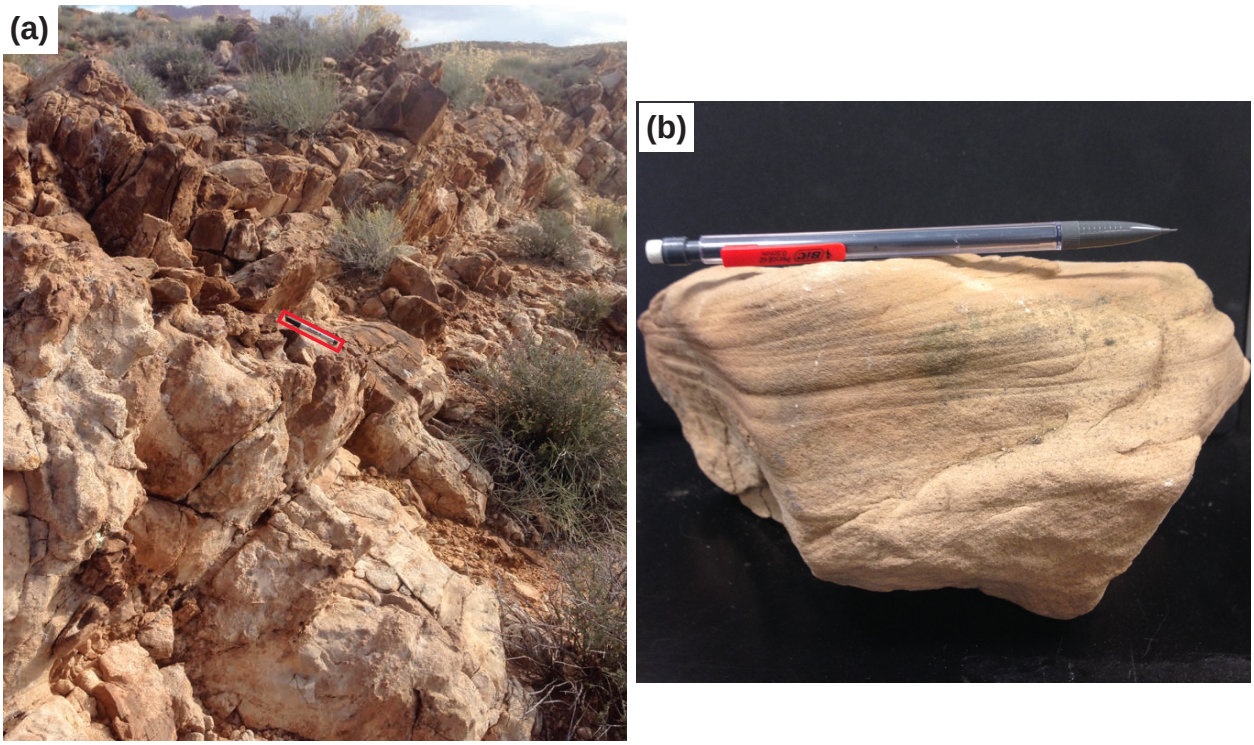

Figure 4.7 (a) Outcrop of interpreted White Rim Sandstone (red rectangle highlights pen for scale); (b) Hand sample of White Rim Sandstone from Professor Valley, exhibiting fine- to very-fine-grained, well-sorted, cross-stratified grains.

existing seismic data has prevented even greater accuracy of these interpretations, but this model serves as an initial 3D representation of the geology at this location in Castle Valley, which previously has not been accomplished for this area.

Structurally, the termination of the Castle Valley salt wall is relatively simple when compared with other salt wall terminations. Relatively small-scale faulting is present within the Cutler Group and overlying White Rim Sandstone, but it is unclear if this faulting extends far into the subsurface (Figure 4.3; Figure 4.8a). An important theory to consider is that Precambrian faulting likely exists along the northeast of the termination (Figure 2.13), acting as a barrier to salt flow. This has been built into the model, showing the abrupt termination of the salt against the interpreted location of this structure (Figure 4.8b; Figure 4.8c). This has been inferred from existing studies suggesting the presence of Precambrian northeast-southwest-striking structures throughout the Paradox Basin that mimic the regional Colorado Lineament (Warner, 1978). In this location, the Colorado River runs along the inferred location of one of these structures, as

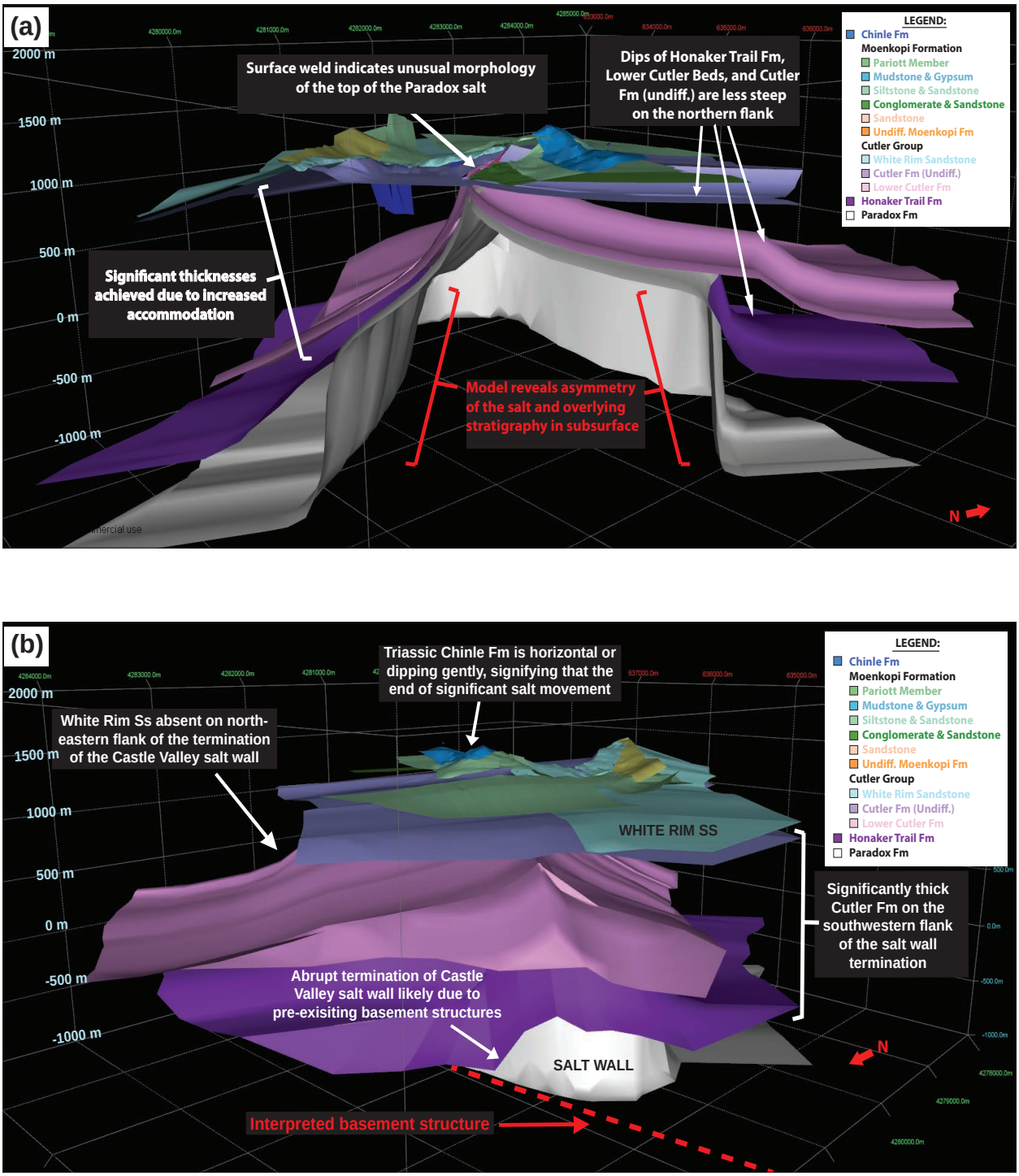

Figure 4.8 (a) Overview of 3D model, illustrating the subsurface asymmetry and unusual morphology of the welded salt; (b) View of plunge with overlying stratigraphy, displaying the differing accomodation on either side of the Castle Valley salt wall and the absence of the White Rim Sandstone along the northeastern flank.

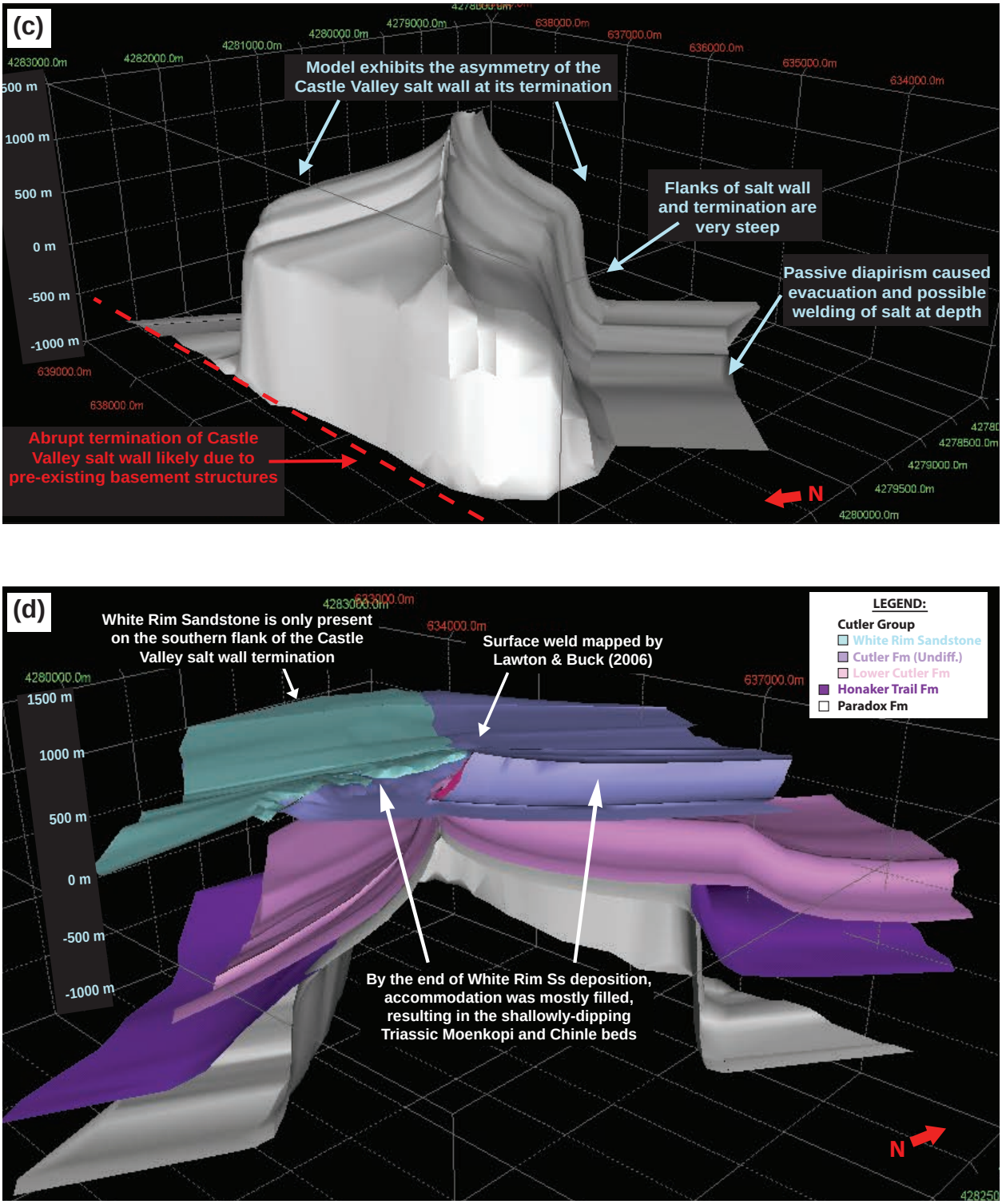

Figure 4.8 (continued) (c) Display of the salt wall termination without the overlying stratigraphy, demonstrating the abrupt termination against an inferred basement structure; (d) Overview of Paleozoic stratigraphy, showing the unusual distribution of the White Rim Sandstone.

can be seen in Figure 4.9 (Trudgill, 2011). This salt isopach map was consulted during creation of the 3D model as it suggests an abrupt change in salt thickness to the north-northwest, likely the result of a preexisting base-salt structure. Another important aspect of this salt isopach map is the location of areas of zero salt thickness, highlighted in purple. This isopach trend suggests that the accommodation was asymmetric on either side of the salt wall termination and that the area southwest of the termination had a relatively large area of welded salt. This would have enabled an anomalously thick package of sediment to accumulate along the southwestern flank of Castle Valley (Figure 4.8d), which in this interpretation would correspond to the Permian White Rim Sandstone. This accommodation rapidly decreases to the southeast, which is also represented by the rapid thinning of the White Rim Sandstone along the southern flank of the Castle Valley salt wall. The proposed 3D model incorporates these thickness trends and asymmetric stratigraphy across the termination, further verifying the interpretations presented in the model.

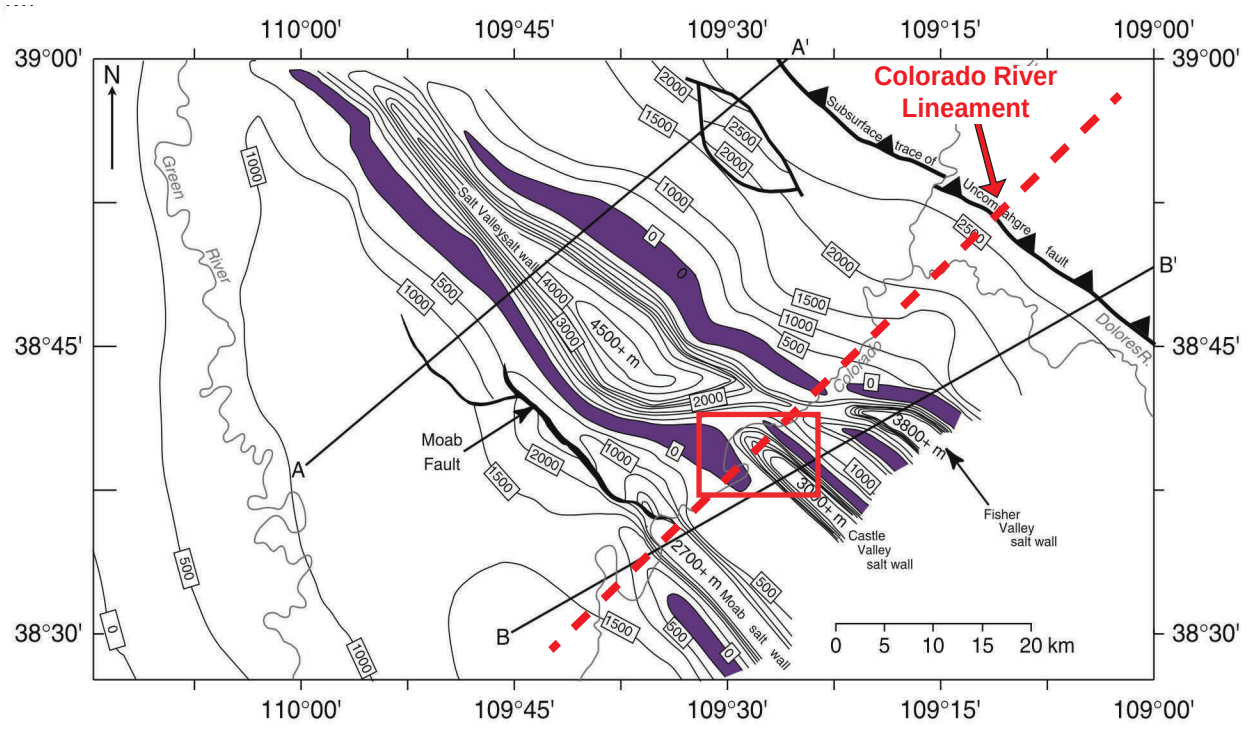

Figure 4.9 Salt isopach map showing the unusual terminations of the salt structures in the northwestern Paradox Basin. Note the rapid decrease in salt thickness (highlighted by red rectangle) along the northwestern termination of the Castle Valley structure and its proximity to the Colorado River Lineament, interpreted by a red dashed line (Trudgill, 2011).

4.5 Depositional Environment During Permian Time

The Permian period in the Paradox Basin was characterized by the uplift of the Uncompahgre Front during the early Permian, followed by extensive movement of the Paradox salt. The Permian Cutler Group is composed primarily of arkosic sandstone that interfingers with marine and eolian deposits to the west. Due to the rise of the salt structures during the Permian, the thickness of the Cutler Group varies significantly within the Salt Wall Region (Figure 4.10).

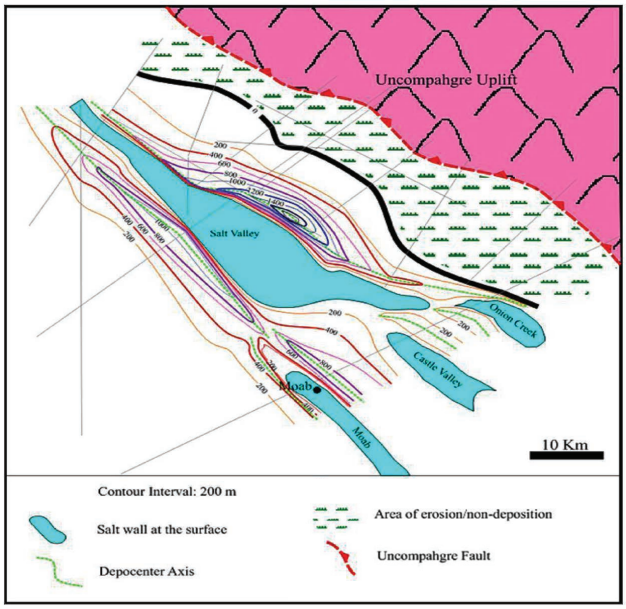

Figure 4.10 Paleogeographic and isopach map of the middle Cutler Formation. Note location of depocenter axes adjacent to the salt structures (from Paz et al., 2009).

Consequently, the unusual topography and the fill of accommodation led to increased diapir growth, which subsequently caused further mini basin subsidence and the creation of accommodation. This process, known as passive diapirism or downbuilding, in which sediment in the surrounding minibasins sinks into the salt, driving the salt into the growing salt wall (Rowan et al., 2003). Additionally, this process resulted in the passive upturning of the Honaker Trail and Cutler Formations. Growth packages observed in Permian through Jurassic strata indicated that the rise of the Paradox salt continued until the Middle to Late Jurassic, although it attenuated following the deposition of the Cutler Group. In addition to growth sequences, inter- and intraformational unconformities are present in these strata, further suggesting that salt growth occurred throughout this 160 m.y. span (Baars et al., 1988).

4.5.1 The Permian White Rim Sandstone

The Cutler Group exhibits different characteristics throughout the basin, from the undivided Cutler Formation proximal to the Uncompahgre Front to more distinguishable members (i.e., Cedar Mesa Sandstone, White Rim Sandstone) to the west (Trudgill, 2011). This is interpreted to represent a transition from a continental setting near the Uncompahgre Uplift, dominated by fluvial processes, to a more coastal and marine environment located west of Moab,

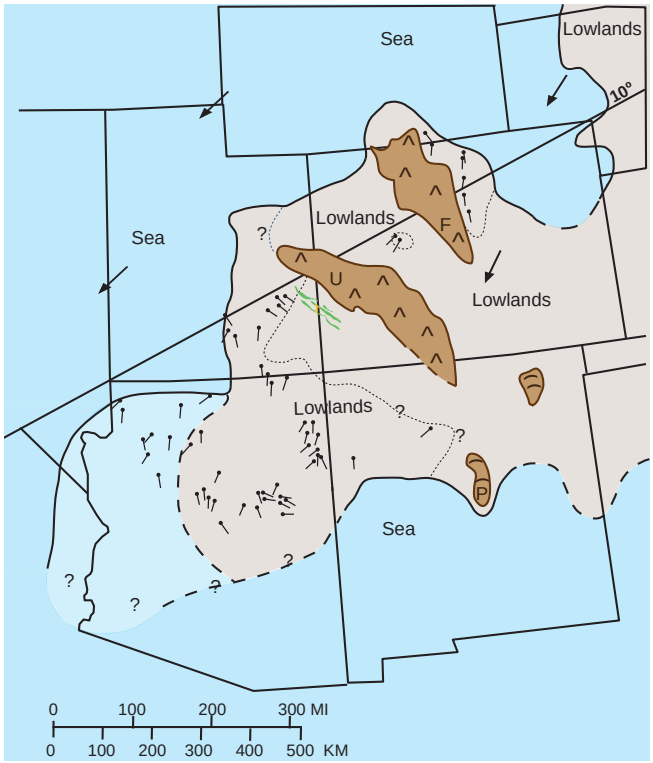

Figure 4.11 Paleogeography during Permian (Leonardian) time. Ball-and-stick symbols point in paleo-wind direction, and black arrows indicate global wind currents. Note paleocurrent direction to the west/southwest of the Salt Wall Region during White Rim Sandstone deposition (modified from Peterson, 1988).

UT. The White Rim Sandstone, found sporadically throughout the western part of the Paradox Basin, has been interpreted as a coastal eolian dune complex (Kamola & Chan, 1988). This interpretation is consistent with the interpretation of the Cedar Mesa Sandstone as a coastal sand facies adjacent to the upper Elephant Canyon Sea (Baars et al., 1988). Although interpretations of the Cedar Mesa Sandstone have varied, its southeast-dipping crossbedding indicates a provenance located to the northwest. Similarly, cross-stratification in the White Rim Sandstone located

along the Castle Valley termination indicates a northerly or northwesterly wind direction. These paleo-currents (Figure 4.11), as described in detail by Peterson (1988), combined with the quartz-rich lithology of these sandstones, seem to suggest a different sediment source than that of the Uncompahgre Range.

Thicknesses of the White Rim Sandstone vary considerably throughout the basin, although it does display some trends in relation to the salt walls. The maximum thickness of the White Rim Sandstone is approximately 240 meters near its western extent, as determined by drill hole data. In outcrop, thicknesses range from 60-120 meters thick, thinning regionally towards the east (Fillmore, 2011). Although the White Rim deposits located in Castle Valley are eolian in nature, the White Rim Sandstone is more generally described as a coastal dune environment. Marine influence is documented further to the west, where marine deposits are recognized in the White Rim Sandstone. However, in the study area, lack of marine signatures indicate that this portion of the White Rim erg was not significantly influenced by marine waters. Preservation of these thicknesses of eolian sand likely resulted from a fluctuating water table, likely influenced by a relatively nearby sea (Kamola & Chan, 1988). Kamola & Chan (1988) recognized a distinct marine overprint of the eolian deposits located at Capitol Reef, suggesting that flooding of the coastal dune environment influenced the dune deposits of the White Rim Sandstone.

With respect to petroleum exploration, the White Rim Sandstone is and has been an excellent petroleum reservoir (Campbell & Ritzma, 1979). Eolian sandstone are characterized as having well-sorted, well-rounded, and uniform grains, usually fine-grained in size or smaller as a result of the carrying capacity of wind currents. The White Rim Sandstone has excellent porosity and permeability as a result, making it a prime candidate for a petroleum reservoir. Additionally, the apparent lack of marine influence in the Castle Valley study area suggests that the reservoir quality of the White Rim Sandstone may be better than in deposits further to the west. The Pennsylvanian Paradox Formation is the primary source rock in the basin, but it has been proposed that the Kaibab Limestone (Baars & Seager, 1970) or Precambrian Chuar Group rocks (Sanford, 1995) may have been an additional organic source rock. Lastly, the overlying Triassic Moenkopi

Formation, predominantly comprised of shale and siltstone, would have acted as the seal atop the White Rim Sandstone reservoir, completing the petroleum system. Today, the White Rim Sandstone constitutes a targeted reservoir flanking the Salt Valley salt wall. An ancient White Rim reservoir in the Elaterite Basin, located southwest of Canyonlands National Park in Utah, was at one time an enormous petroleum reservoir. Confinement of this reservoir is estimated to have existed until approximately 5 million years ago, when the incision of the modern Colorado River breached the White Rim reservoir. Breaching of the reservoir would have released the volatile petroleum gases and liquids and altered the remaining hydrocarbons to the solid, tarry substance that presently remains in the reservoir (Campbell & Ritzma, 1979). Today, it has been estimated that the White Rim Sandstone (and to a minor extent the Cedar Mesa Sandstone) holds the largest tar sand deposit in the United States, with an estimated 12.5 to 16 billion barrels of oil in place (Campbell & Ritzma, 1979). However, this tar, from both and economic and technological standpoint, is unrecoverable. Nonetheless, the White Rim Sandstone petroleum system provides valuable information, particularly concerning eolian reservoirs located in other petroleum basins around the world.

CHAPTER 5

GYPSUM VALLEY SALT WALL TERMINATION AND KLONDIKE RIDGE

5.1 General Characteristics

The Gypsum Valley salt wall is located south of the town of Naturita, CO and the Paradox Valley salt wall (Figure 5.1). The Gypsum Valley salt structure trends northwest-southeast and is bisected by the Dolores River. The study area is located at the southeastern termination of the Gypsum Valley salt wall in an area known as Klondike Ridge. Just north of Klondike Ridge, the Gypsum Valley transitions abruptly from a wide, flat-floored valley to a narrow valley dominated by mounds of caprock of the Paradox Formation. The Klondike Ridge study area boasts several striking features, including the Klondike Amphitheater and the Gypsum Valley "megaflap" (Deatrick et al., 2014). Despite the abundance of caprock located just north of Klondike Ridge, caprock is seemingly absent within Klondike Ridge, indicating that salt may not have breached the surface in this area. A detailed stratigraphic column was produced for this study area (Figure 5.2), incorporating lithologic characterization from several publications

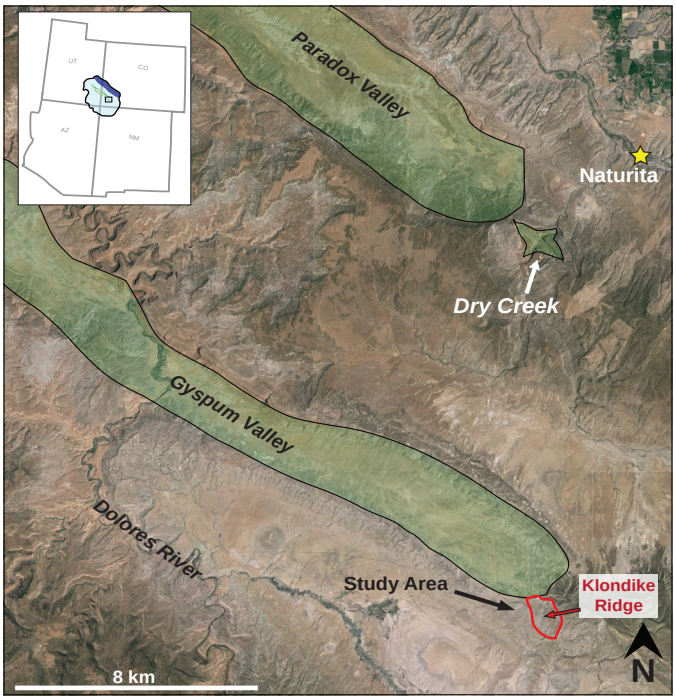

Figure 5.1 Aerial map highlighting the location of Klondike Ridge in the Gypsum Valley area. Inset of regional map indicates location of aerial map in the basin.

(Vogel, 1960; Cater, 1970).

The Klondike Ridge area at the termination of the Gypsum Valley structure was an ideal study region for several reasons. First, it offered a unique perspective of the Gypsum Valley salt wall termination, essentially providing a window into some of the underlying structure. Second, much of the stratigraphy and structure were accessible, allowing for data collection throughout the field area. Lastly, spectacular exposures of halokinetic sequences, including the megaflap discussed by Deatrick and others (2014), provide insight into the growth of the salt wall termination through time. Therefore, detailed mapping and 3D modeling of the Gypsum Valley termination was essential to better understanding its evolution.

5.2 Stratigraphy

Within the Klondike Ridge area, the stratigraphic units range from Pennsylvanian to Cretaceous in age (Figure 5.2). The stratigraphic units present include, from oldest to youngest: the Paradox Formation and Honaker Trail Formation of the Pennsylvanian Hermosa Group, the Permian Cutler, the Triassic Chinle Formation, the Wingate Sandstone and Kayenta Formation of the Jurassic Glen Canyon Group, the Jurassic Entrada Sandstone, the Jurassic Summerville Formation, the Salt Wash Member and Brushy Basin Member of the Jurassic Morrison Formation, the Cretaceous Burro Canyon Formation, the Cretaceous Dakota Sandstone, and the Cretaceous Mancos Shale.

It is important to note that the boundary between the Pennsylvanian Honaker Trail Formation and the overlying Permian Cutler Formation was difficult to determine in the field. The Honaker Trail Formation is predominantly marine, whereas the Cutler Formation is a wholly non-marine, arkosic unit. However, a transitional unit between these two formations contains arkosic sandstones (Figure 5.3) interbedded with thin, laterally-continuous limestone beds (Figure 5.4a). This zone of interbedded arkosic sandstone and marine limestone between these two forma- tions was previously classified as the Rico Formation (Vogel, 1960). However, this classification is outdated, and instead, geologists have grouped this unusual transition into either the Honaker Trail Formation or the Cutler Formation. For the purpose of this study, this transitional

AGE	FORMATIONS & MEMBERS		MAP SYMBOL	THICKNESS (Meters)	DESCRIPTION
CRETACEOUS	Mancos Shale		Km	**797**	Soft, drab-gray, fissile marine shale. Crops out in Disappointment Valley and Dry Creek Basin.
	Dakota Sandstone		Kd	**46-53**	Gray to buff, medium- to fine-grained cross-bedded sandstone. Deposited in floodplain environment.
	Burro Canyon Formation		Kbc	**15-48**	Gray to light-brown cross-bedded conglomerate and sandstone.
JURASSIC	Morrison Formation	Brushy Basin Member	Jmb	**146-157**	Predominantly fluvial in origin. Consists of varicolored shales, ranging in color from green to blue, red, or white.
		Salt Wash Member	Jms	**73-134**	Predominantly fluvial in origin. Consists of thick, resistant sandstone units. Fossilized plant remains common.
	Summerville Formation		Js	**0-27**	Thin, evenly-bedded shale units, red to gray-green in color. Fluvial to lacustrine in origin.
	Entrada Sandstone		Jes	**0-29**	Buff-tan eolian sandstone. Cliff-former in the Klondike amphitheater.
	Glen Canyon Group	Kayenta Formation	Jk	**0-61**	Maroon sandstone, poorly sorted and containing minor shales and calcareous siltstone. Primarily fluvial in origin.
		Wingate Sandstone	Jw	**0-7**	Pale-orange cliff-forming sandstone, primarily eolian in nature.
TRIAS.	Chinle Formation		Trc	**0-15**	Mostly cross-bedded and fluvial in origin. Only the upper part of the formation, comprised of lacustrine gray-green shale and limestone, in present in southwest CO.
PERMIAN	Cutler Formation		Pc	**116+**	Wholly non-marine, characterized by banded and mottled arkosic sandstones and siltstones. Composed of mixed alluvial fan and fluvial deposits. Basal contact marked at top of highest marine unit.
PENNSYLVANIAN	Hermosa Group	Honaker Trail Formation	Phl	**195-700+**	Fossiliferous gray limestone, dolomite, and minor gray-green/maroon calcareous shale. Upper part of the unit contains interbedded arkosic sandstone, siltstone, and fossiliferous limestone.
		Paradox Formation	Php	**1,219+** (depositional) **3,000+** (diapirs)	Consists of drab gray gypsum with minor beds of black shale, sandstone, and limestone. Typically weathers to low, rounded hills and mounds, but forms high hills near the southeastern end of Gypsum Valley.

Figure 5.2 Stratigraphic column of units in the Klondike Ridge study area showing colors, thickness variations, and general characteristics (after Vogel, 1960; Cater, 1970).

unit has been classified as the upper Honaker Trail Formation. Utilizing the definition published by DuChene and others (2009), the top of the Honaker Trail Formation is defined at the top of the last limestone bed. In the field, this limestone bed is often overlain by purple sandstone, signifying a transition into the wholly terrestrial, arkosic Cutler Formation. In order to establish a definitive contact, fossil assemblages (e.g., Virgilian fusulinids) would need to be dated to determine the location of the Pennsylvanian-Permian boundary.

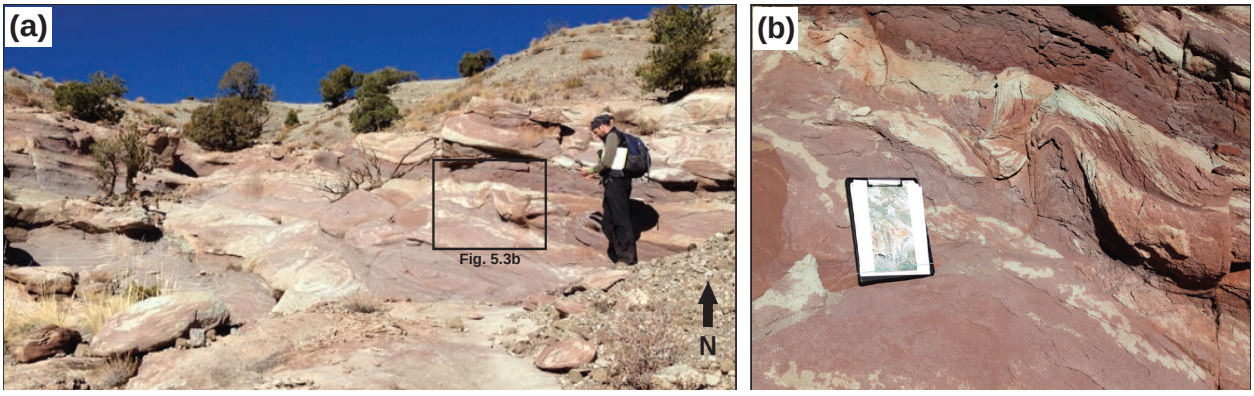

Figure 5.3 (a) View of unusual arkosic sandstone interbedded with marine limestone beds within the upper Honaker Trail Formation; (b) Close-up of contorted nature of these arkosic sandstones.

5.3 Mapping Results

Field mapping was vital to understanding the structural complexity within Klondike Ridge and the Gypsum Valley termination as a whole. Structural and stratigraphic data were collected and compiled into a comprehensive geologic map (Figure 5.5). In addition to these field measurements, key publications (Vogel, 1960) and aerial imagery allowed for greater data coverage than was achievable in the field.

Unlike the Castle Valley salt wall, the Gypsum Valley salt wall displays much greater structural complexity. Several large faults (shown in Figure 5.4b on a smaller field scale) dissect the Klondike Ridge area, juxtaposing Jurassic-age formations against Pennsylvanian and Permian units. The central portion of Klondike Ridge, which is structurally similar to a graben, lies lower than the surrounding stratigraphy, providing exceptional views of the halokinetic sequences present in the footwall blocks of both faults. To the west, the megaflap described by Deatrick and others (2014) exhibits vertical to sub-vertical bedding within the Paradox and Honaker Trail Formations (Figure 5.6). The beds in the Honaker Trail Formation are sub-parallel to the underlying salt wall, justifying the classification of this feature as a megaflap. These vertical dips quickly decrease to the south, resulting in the anomalously thick Honaker Trail Formation. It is highly likely that the Permian Cutler Formation exhibits similar thickening (as is seen throughout the basin and in the subsurface), but only a thin section is observed here beneath the overlying unconformable Summerville Formation.

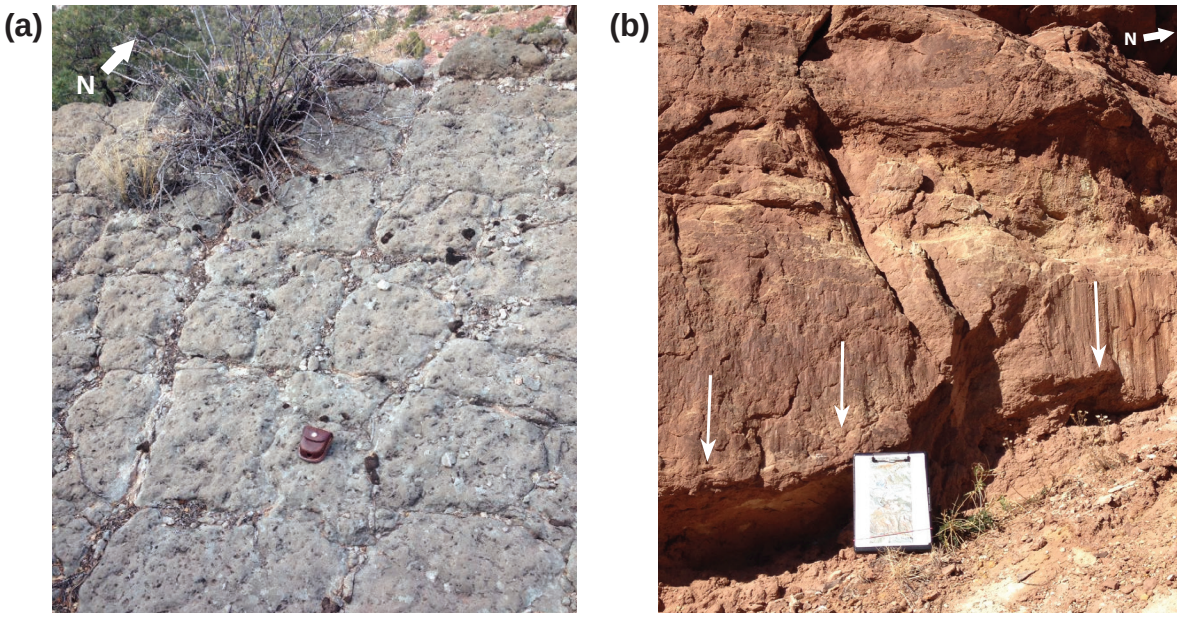

Figure 5.4 (a) Example of one of the uppermost limestone beds interbedded with arkosic sandstone within the upper Honaker Trail; (b) Slickenlines on a near vertical fault plane within the Jurassic Salt Wash Member, reflecting the large-scale faulting present at Klondike Ridge.

To the east of the Klondike Ridge graben, the Klondike Amphitheater (Figure 5.7) boasts a textbook example of growth sequences within the strata. These growth sequences correspond to the rotation and variable accommodation during salt growth, allowing for relative timing of the diapirism of the Gypsum Valley salt wall and its termination to be established. The Amphitheater also displays a gently dipping Summerville Formation blanketing these growth packages, illustrating the end of significant salt growth prior to end of Morrison Formation deposition. It has been proposed that the Jurassic Morrison Formation was the first to fully cover the diapir (Trudgill, 2011), and this hypothesis is seemingly confirmed in the Klondike Amphitheater.

5.4 Modeling Results

The model of Klondike Ridge constructed in 3D Move yielded intriguing and encouraging results. This process allowed for better visualization and interpretation of the subsurface, and revealed a great deal about the structural framework that characterizes this area. While seismic data would further resolve the structural and stratigraphic complexity at Klondike Ridge, regional well data provided a reasonable control for the formations at depth. This enabled more accurate thickness estimates and determination of stratigraphic relationships as it

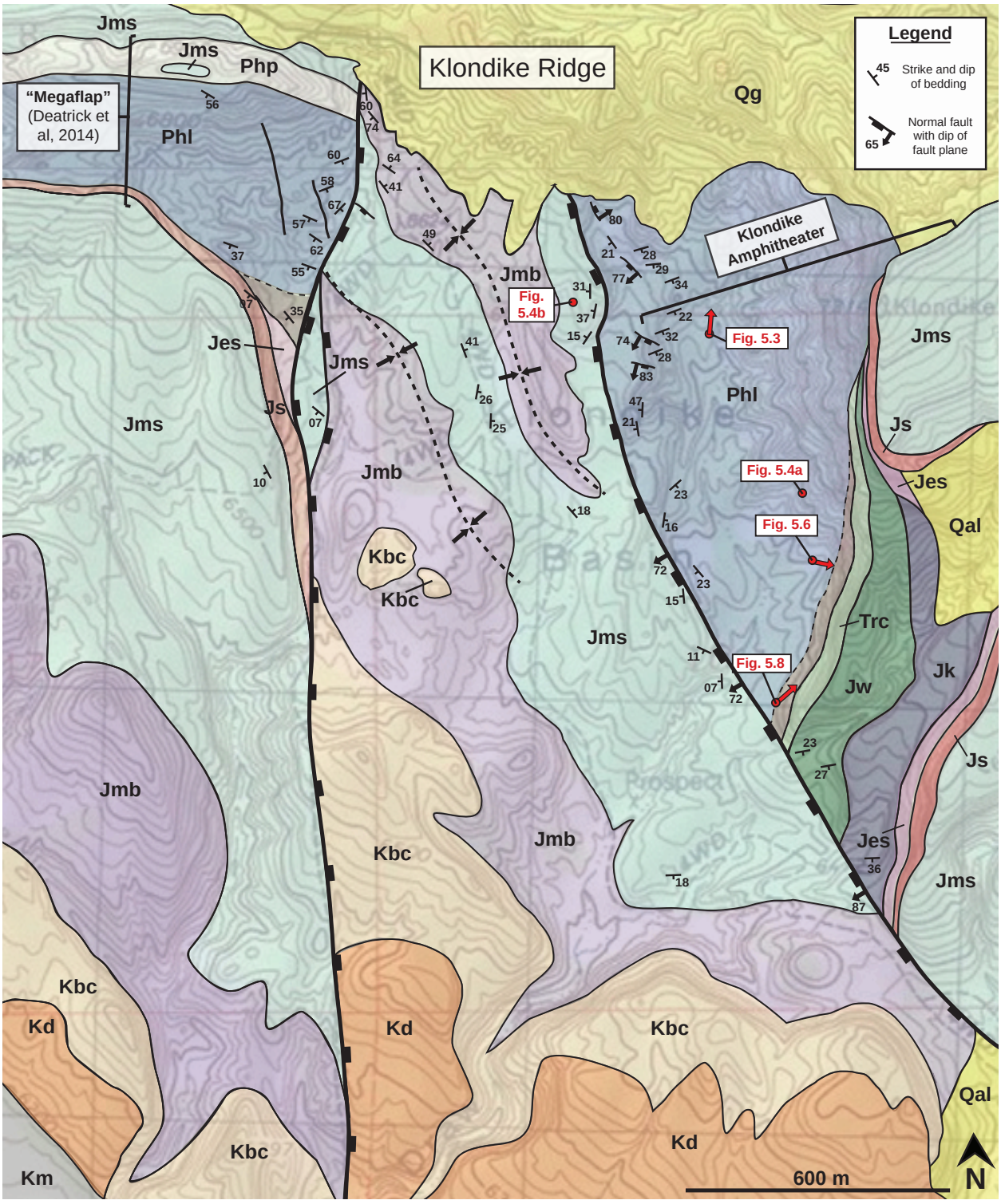

Figure 5.5 Geologic map of the Gypsum Valley salt wall termination (revised from Vogel, 1960). Geologic units correspond to those described in Figure 5.2. Locations of Figures 5.3, 5.4 a-b, 5.6, and 5.8 are designated on the map, and an explanation of symbols is provided.

constrained the base of the model, which previously has not been interpreted in this area.

Structurally, the Klondike Ridge area is characterized by two major faults that strike approximately north-south and bound the central, low-lying area at Klondike Ridge (Figure 5.7). These are mappable at the surface (Figure 5.5), but the 3D model suggests that these faults likely penetrate all strata lying atop the salt, as salt frequently acts as a detachment surface along the flanks and terminations of the salt walls in the basin. As shown on the geologic map (Figure 5.5), the magnitude of throw on these faults decreases considerably from north to south. In the northern part of Klondike Ridge, the Jurassic Salt Wash Member is juxtaposed against the Pennsylvanian Honaker Trail Formation. In the southern portion of the field area, units in the Jurassic Morisson Formation are faulted against lower Cretaceous units, suggesting a much smaller amount of throw on the faults. This interesting field pattern may suggest that the down-dropped block present in the center of Klondike Ridge is not a classic graben but instead a pivoting hangingwall block, where throw increases towards the north (and towards the salt wall). Figure 5.6 shows that the central block also decreases in width towards the north, which is also reflected in the subsurface. Folding within this hangingwall block as well as synthetic faulting adjacent to the western bounding fault appear to have formed as a result of decreased structural accommodation for the downthrown block to the north. This folding and faulting is present at the surface and diminishes to the south. Furthermore, it is likely that units thicken to the north within this hangingwall block. It is interpreted that the major faults at Klondike Ridge do not represent a discrete faulting event, but instead continuous growth or accommodation faulting. The throw on the faults was greater to the north, resulting in increased accommodation. However, since the faults converge gradually to the north, the decreased width of the faulted area resulted in the faulting and folding observed at the surface and within the subsurface.

Another important implication of this model is the resolution of the behavior of halokinetic features within Klondike Ridge. Prior to this modeling, the megaflap that lies west of the western bounding fault appeared to be an anomaly, seemingly terminating abruptly against the western fault. However, it appears that the megaflap is likely related to the Klondike Amphi-

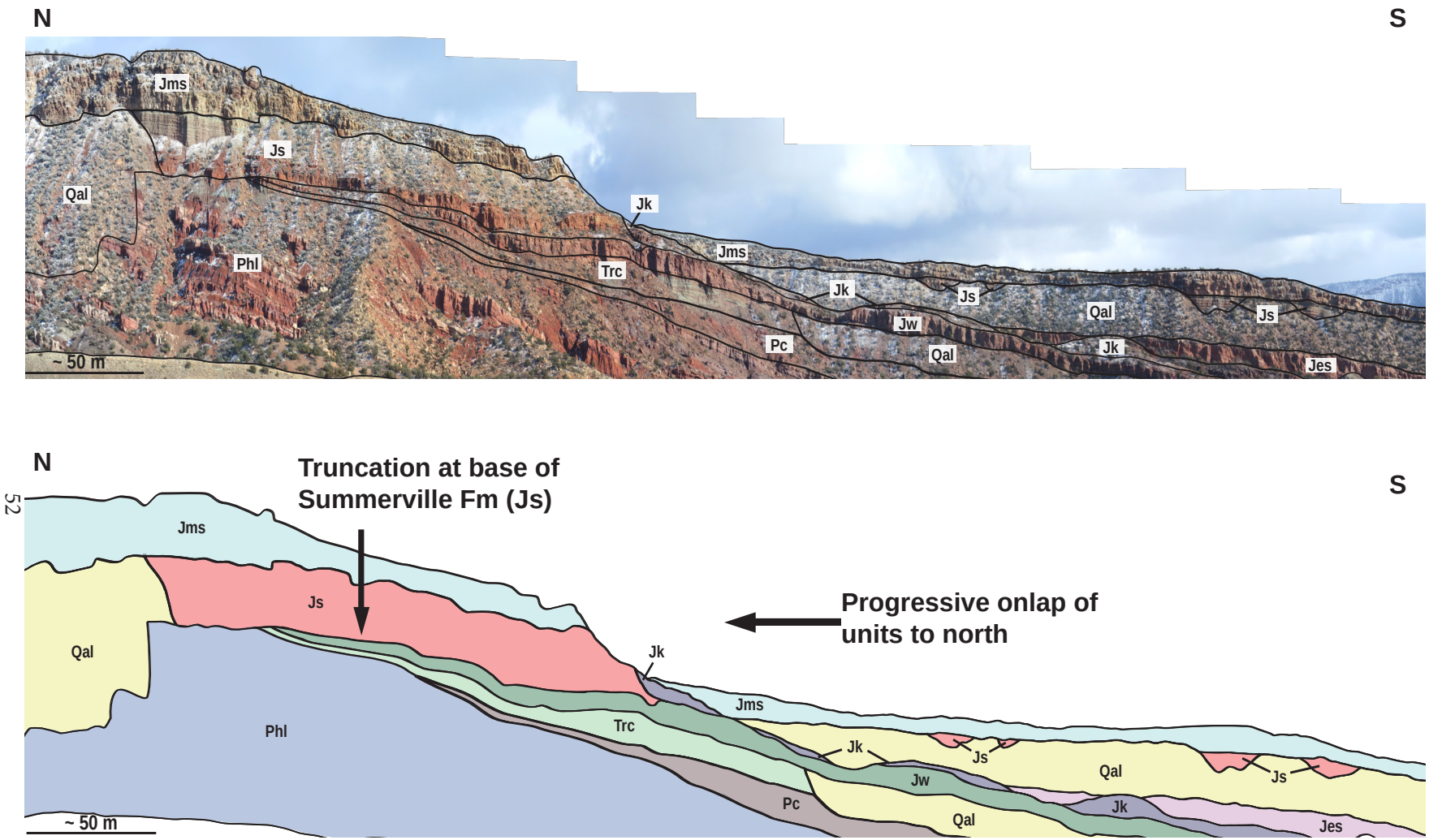

Figure 5.6 View to east of Klondike Amphitheater, showing stratigraphic thickening of Pennsylvanian through Middle Jurassic (Phl - Jes) units away from the Gypsum Valley salt wall.

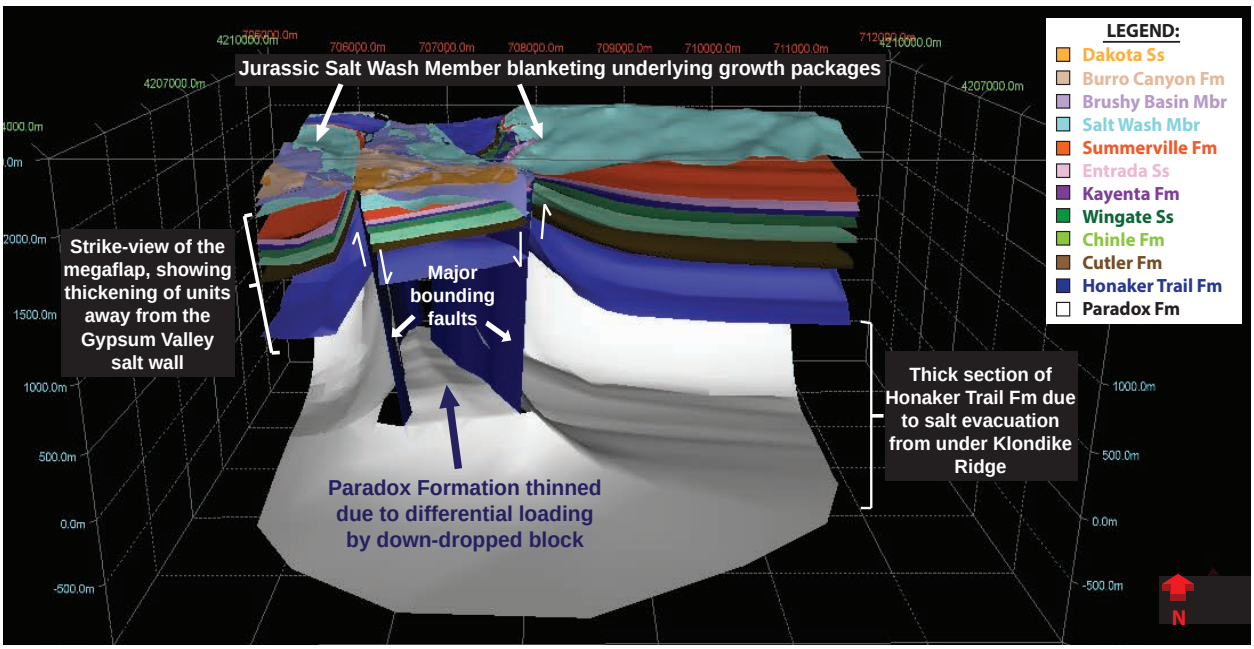

Figure 5.7 Overview of 3D model for Klondike Ridge, illustrating structural and stratigraphic relationships present at the surface and in the subsurface. Although constrained by field and regional well data, this model is presented as a schematic representation of the area.

theater structure that lies east of the eastern fault (Figure 5.6). While it is unclear if the Klondike Amphitheater exhibits the exact geometries observed in the megaflap, it is evident that the megaflap and Klondike Amphitheater illustrate the response of the strata to the formation and continued growth of the Gypsum Valley salt wall. Observations of the Klondike Ridge and southeastern Gypsum Valley in conjunction with the near vertical behavior of the salt in seismic data northeast of Klondike Ridge (Thomas Hearon, personal communication) lead to the interpretation of a preexisting structural feature east of the southeast termination of Gypsum Valley. This structure, which is likely a large fault or fault array, acted as a buttress to lateral salt flow, resulting in the flow of salt to the southeast beneath Klondike Ridge. The overlying strata reflect the presence of this salt feature, both in the megaflap and Klondike Amphitheater but also in the younger strata blanketing these growth sequences. Figure 5.8 illustrates the continuation of this interpreted trend from the megaflap to the Klondike Amphitheater, suggesting that the Klondike Ridge faulted structure represents the zone of failure in this trend. The faulting of Klondike Ridge likely would have displaced even more salt into the footwall blocks, perhaps contributing to the

considerable halokinetic relationships observed in the strata in the megaflap and Klondike Amphitheater.

As was detailed in Chapter 3, this 3D model was constructed from a number of 2D sections throughout the area, which not only allowed for better constraint of the interpretations but also enabled more careful interpretation of the subsurface. Stratigraphic and structural relationships to the salt were better resolved in the 3D model (Figure 5.9a) and allowed for the recognition of a potential petroleum trap (Figure 5.9b). This trap, located in the northern, folded portion of the down-dropped fault block, consists of thickened Pennsylvanian and Permian units as a result of growth faulting. The trap is sealed on three sides by major faults and salt, and the slightly higher elevation of the folded region would prevent hydrocarbon migration to the south. However, since seismic surveys in and around the Gypsum Valley termination were not accessible for this study, it is important to recognize that these models, although constrained by field and regional well data, are schematic in nature. The future addition of seismic interpretation would greatly increase the accuracy of the model and its usefulness in petroleum exploration. Figures 5.8 and 5.9 show several displays of the model, illustrating the subsurface trends present throughout the Klondike Ridge area. Interpretations of the 2D sections utilized in this model may be located in Appendix B and provide greater insight into the 3D interpretations in Figure 5.8 and 5.9.

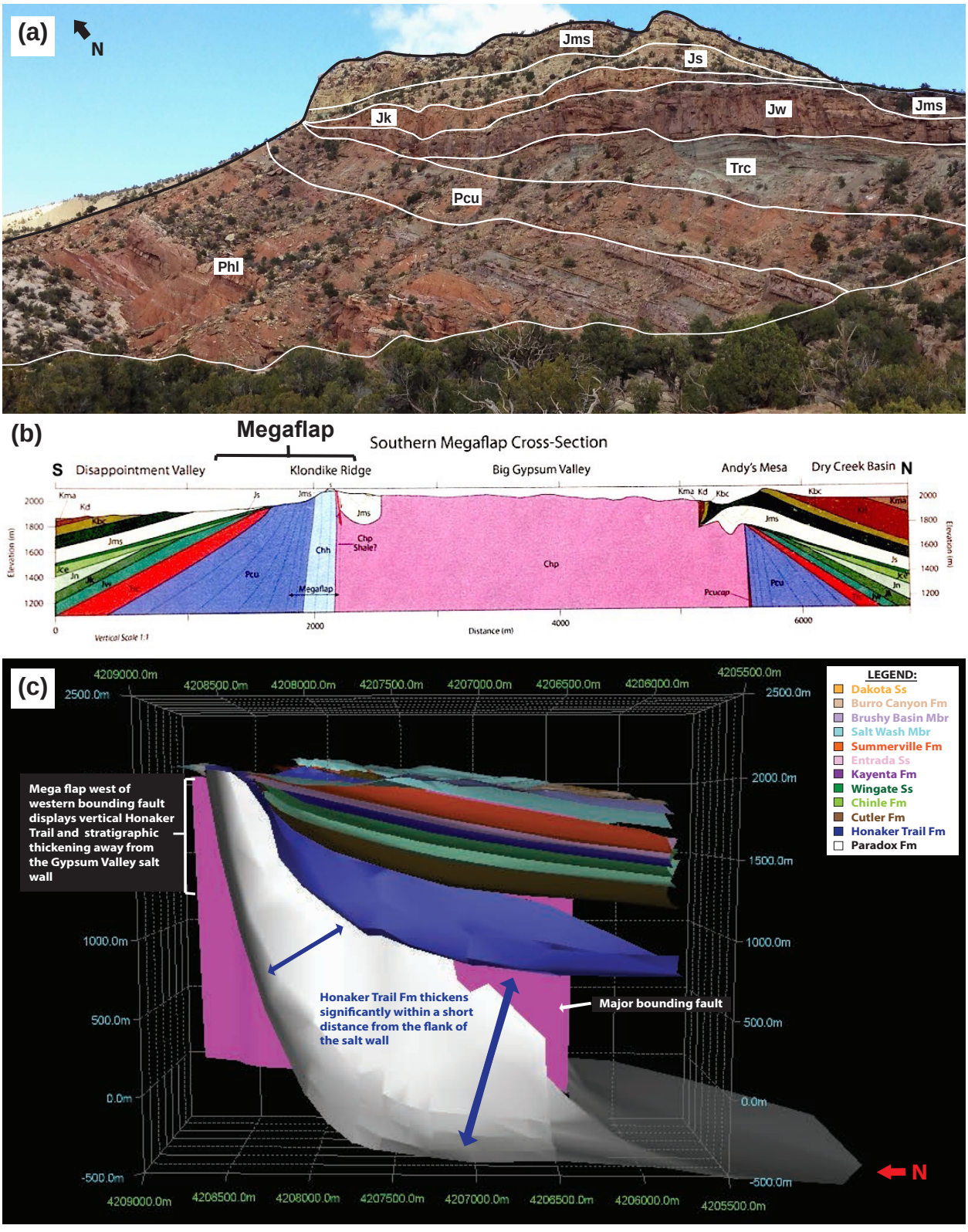

Figure 5.8 (a) View of Klondike Amphitheater from the south, showing the thickened stratigraphic units flanking the Gypsum Valley salt wall; (b) Megaflap interpretation by Deatrick and others (2014); (c) View of megaflap located west of the western bounding fault, showing similar thickening patterns to those seen in the Klondike Amphitheater.

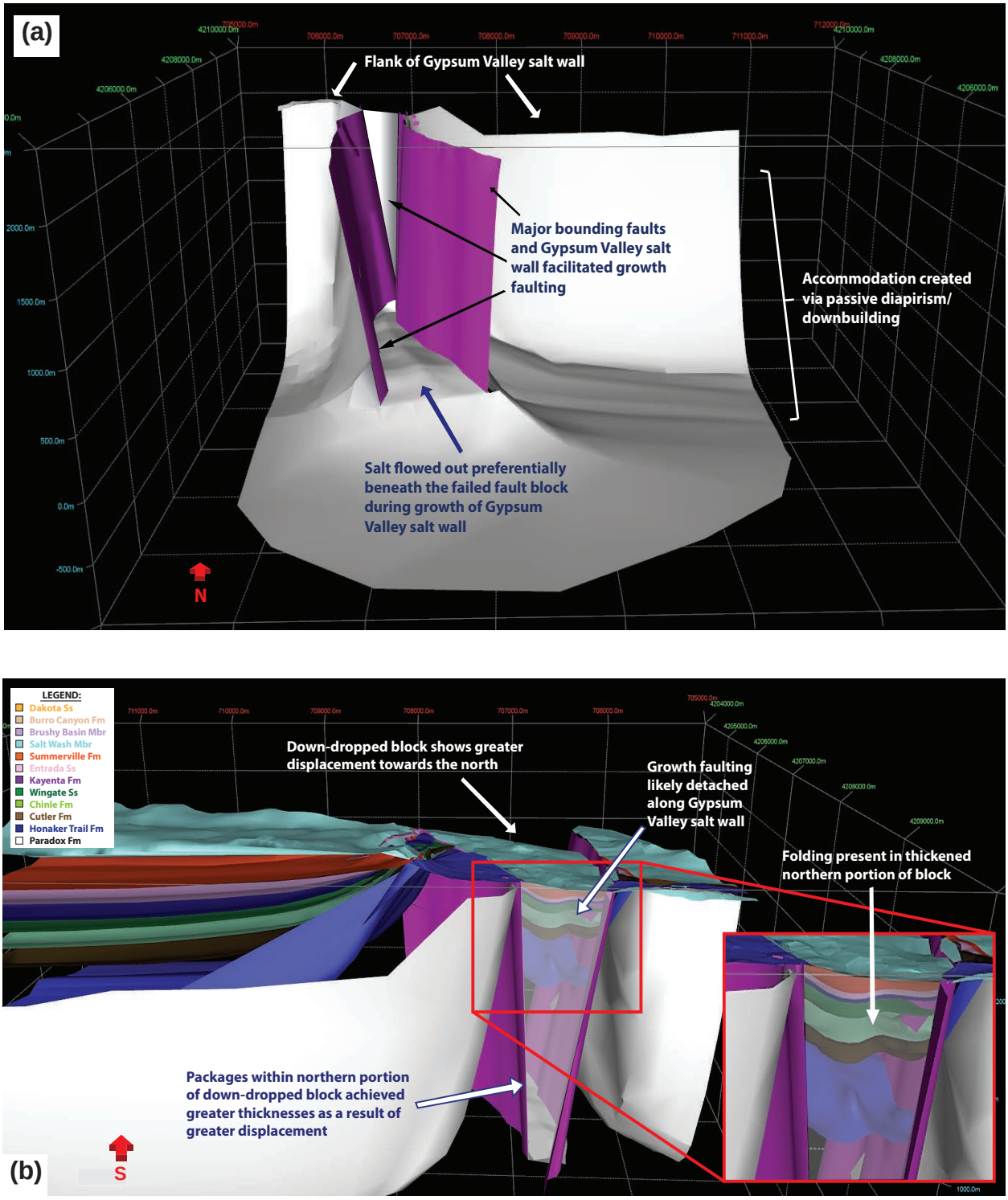

Figure 5.9 (a) 3D model showing only the Paradox salt and major bounding faults to illustrate interpreted behavior of the salt and its relation to faulting at Klondike Ridge; (b) View from north of proposed trap, showing growth within pivoted fault block. This down-dropped block is bounded by faults to the east and west and the Gypsum Valley salt wall to the north.

CHAPTER 6

DISCUSSION

6.1 Overview of Stratigraphic Trends

As has been detailed in the preceding sections, the Castle Valley salt wall termination is a complex and irregular geologic setting. Stratigraphically, it is defined by the presence of the thick White Rim Sandstone perched atop the salt wall termination. The prominent eolian sandstone pinches out to the southeast, and is absent on the northeastern flank of the salt wall. The 3D model proposed for this area reveals that the White Rim Sandstone is reflective of the unusual stratigraphic and structural geometries present in the subsurface.

6.1.1 The White Rim Sandstone at Castle Valley and Future Petroleum Exploration

Several factors were likely responsible for the anomalous deposition of the White Rim Sandstone. The unusual morphology of the underlying salt provided a irregular surface on which the younger stratigraphy was deposited. The irregular geometry of the underlying Paradox salt

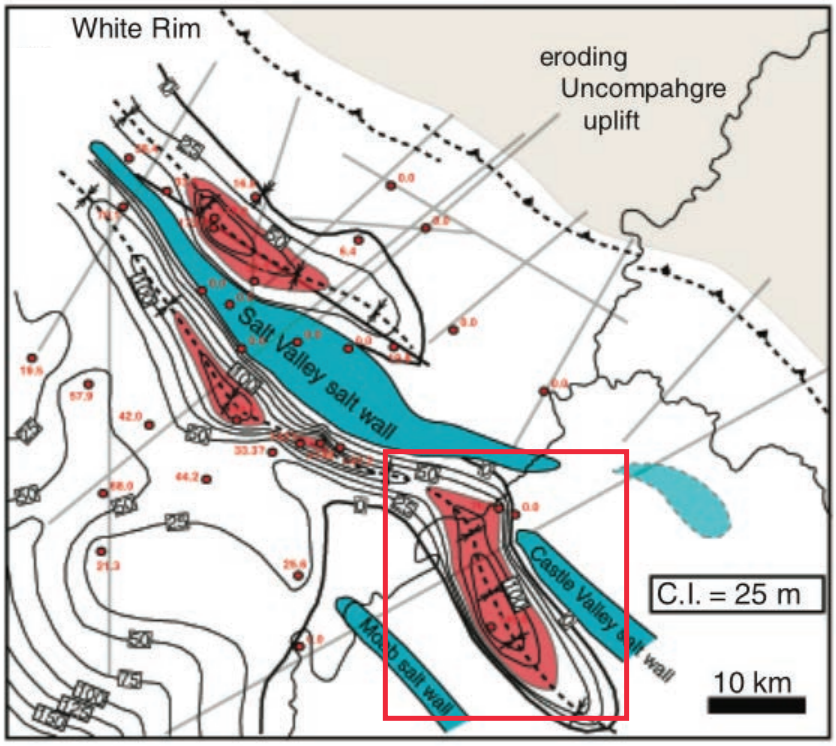

Figure 6.1 Isopach and paleogeographic map for Permian White Rim Sandstone deposition. Note thick depocenter to the west-southwest of the Castle Valley salt wall termination, highlighted within the red rectangle (Trudgill, 2011).

resulted from the asymmetry of the salt wall (steeper on the southern flank) as well as Precambrian faults present in the area. The depocenters present during White Rim deposition reflected this abnormal paleotopography (Figure 6.1). Additionally, the paleocurrent directions proposed by Peterson (1988) and the salt isopach thicknesses detailed by Trudgill (2011) suggest that the White Rim Sandstone was deposited on the southwestern flank of the salt wall termination via north-northwesterly winds. This was likely due to a combination of increased accommodation and deflection of eolian flow by the rising salt structure. The deposition of the White Rim Sandstone fueled the evacuation of the underlying salt, causing further salt wall growth and increased accommodation. This positive feedback cycle may also be represented in the Professor Valley outcrop, although on a smaller scale than Castle Valley. The evolution of the Paradox salt directly influenced the distribution and thickness of the White Rim Sandstone (and the Paleozoic units as a whole), suggesting that similar forces may have had similar results elsewhere in the basin. This has important implications for exploration of the White Rim Sandstone as a potential petroleum reservoir. At Castle Valley, surface exposure of the White Rim Sandstone on its southern flank

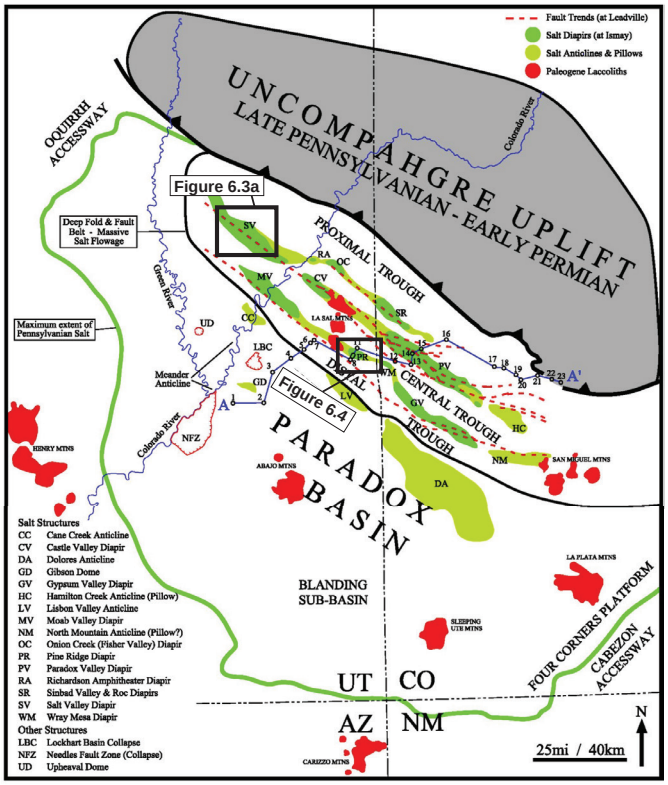

Figure 6.2 Reference map for Figures 6.3 and 6.4, with the locations of the Salt Valley (SV) salt wall and Pine Ridge (PR) diapir highlighted (Rasmussen, 2014).

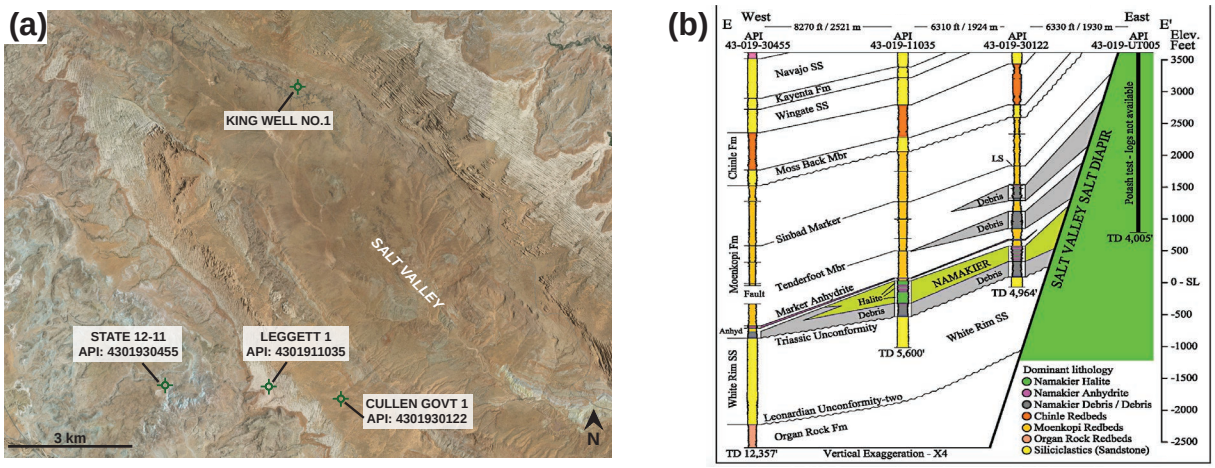

Figure 6.3 (a) Aerial photo of Salt Valley, showing the location of the wells in Figure 6.3b; (b) Cross-section of the southwestern flank of the Salt Valley salt wall, showing a thick White Rim Sandstone section. The "King Well No. 1" drilled on the northeastern flank of the salt wall did not encounter any White Rim Sandstone in the subsurface (Rasmussen, 2014).

and the absence of the eolian unit on the northern flank (verified by well data) make it an improbable hydrocarbon reservoir in the subsurface. However, well data have revealed similar trends of the White Rim Sandstone along other salt walls in the region, and these deposits are primarily located in the subsurface. The Salt Valley salt wall and the Pine Ridge salt diapir (Figure 6.2) exhibit an asymmetric distribution of the White Rim Sandstone, with noticeably thicker sections of the eolian sandstone on the southwestern flank of each structure (Figures 6.3 and 6.4; Rasmussen, 2014). It is important to note that the cross-sections in Figures 6.3 and 6.4 are interpretive: some of the wells may have tops interpreted by Rasmussen (2014).in Figure 6.3 (see Appendix C; well # 4303711300 in Figure 6.4; see Appendix C for well files). However, the remaining wells suggest thickness patterns similar to those interpreted in Figures 6.3b and 6.4b. The recognition of this pattern amongst salt structures in the western portion of the Salt Wall Region is highly significant with regards to exploration of White Rim Sandstone reservoirs. As discussed in Chapter 4, the White Rim Sandstone has the characteristics of a high-quality reservoir and has acted as such in the past. The study of the White Rim Sandstone outcrop atop the Castle Valley salt wall termination revealed an important relationship between the timing of salt wall evolution and the paleocurrent direction for the White Rim Sandstone. The hypothesis that the White Rim Sandstone was deposited and preserved along the southwestern flank of the Castle Valley salt

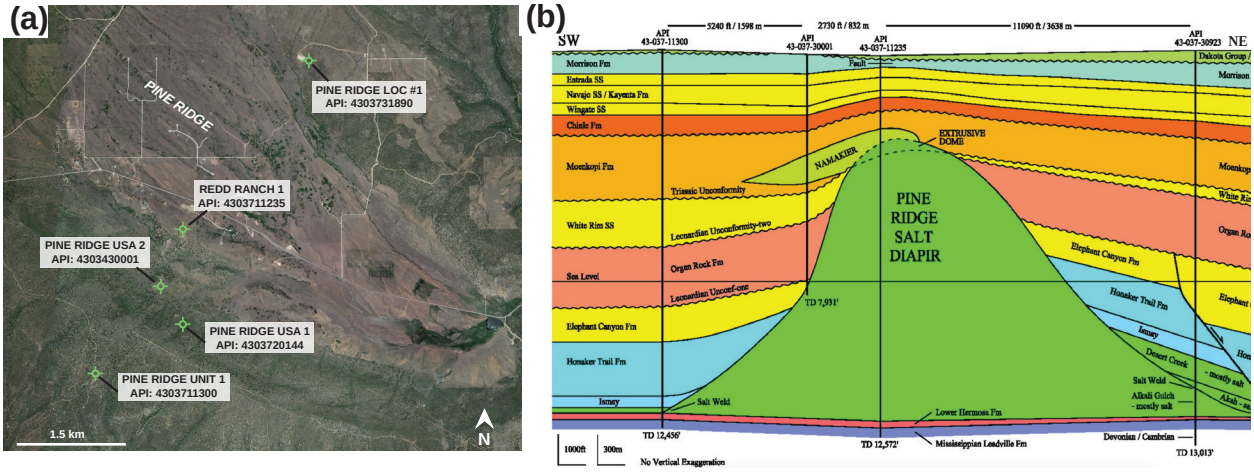

Figure 6.4 (a) Aerial photo of Pine Ridge, showing the location of the wells in Figure 6.4b; (b) Cross-section of the southwestern flank of the Pine Ridge diapir, showing a significantly thicker White Rim Sandstone section on its southwestern flank (Rasmussen, 2014).

termination as a result of this dynamic relationship is seemingly verified by similar patterns seen in the subsurface at Salt Valley and Pine Ridge. To fully constrain the volume of White Rim Sandstone deposits along these structures, additional seismic and well data would need to be consulted. However, in terms of the elements necessary for a petroleum system, the Paradox Formation would act as an excellent lateral seal and source rock for White Rim reservoirs. Furthermore, the prominent shales in the overlying Triassic Moenkopi Formation would provide a necessary top seal to a White Rim reservoir. Therefore, study of paleocurrent directions on a more detailed, field-sized scale as well as further resolution of the timing of salt rise for salt structures in the basin would improve prediction of the location of White Rim Sandstone reservoirs, potentially resulting in renewed petroleum production in the Paradox Basin.

6.1.2 Halokinetic Sequences: the Megaflap and Klondike Amphitheater

The stunning Klondike Amphitheater and megaflap that define the eastern and western extents of Klondike Ridge, respectively, allow a unique view into the subsurface stratigraphy. In salt tectonic regimes where passive diapirism is dominant, the study of halokinetic sequences is essential to understanding the relationship between salt rise and sedimentation (Giles & Rowan, 2012). These halokinetic sequences are frequently identified in seismic, and often are the targets of petroleum exploration. Therefore, the field study and subsurface interpretation of the megaflap

and Klondike Amphitheater provide valuable information with regards to halokinetic sequences in other salt provinces.

Kyle Deatrick, Kate Giles, and others (2014) have extensively studied the megaflap present in Klondike Ridge in an effort to better resolve the stratigraphy flanking the Gypsum Valley salt wall. In the field, steeply-dipping (>80 degrees) to vertical beds within the Paradox caprock and the Honaker Trail Formation can be observed and measured; additionally, the Permian Cutler Group contains steeply dipping beds as well, suggesting that these Paleozoic Formations have been significantly deformed by drape folding adjacent to the salt wall flank.

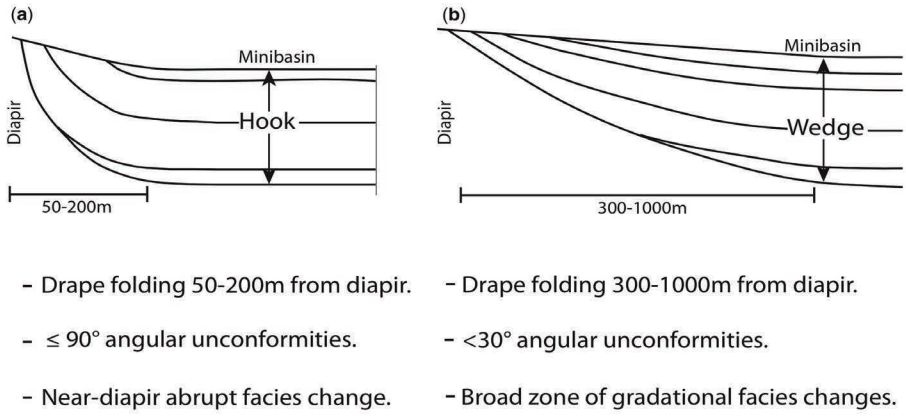

Figure 6.5 End-member types of halokinetic sequences: (a) hook-type halokinetic sequence; (b) wedge-type halokinetic sequence (Giles & Rowan, 2012).

The evacuation and growth of the Gypsum Valley salt wall not only forced existing stratigraphy to its current vertical state but also generated the present halokinetic sequence. Giles and Rowan (2012) detailed two end-member types of halokinetic sequences that form during passive diapirism: hook-type halokinetic sequences and wedge-type halokinetic sequences (Figure 6.5). The 3D model presented in this study shows both end-member types of halokinetic sequences are present within the megaflap (Figure 6.3a). member types of halokinetic sequences are present within the megaflap (Figure 6.6a).

The Klondike Amphitheater is similar to the megaflap in many ways but differs in its orientation and lack of ~vertical bedding close to the salt wall. The Klondike Amphitheater boasts steeply dipping beds that decrease in dip throughout the Permian and Triassic. During

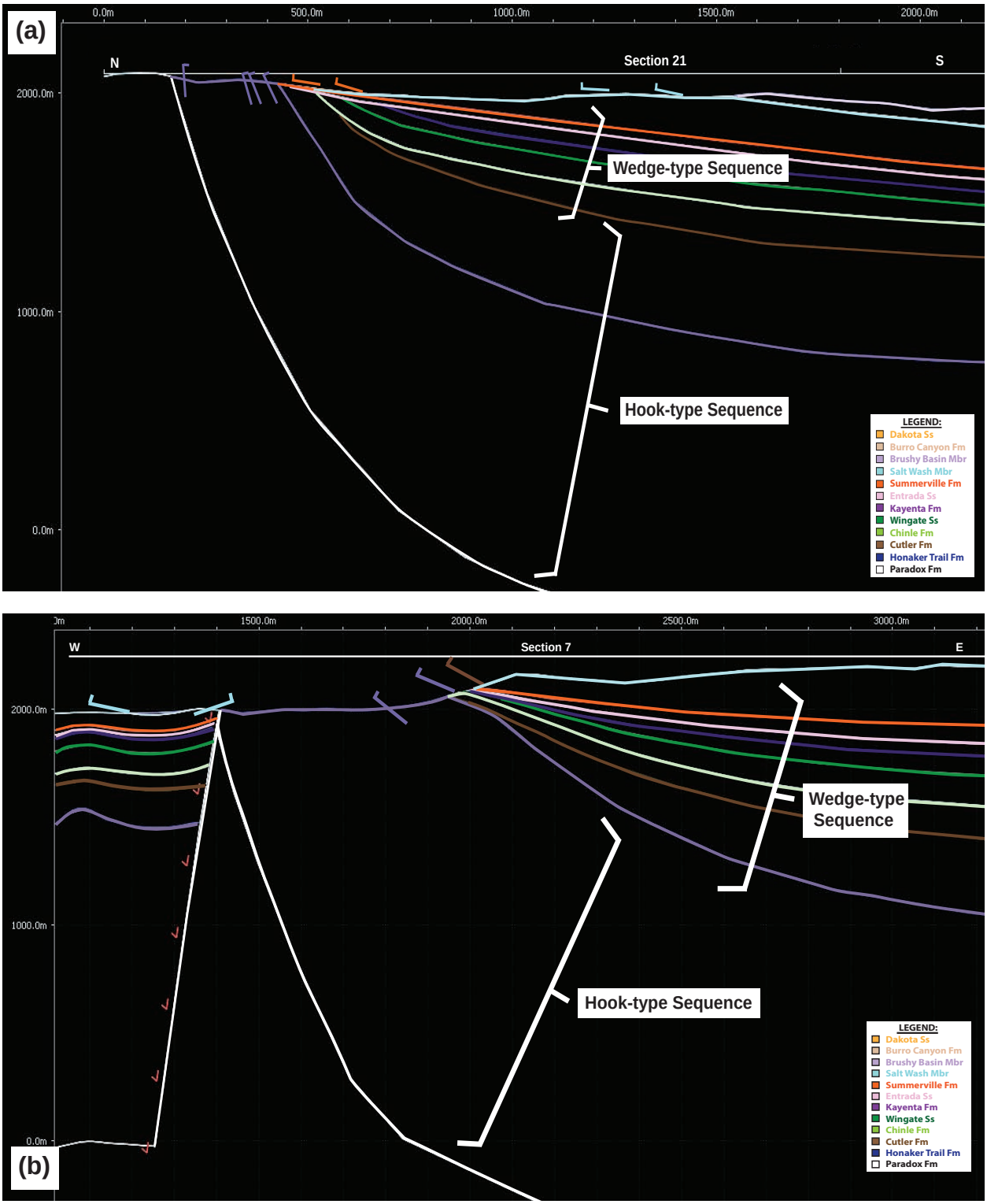

Figure 6.6 (a) 2D section through the megaflap, showing the two end-member types of halokinetic sequences, showing a decreasing rate of salt rise and/or increasing sedimentation with the transition from the hook-type to the wedge-type sequence; (b) 2D section through Klondike Amphitheater, showing a similar transition, although the transition from a hook-type to a wedge-type sequence occurs earlier than in the megaflap.

Jurassic time, the Summerville and Morrison Formations eventually blanketed the Gypsum Valley salt wall and the Amphitheater atop an erosional unconformity. The strike of the megaflap is approximately east-west, whereas the Amphitheater strikes approximately northeast-south-west (Figure 5.6). The Amphitheater similarly consists of both end-member types of halokinetic sequences found in the megaflap (Figure 6.6b), suggesting that the megaflap and Klondike Amphitheater may be related. Additionally, the hook sequence present in the megaflap appears to persist through Cutler Time, longer than is seen in the Amphitheater. The near-diapir abrupt facies changes characteristic of hook sequences is seemingly manifested in the field in the Honaker Trail and Cutler Formations. These facies changes may be an important contributing factor to the difficulty in the stratigraphic correlation of these units. Additionally, the earlier transition to a wedge sequence in the Amphitheater may suggest that the rate of salt rise slowed earlier than in the megaflap. This interpretation is consistent with the notion that salt walls are more constricted at their terminations, whereas salt that is more centrally located would be slightly less restricted

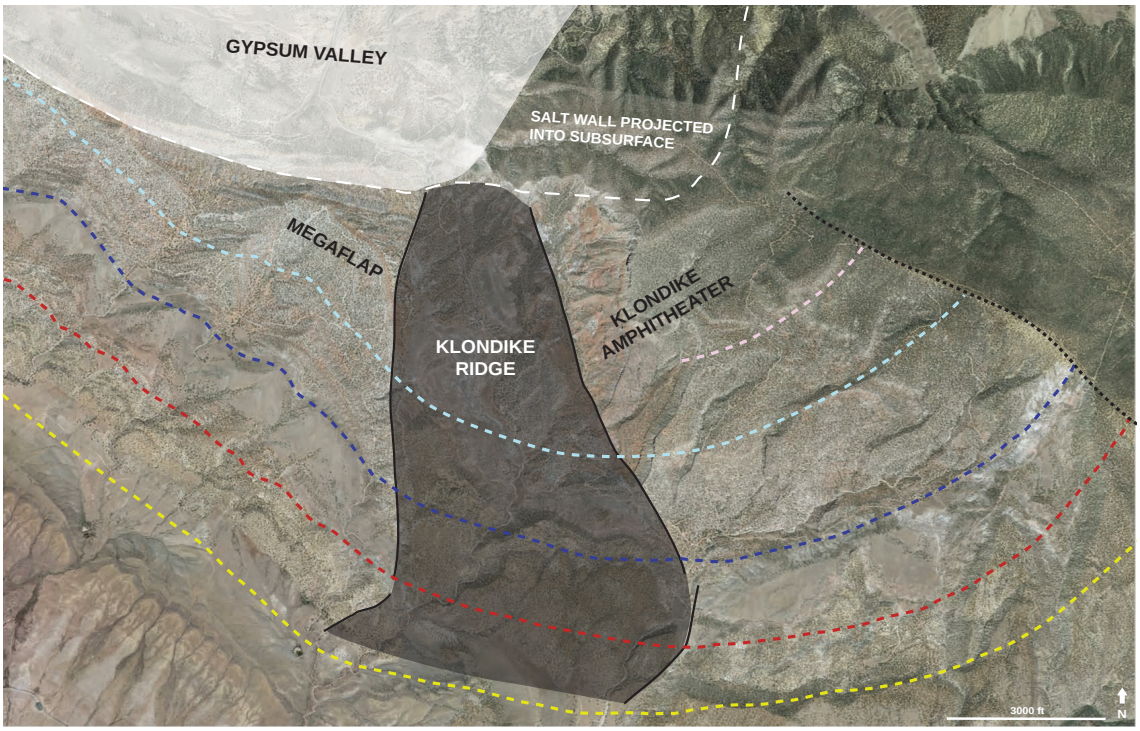

Figure 6.7 Aerial photograph of the Gypsum Valley salt wall termination, with Klondike Ridge obscured. Dashed lines are interpreted trends of changing strike directions of beds, showing the bending of the strata around the nose of the Gypsum Valley salt wall. Klondike Ridge can be interpreted as a zone of failure in which the rigid beds were unable to wrap around the salt wall termination.

during its growth. This may also explain how beds within the Honaker Trail Formation achieved vertical dips in the megaflap but not in the Klondike Amphitheater. The addition of seismic interpretation would allow for better classification of the halokinetic sequences, thereby resolving the timing of growth of the Paradox Formation near and adjacent to the salt wall termination.

The abrupt disappearance of the megaflap at its eastern end has led to confusion regarding the evolution of the Gypsum Valley salt wall. However, study of the Klondike Amphitheater provides further evidence that the Amphitheater is an apparent continuation of the megaflap to the east. 3D modeling of the Klondike Ridge has revealed many similarities between the two structures; additionally, the proposed faulting history at Klondike Ridge may also support the hypothesis that these features are related. Examination of aerial images of the Klondike Ridge and greater Gypsum Valley salt wall termination has revealed intriguing patterns in the stratigraphy (Figure 6.7). It is plausible that the megaflap and Klondike Ridge reflect the vertical and lateral

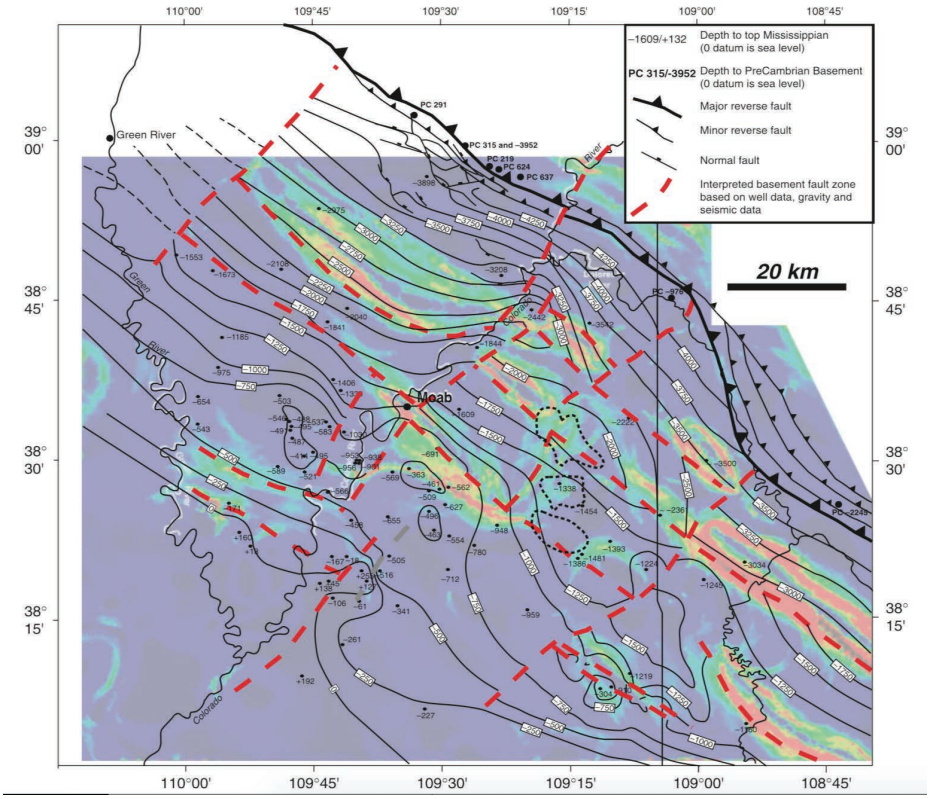

Figure 6.8 Top Mississippian structure map and interpreted basin compartmentalization controlled by basement fault zones. NW-SE-trending Mississippian-level faults, responsible for influencing the location and orientation of the linear salt walls in the Paradox Basin, and NE-SW-trending basement faults, which run sub-parallel to the regional Colorado Lineament, are designated by red dashed lines.

response of the overlying stratigraphy to salt movement; moreover, the change in strike of the beds appears to show the strata "wrapping" around the termination of the Gypsum Valley salt wall. Along this reasoning, the down-dropped block present within Klondike Ridge may represent a zone of failure in which the brittle rocks were unable to mimic the morphology of the salt wall termination. This has significant application to other basins characterized by salt tectonics. The inability of brittle rock to accommodate abnormal geometries of rising salt structures has undoubtedly resulted in failure zones and potential petroleum traps, both within and outside of the Paradox Basin. The interpretation proposed by this study (Figure 5.8) supports this hypothesis, but study of seismic data would be necessary to verify this pattern in the subsurface. Nonetheless, the recognition of these apparent relationships in Klondike Ridge has important implications for resolving salt-sediment relationships as well as petroleum exploration around the terminations of salt structures.

6.2 Overview of Structural Trends

The anomalous trends observed in the Paradox Basin have frequently been attributed to the structural fabric in the Precambrian basement by numerous authors (Kelley & Clinton, 1960; Case, 1966; Case & Joesting, 1973; Hite, 1975; Warner, 1978; Baars et al., 1988; Ross, 1998; Trudgill, 2011). Figure 6.8 illustrates the influence of existing northeast-southwest-trending basement structures on the compartmentalization of the basin (Trudgill, 2011). Utilization of previous publications and existing subsurface geophysical data in conjunction with the models presented here indeed suggest that pre-existing structures were likely a major control in the development and evolution of the Castle Valley and Gypsum Valley salt wall terminations.

6.2.1 Role of Pre-existing Structure

Regarding the Castle Valley salt wall termination, the geometry of the salt and overlying strata strongly infer the presence of a northeast-southwest-trending structure directly northwest of the Castle Valley salt wall. This structure appears to parallel the route of the modern-day Colorado River. In addition to the salt isopach map published by Trudgill (2011) in Figure 4.9, geophysical data published by Case & Joesting (1973) helps resolve some of the Precambrian trends and

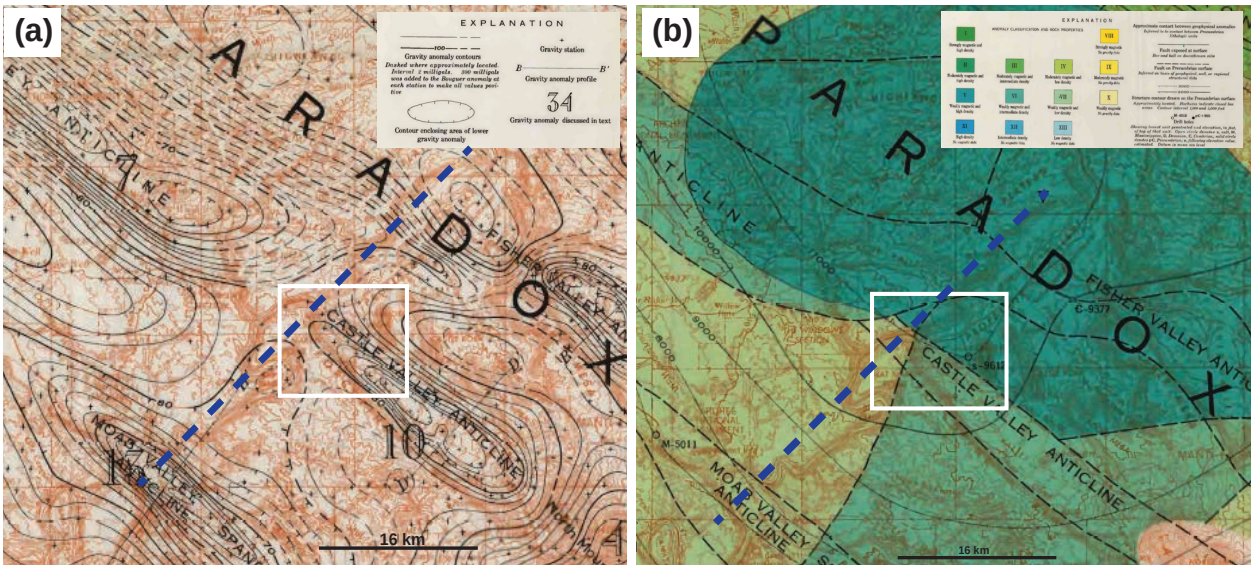

Figure 6.9 (a) Gravity gradient map of the Precambrian basement, with a contour interval of 2 milligals. Note the unusual gravity pattern around the termination of the Castle Valley salt wall highlighted by a blue dashed line; (b) Combined magnetic anomaly and gravity map of the Precambrian basement, showing a similar anomalous pattern at the termination of Castle Valley highlighted by a blue dashed line (Case & Joesting, 1973).

subsurface salt geometries. Figure 6.9 shows an unusual trend present in the basement-level gravity gradient and magnetic anomaly maps at the termination of the Castle Valley salt wall. This may suggest that a structure is present that is causing the unusual patterns observed at the end of Castle Valley, which would further support the idea that a basement structure is controlling the development of the Castle Valley termination. Furthermore, it is unlikely that the original Paradox salt within the Castle Valley salt wall was present west of the Colorado River as a result of this Precambrian structure beneath the present-day Colorado River. Salt flow was buttressed by this structure, impacting the morphology and asymmetric distribution of the rising salt. The structural framework of Castle Valley resulted in unequal accommodation on the flanks of the Castle Valley salt wall termination, with greater accommodation on the southwestern flank. The increased accommodation likely aided the deposition and preservation of the thick White Rim Sandstone, in addition to the factors described in section 6.1.1. The evolving Paradox Formation was close to or at the surface throughout the Paleozoic, and the Castle Valley salt wall was not fully buried until Late Triassic time (Trudgill, 2011). The Castle Valley salt wall likely had an unusual morphology throughout its evolution, and welding at the surface juxtaposed upturned Pennsylvanian and

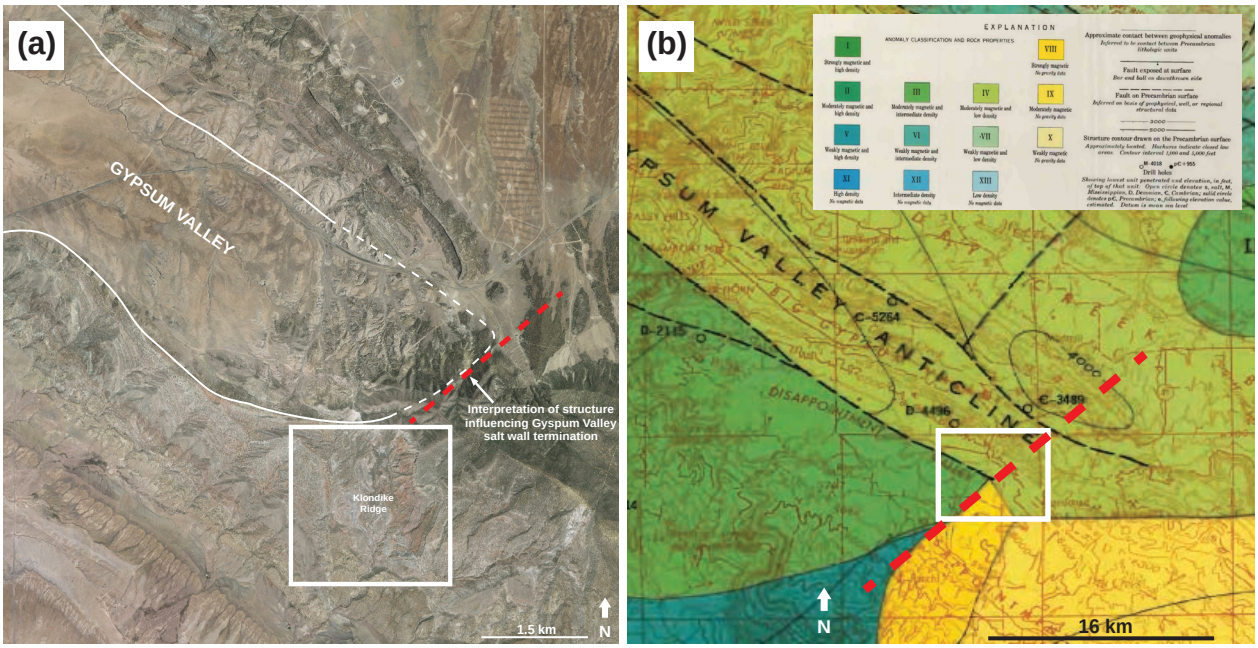

Figure 6.10 (a) Aerial photo of the Gypsum Valley salt wall termination, showing an interpretation of the behavior of the salt in the subsurface and interpreted Precambrian structure (red dashed line); (b) Combined magnetic anomaly and gravity map, showing an unusual pattern at the Gypsum Valley salt wall termination highlighted by a red dashed line (Case & Joesting, 1973).

Permian beds against younger Triassic strata.

Similarly, the Gypsum Valley salt wall termination displays evidence of a Precambrian structural control on its evolution. At the termination of Gypsum Valley, there appears to be an inferred NE-SW trending structure causing the salt wall to have an unusual morphology (Figure 6.10a). Seismic data show a steep 80° dip of the Gypsum Valley salt wall at its termination, suggesting that the salt was buttressed by an existing structure that prevented the lateral flow of salt (Thomas Hearon IV, personal communication). Gravity gradient data are not available over the southeastern termination of Gypsum Valley, but a combined gravity and magnetic anomaly map has been constructed for the area (Figure 6.10b). This trend, although very generalized due to minimal data coverage, does mirror the structural trend interpreted from field and apparent seismic trends. In addition to the subsurface data, the Gypsum Valley salt wall appears to thicken slightly towards its termination. This behavior seems to suggest that this termination is structurally controlled, and a northeast-southwest-trending basement structure would produce the observed features of the Gypsum Valley termination.

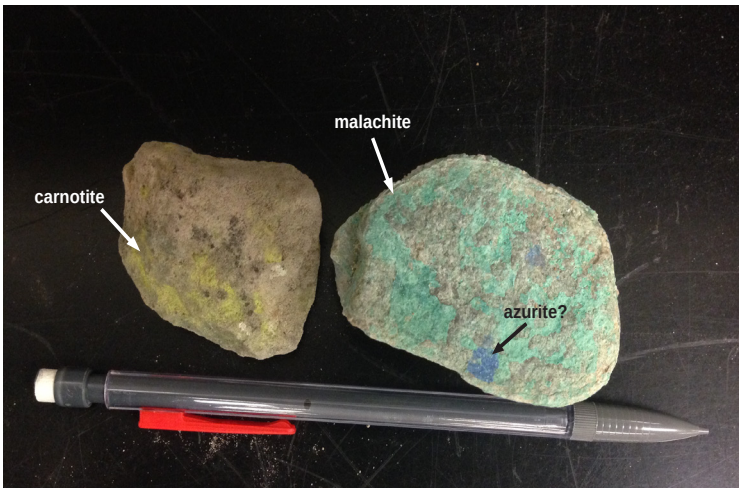

Figure 6.11 Hand samples from mineral ores found in the basal units of the Jurassic Salt Wash

6.2.2 Faulting at Klondike Ridge and the Potential for Hydrocarbon Traps

The extensive faulting observed at Klondike Ridge reveals a complex history of the Gypsum Valley salt wall termination. Although the timing and extent of faulting are not yet fully resolved, the data suggest that faulting along the major bounding faults likely took place continuously throughout the evolution of the Gypsum Valley salt wall. As was proposed in the preceding section, these faults likely developed during the early stages of salt growth. The inability of the rigid rocks to wrap around the evolving salt wall termination may have resulted in failure at the location of Klondike Ridge (Figure 6.7). As the faults at Klondike Ridge developed, salt was evacuated from beneath the pseudo-graben, creating even more accommodation. Faulting continued in order to fill the accommodation created by salt withdrawal, and this process continued throughout the development of Gypsum Valley.

This faulting has generated great interest since the early 20th century, primarily with regards to mineral exploration. Vogel (1960) published an extensive report on the ore deposits found in Klondike Ridge, providing the first detailed geologic map of the area as well as a thorough discussion of the evolution of the Gypsum Valley salt wall. Of particular interest were the uranium-, vanadium-, and manganese-bearing ores found predominantly in the lower part of the Jurassic Salt Wash Member of the Morrison Formation (Figure 6.11). The uranium-bearing ores are all of the carnotite-type, and it is estimated that only 1,000 tons of ore have been shipped

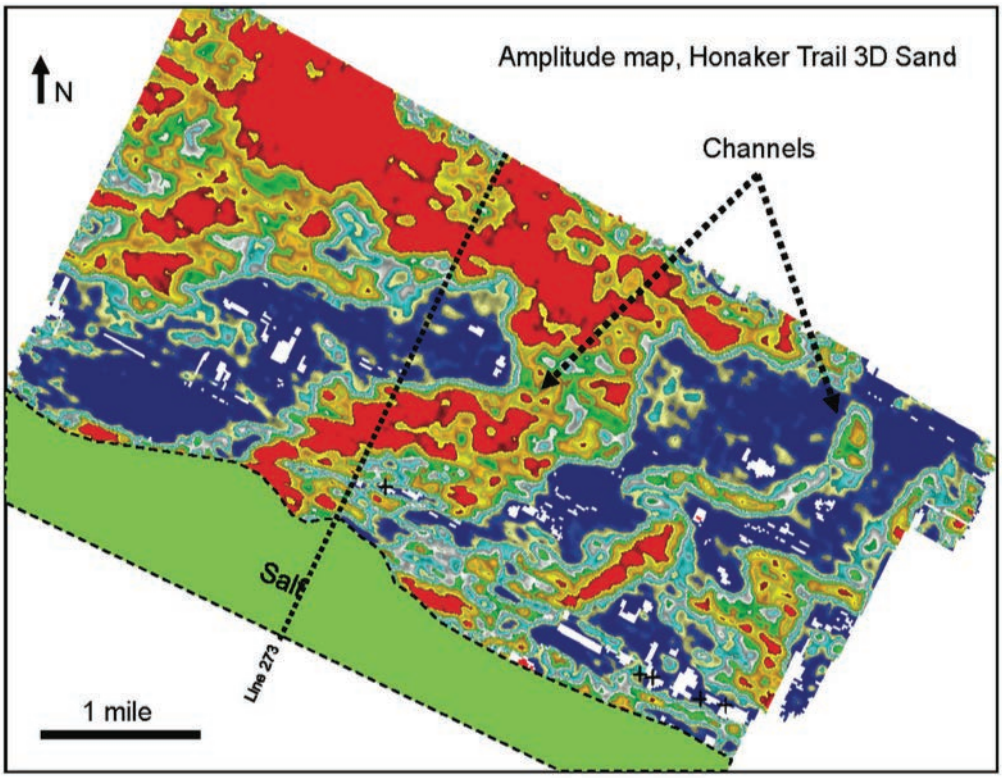

Figure 6.12 Horizon slice amplitude map of the Honaker Trail horizon, showing channelized features in light blue, green, yellow, and red and non-channel ares in dark blue (DuChene et al., 2009).

from the district since 1950. Dating of the carnotite deposits suggests they were deposited in the lower Salt Wash Member around 60-70 million years ago (Vogel, 1960). These uranium deposits are confined to the vicinity of the faults, suggesting a structural control on their deposition. The relatively small mineral/ore deposits found in Klondike Ridge discouraged prospectors shortly thereafter, but interest in these deposits continued due to the association of manganese and copper deposits with carnotite, which is unusual on the Colorado Plateau (Vogel, 1960). Manganese deposits, primarily in the form of pyrolusite, are located in the center of the district and are almost entirely hosted by red beds in the Cutler Formation. Like the carnotite deposits, all deposits are located in or near faults and fractures, suggesting a similar structural control. The copper deposits, in the form of malachite, copper sulfide, and minor jasper, also show the influence of structure and stratigraphy on their formation. Structurally, these deposits are located in and around faults and fractures, as are the other major deposits in Klondike Ridge. Stratigraphically, these deposits are primarily found in the Jurassic Morrison or Summerville Formations, with few

deposits found in red bed units of the Cutler Formation (Vogel, 1960).

The recognition of these ore deposits and their association with faulting and fracturing has implications for petroleum exploration. It is plausible, according to Vogel (1960), that, in addition to groundwater, migrating hydrocarbons may have transported the ore minerals to their current location, suggesting that a petroleum system is or was active in Klondike Ridge. The major bounding faults present in Klondike Ridge allowed for the juxtaposition of younger units against common hydrocarbon sources. At Andy's Mesa Field, located on the northeastern side of the Gypsum Valley salt wall termination (Figure 2.16, the primary producing units are located predominantlywithin the Pennsylvanian Honaker Trail Formation, with lesser production from the Pennsylvanian Paradox Formation and Permian Cutler Formation (DuChene et al., 2009). Gas is trapped within these upturned Pennsylvanian and Permian beds truncated against the Gypsum Valley salt wall. Channelized sandstone (Figure 6.12) and marine limestone within the Honaker Trail Formation are upturned and truncated against salt and faults to form 3-way traps. Depositional environments for the sandstone reservoirs include braided and meandering fluvial with minor delta front, distributary channel, and eolian environments. Reservoirs tend to be under-pressured at Andy's Mesa Field, and average porosities and permeabilities can be as high as 15% and 150 md, respectively (Amador et al., 2009). The most prolific Honaker Trail wells in the Double Eagle Unit in Andy's Mesa Field are located within the up-thrown block adjacent to the west side of a keystone graben within the field (DuChene et al., 2009). The pseudo-graben present in Klondike Ridge may similarly contain a prolific petroleum system. The mega-flap and Klondike Amphitheater exhibit beds that dip away from and are bound by salt and faults. The down-dropped block, containing thickened Pennsylvanian and Permian units, is bound on the east and west by the large bounding faults and to the north by the Gypsum Valley salt wall. The production at Andy's Mesa Field combined with the interpreted subsurface structural and stratigraphic geometries at Klondike Ridge support the hypothesis that Klondike Ridge is a viable target for petroleum exploration and development.

6.3 Incorporation of Results in Petroleum System Assessment

In the preceding sections, the models generated for the Castle Valley and Gypsum Valley salt wall terminations suggest potential for new or renewed petroleum plays. Reservoir quality, trap geometry, and sealing mechanisms were highlighted, utilizing existing subsurface data and information regarding historic production in the Paradox Basin. Another important consideration in this assessment of petroleum systems is the source of hydrocarbons for the proposed traps and reservoirs.

6.3.1 Thermal Maturity Trends in the Paradox Basin

In general, several intervals within the Pennsylvanian Paradox Formation constitute the hydrocarbon sources for the basin. The Ismay and Desert Creek intervals within the Paradox Formation are rich in organic matter, with total organic carbon (TOC) values between 5-15% (Hite, 1970). Nuccio and Condon (1996) published an important study of the burial and thermal history of the key source rock intervals, illustrating regional trends in thermal maturity within the Paradox Basin. They assessed the petroleum potential of two intervals in particular: the Ismay-Desert Creek interval and the Cane Creek cycle of the Middle Pennsylvanian Paradox Formation. Samples from these intervals verified that these horizons contained good to excellent source rocks, with TOC values greater than 0.50% and as high as 11% in some instances (Nuccio & Condon, 1996). With respect to kerogen types, the Cane Creek cycle contains Types I, II, and III, whereas the Ismay-Desert Creek interval contains mostly Types II and III. For both intervals, however, samples from the eastern part of the region are more terrestrial in origin.

Thermal maturity trends in the basin are influenced by structural and burial trends, but generally increase in a southwest to northeast direction according to Nuccio and Condon (1996). To calculate thermal maturity for the basin, they used T_{max}, PI, and R_o values. T_{max} represents the temperature at which the maximum yield of hydrocarbons occurs. PI, or production index, is the ratio of volatile hydrocarbon yield to total hydrocarbon yield, which increases with heating if there is no hydrocarbon migration. R_o, or vitrinite reflectance, is the measure of the proportion of light reflected from a polished vitrinite grain. The amount of reflectance is related to the degree

of metamorphism of the organic-rich sample and therefore is useful as another thermal maturity indicator. Figure 6.14 illustrates these thermal maturity trends in terms of the production indices throughout the basin. For reference, the beginning of oil generation occurs around PI values of 0.08-0.10, and thermal cracking of oil to gas and condensate occurs in the range of 0.40-0.50 (Nuccio & Condon, 1996). Table 6.1 illustrates how Nuccio & Condon (1996) related T_{max}, PI, and R_o to calculate thermal maturity:

Table 6.1 Levels of thermal maturity based on the temperature of maximum hydrocarbon yield, production index, and vitrinite reflectance (Nuccio & Condon, 1996).

	T_{max} °C	PI	R_o (percent)
Immature for oil, biogenic gas	<435	<0.08	<0.60
Mature for oil	435-460	0.08-0.50	0.60-1.35
Overmature for oil-dry gas zone	>460	>0.50	>1.35

Figure 6.13 shows interpreted thermal maturity maps for the Ismay-Desert Creek interval and the Cane Creek cycle. Note the general trend of increasing maturity from southwest to northeast. For the Ismay-Desert Creek interval (Figure 6.13a), the Gypsum Valley salt wall termination appears to be out of the oil window, with values greater than 0.50. The salt structures in the western part of the Salt Wall Region appear to lie within the oil window or in the transition zone between oil

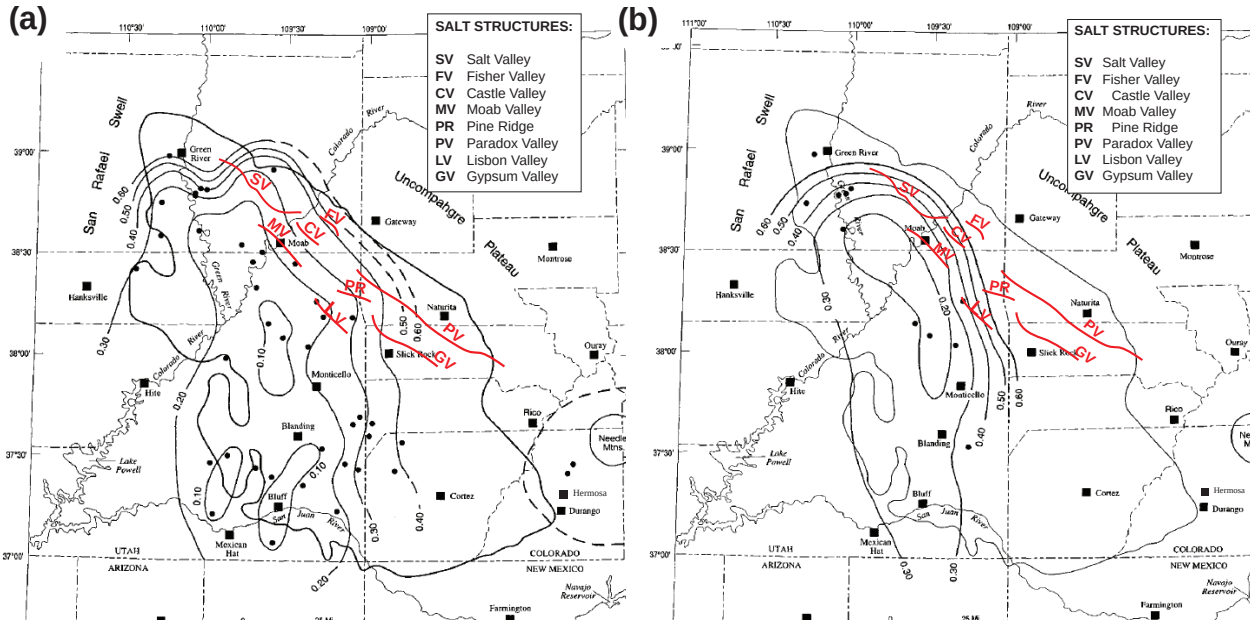

Figure 6.13 Thermal maturity map of the Paradox Basin at the (a) Ismay-Desert Creek Interval, and (b) Cane Creek cycle. Contours are production indices (interval = 0.10) and salt walls are indicated in red (modified from Nuccio & Condon, 1996).

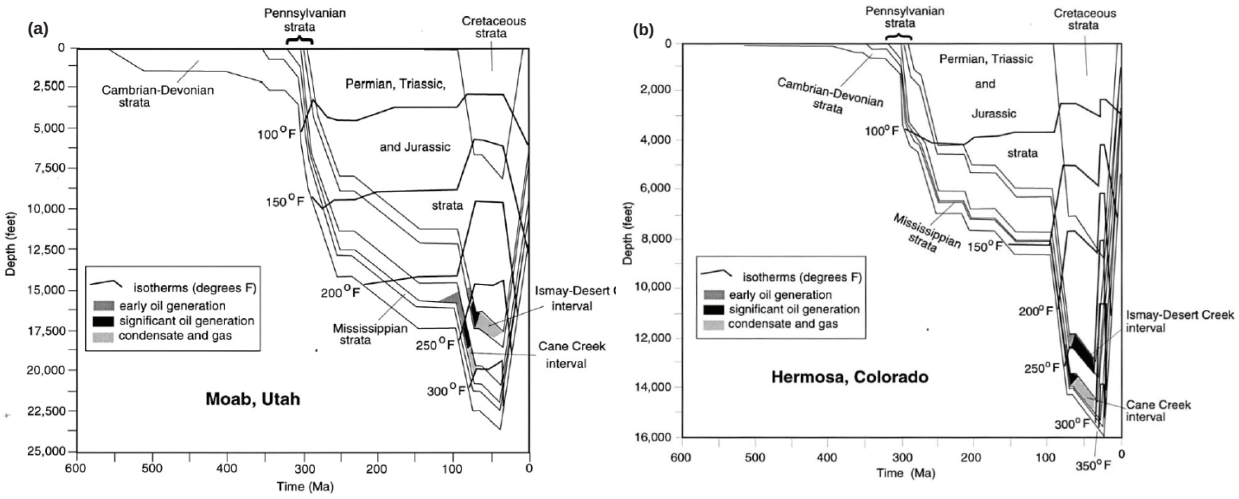

Figure 6.14 Burial, thermal, and petroleum generation model of the (a) Moab, Utah area, and (b) Hermosa, Colorado area. It is likely that gas is still present in reservoirs in areas where hydrocarbons have overmatured (Nuccio & Condon, 1996).

and condensate/gas. For the Cane Creek cycle (Figure 6.14b), Gypsum Valley is well outside of the oil window and likely within the gas window. Castle Valley and the other salt walls in Utah appear to be within the upper oil window or transitioning into the condensate/gas window. Figure 6.14 illustrates burial, thermal, and petroleum generation models for Moab, Utah, and Hermosa, Colorado (see Figure 6.13 for location). These models illustrate the significant differences between the eastern and western parts of the basin. In Colorado, burial depths were considerably shallower, and oil generation for both intervals took place later than in the Moab area. Around Moab, greater burial depths were achieved, and the oil generation window for both intervals occurred earlier than in Colorado and lasted for a shorter amount of time. This indicates that significant differences in burial history can occur over relatively short distances and that field-based models are necessary for an accurate local assessment of thermal maturity.

Study of the thermal history of the source rock intervals in the Paradox Basin is very important when assessing the potential for petroleum production. In general, the oil (and associated gas) produced from the interval within the Honaker Trail to cycle 9 in the Paradox Formation lies within the oil generation window for the Ismay-Desert Creek interval (PI< 0.30-0.40). At Andy's Mesa Field and other fields located in the eastern part of the basin, where

production indices are greater than 0.60, primarily gas is produced (Nuccio & Condon, 1996). Therefore, in assessing the prospectivity of plays near Castle Valley or at Klondike Ridge, it is important to understand what type of petroleum will ultimately be produced in a given location. As the research published by Nuccio & Condon (1996) reveals, the study of thermal maturity and burial history is crucial to understanding the various petroleum systems found in the Paradox Basin.

6.3.2 Similarities to Existing Petroleum Plays

The models produced for this study allow for comparison with other basins characterized by salt tectonics. The importance of studying outcrop and field analogues to understand sub-surface plays is profound; study of structures in the Paradox Basin in particular has allowed for better interpretation of other salt structures around the world (e.g. Gulf of Mexico, North Sea). The research presented in this study may also be helpful in resolving the geology in salt systems, particularly in understanding the evolution of salt structures in three dimensions.

The Gulf of Mexico is one of the most economically significant petroleum basins in the world, exhibiting interesting and complex geology (Figure 6.15). The basin formed during a major rifting episode in the Triassic-Jurassic associated with the opening of the Gulf of Mexico.

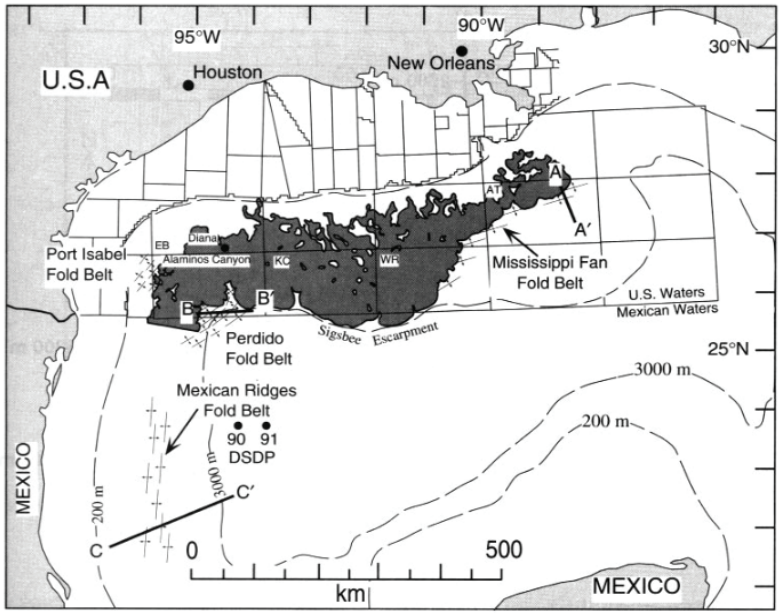

Figure 6.15 Regional map of the Gulf of Mexico, highlighting key regions and the extensive Sigsbee salt canopy in dark gray (Trudgill et al., 1999).

Post-rift subsidence of the crust and restricted waters resulted in the widespread deposition of the Jurassic Louann Salt (Rowan et al., 2003). The Louann salt was overlain in places by the Jurassic Norphlet Formation, which consists of well-sorted eolian sandstone. The Late Jurassic to Early Cretaceous succession consists of predominantly shallow- to deep-water marine carbonates, most notably the Jurassic Smackover Formation (Ajdukiewicz et al., 2010). Extensive siliciclastic sedimentation during the Late Cretaceous to Eocene differentially loaded the autochthonous Louann Salt, leading to the evacuation and diapirism of the salt. Amalgamation of salt diapirs into the extensive Sigsbee canopy has resulted in the present-day configuration of the Gulf of Mexico.

The Jurassic Norphlet Formation has been a successful and ongoing play in the Gulf of Mexico since 1967 (Schmoker & Schenk, 1994). The eolian sandstone was deposited on the Louann Salt in the Middle to Late Jurassic, effectively loading the salt sporadically and creating isolated reservoirs in the subsurface. In the Mobile Bay area, the Norphlet is buried to depths as great as 6,645 m. In terms of porosity, the upper Norphlet, characterized as the "tight zone", is well-cemented and has porosities less than 8%. Beneath the cemented zone lies the main reservoir, where porosities can range from 10-20% and contain less than 1% quartz cement (Ajdukiewicz, 2010). The Norphlet Formation, similar to the White Rim Sandstone at Castle Valley, was deposited on top of mobile salt. The loading of the salt by both of these eolian units resulted in the evacuation of the underlying salt and increased accommodation, facilitating further eolian deposition. Both the Paradox and Louann salt act as lateral seals for the White Rim Sandstone and Norphlet Formation, respectively, and allowed for anomalously thick sections of eolian sandstone to accumulate. While the salt in the Paradox Basin is much more restricted than that of the diapiric Gulf of Mexico salt, the Castle Valley model presented here may have implications for future research of the Norphlet Formation. Further study of paleocurrents and the relationship between the timing of eolian deposition and of salt evolution in the Paradox Basin may reveal new information regarding the Norphlet play. Conversely, study of the Norphlet reservoir could shed light on the nature of the White Rim Sandstone, particularly with regards to porosity, permeability, and diagenetic cementation.

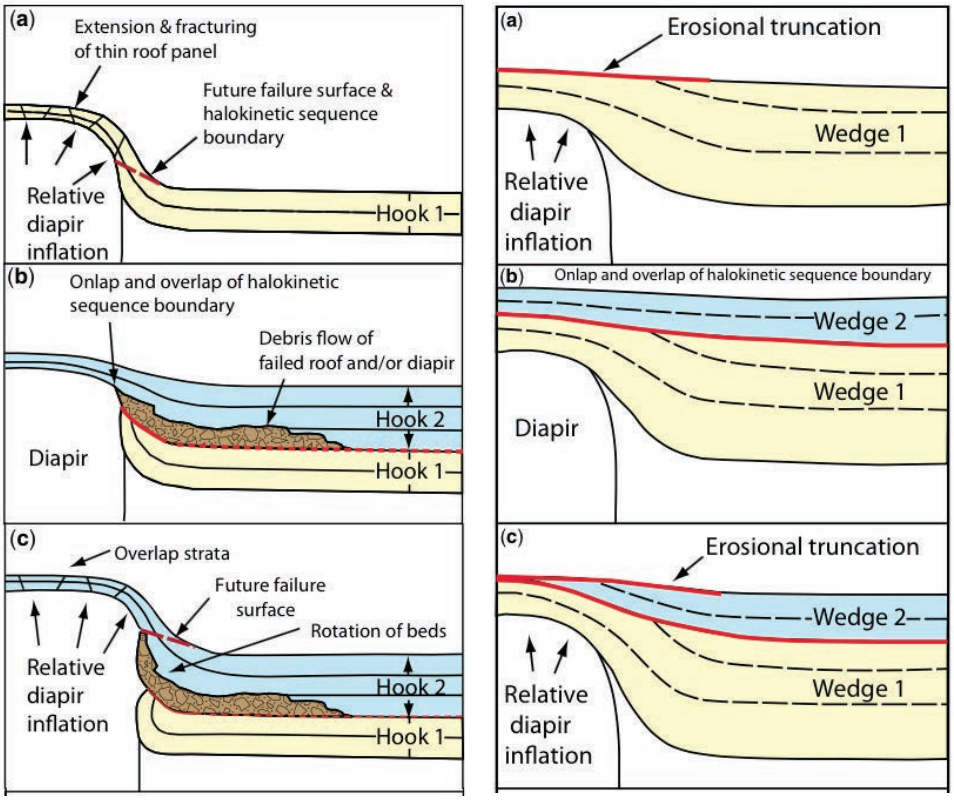

Figure 6.16 Schematic diagram illustrating composite halokinetic sequence end-members: tabular (left panel), comprised of hook sequences, and tapered (right panel), comprised of wedge sequences (Giles & Rowan, 2012).

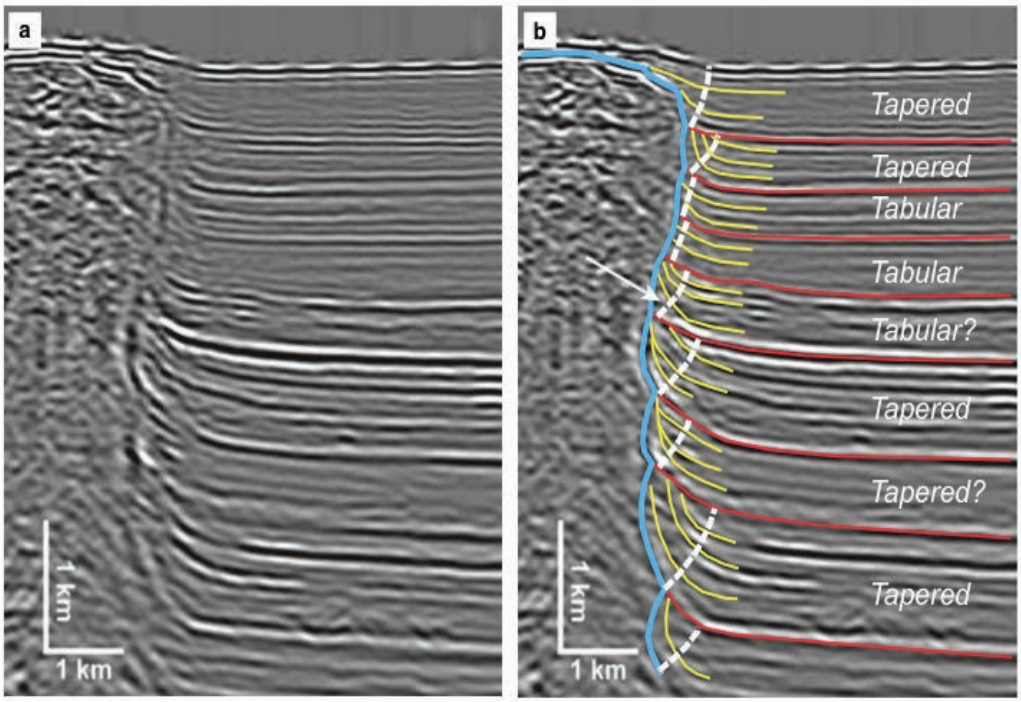

Figure 6.17 Prestack depth-migrated seismic profile from the northern Gulf of Mexico, (a) uninterpreted, and (b) interpreted. Both tabular and tapered composite halokinetic sequences are represented (Giles & Rowan, 2012).

The Gulf of Mexico, in addition to the unique Jurassic Norphlet formation, has incredible examples of near-salt deformation and halokinetic sequences. Giles & Rowan (2012) detail the formation of the two end-member types of halokinetic sequences and the composite sequences they form. Halokinetic sequences have been identified in many places throughout the Gulf of Mexico (Figure 6.17), and in many cases are the focus of petroleum exploration and production. As was discussed in section 6.1.2, halokinetic sequences have previously been interpreted for the megaflap at Gypsum Valley (Deatrick et al., 2014). Furthermore, generalized halokinetic sequences have been interpreted for the megaflap and Klondike Ridge from the model proposed in this study.

examples of near-salt deformation and halokinetic sequences. Giles & Rowan (2012) detail the formation of the two end-member types of halokinetic sequences and the composite sequences they form. Halokinetic sequences have been identified in many places throughout the Gulf of Mexico (Figure 6.17), and in many cases are the focus of petroleum exploration and production. As discussed in section 6.1.2, halokinetic sequences have previously been interpreted for the megaflap at Gypsum Valley (Deatrick et al., 2014). Furthermore, generalized halokinetic sequences have been interpreted for the megaflap and Klondike Ridge from the model proposed in this study. Similarly, the asymmetry observed in salt walls in the Paradox Basin has also been recognized in the Gulf of Mexico (Figure 6.18). The Gypsum Valley and Castle Valley models both exhibit asymmetry of strata on their limbs, both in thickness and in attitude. The Gypsum Valley salt wall

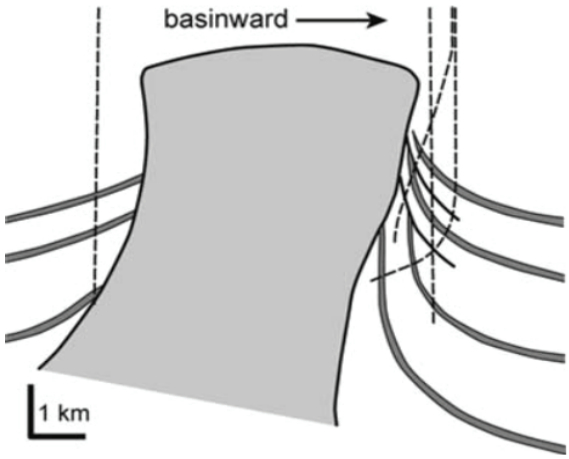

Figure 6.18 Cross-section of a diapir from the Louisiana shelf, northern Gulf of Mexico. Asymmetry and basinward tilt of the diapir is analogous to the Gypsum Valley salt wall, which dips towards the southwest and exhibits steeper strata against its southern limb (Giles & Rowan, 2012).

in particular dips towards the southwest, resulting in more steeply dipping strata on its southern limb, exemplified by the megaflap and Klondike Amphitheater. A significant contribution of the 3D model of the Gypsum Valley salt wall termination presented here is the insight it provides regarding the response of strata to salt movement in a three-dimensional sense. As seen at Klondike Ridge, failure zones may result from the inability of strata to wrap around the terminations of salt structures. Faults that radiate from diapirs in the Gulf of Mexico have been mapped extensively; however, further study of the salt wall terminations in the Paradox Basin will allow for a better understanding of this faulting and perhaps aid in the mapping of reservoirs in the Gulf of Mexico.

CHAPTER 7

CONCLUSIONS

7.1 Summary

The study of the Castle Valley and Gypsum Valley salt wall terminations using field and existing map/well data resulted in:

1. The creation of more detailed geologic maps for the Castle Valley and Gypsum Valley salt wall terminations, incorporating published maps and field measurements collected during this study. Additionally, a new map was created for an outcrop in Professor Valley, providing a new interpretation to the geological setting of the area.
2. The generation of annotated field photographs and photomosaics, illustrating important stratigraphic relationships in the field.
3. The digitization of field and map data to use in 2D and 3D modeling.
4. 3D modeling of the Castle Valley and Gypsum Valley salt wall terminations, constrained by well and field data. This modeling was achieved by interpreting numerous 2D sections in *2D Move* and *3D Move*.
5. The interpretation of structural and stratigraphic relationships at the surface and in the subsurface. Additionally, these interpretations were applied to other salt structures to explain trends observed in other parts of the Paradox Basin.
6. The assessment of potential and existing petroleum systems in the basin using the results of this study. This involved the consultation of past and current production figures and an evaluation of the key components necessary for a successful petroleum system.

7. The application of these models to the Gulf of Mexico, illustrating the benefits of field-based analogues and the similarities and difference between the Paradox Basin and the Gulf of Mexico.

Overall, this study provided new insight into the three-dimensional architecture of two salt wall terminations in the Paradox Basin. The use of regional well data allowed for a complete model to be generated, from the surface to the base of the Paradox salt. Furthermore, 3D modeling revealed trends in the Castle Valley and Gypsum Valley salt wall terminations that were not apparent in 2D interpretations.

7.2 Future Work

To fully understand the subsurface framework of these complex salt wall terminations, the incorporation of 2D and 3D seismic surveys is essential. Re-evaluation of the Castle Valley and Gypsum Valley salt wall terminations using seismic data would allow for a more refined 3D model to be produced. Once the 3D models have been corrected using seismic data, new well locations can be proposed. This process could then be applied to other salt wall terminations in the Paradox Basin.

Additionally, 3D modeling of salt wall terminations in the Paradox Basin will help resolve the 3D architecture in other salt basins (e.g., Gulf of Mexico, North Sea). Understanding these petroleum-evaporite systems in three-dimensions is crucial to predicting migration pathways, trap and seal integrity, and potential volume of recoverable resource. Studying field analogues in the Paradox Basin will not only enable more successful petroleum exploration but may also mitigate the risks involved with drilling through and around evaporates, both on- and offshore. Therefore, continuing this research in the Paradox Basin is essential towards advancing

scientific understanding of salt systems and improving petroleum exploration and production around the world

APPENDIX A

SUPPLEMENTAL 2D SECTION INTERPRETATIONS

The following 2D section interpretations of the Castle Valley salt wall termination model illustrate the general workflow used for this study. These are examples of the number of 2D lines interpreted to generate the 3D surfaces in the model. These are important to reference when considering the methods employed for this research as they show the time and amount of interpretation that went into the creation of the 3D model.

APPENDIX B

SUPPLEMENTAL 2D SECTION INTERPRETATIONS

The following 2D section interpretations of the Gypsum Valley salt wall termination model illustrate the general workflow used for this study. These are examples of the number of 2D lines interpreted to generate the 3D surfaces in the model. These are important to reference when considering the methods employed for this research as they show the time and amount of interpretation that went into the creation of the 3D model.

APPENDIX C

SUPPLEMENTAL WELL FILES

The following files include publicly available well files for wells mentioned in this study. These files will highlight the available well data as well as interpretations made regarding these wells. The inclusion of these well files is important when considering the quality of the well data used in this study as well as when studying the interpretations of several of the authors referenced in this research.

APPENDIX D

SUPPLEMENTAL ELECTRONIC FILES

The following electronic files are Quicktime Movie files (.mov), showing the 3D models for the Castle Valley and Gypsum Valley salt wall terminations spinning in 3D space. These files allow for a better understanding of the three-dimensional features present in these two models, which two-dimensional views of the model could not provide. The inclusion of the files is important to fully grasping the results of this study and understanding the implications of these models.

Castle Valley Salt Wall Termination Model.mov	Quicktime movie of spinning 3D Castle Valley salt wall termination model
Gypsum Valley Salt Wall Termination Model.mov	Quicktime movie of spinning 3D Gypsum Valley salt wall termination model

REFERENCES

Ajdukiewicz, J.M., Nicholson, P.H., and Esch, W.L., 2010, Prediction of deep reservoir quality using early diagenetic process models in the Jurassic Norphlet Formation, Gulf of Mexico: AAPG Bulletin, v. 94, no. 8, p. 1189-1227.

Amador, C.M., Schurger, S.G., and Miller, B.L., 2009, Andy's Mesa Unit, San Miguel County, Colorado: *in* Houston et al., The Paradox Basin Revisited – New Developments in Petroleum Systems and Basin Analysis: RMAG Special Publication, p. 497-518.

Baars, D.L., 1966, Pre-Pennsylvanian paleotectonics – key to basin evolution and petroleum occurrences in the Paradox Basin, Utah and Colorado: AAPG Bulletin, v. 50, no. 10, p. 2082-2111.

Baars, D.L., Bartleson, B.L., Chapin, C.E., Curtis, B.F., De Voto, R.H., Everett, J.R., Johnson, R.C., Molenaar, C.M., Peterson, F., Schenk, C.J., Love, J.D., Merin, I.S., Rose, P.R., Ryder, R.T., Waechter, N.B., and Woodward, L.A., 1988, Basins of the Rocky Mountain region: *The Geology of North America, Sedimentary Cover – North American Craton, U.S.*, The Geological Society of America, p. 109-122.

Baars, D.L., and Seager, W.R., 1970, Stratigraphic control of petroleum in White Rim Sandstone (Permian) in and near Canyonlands National Park, Utah: AAPG Bulletin, v. 54, p. 709-718.

Baars, D.L., and Stevenson, G.M., 1981, Tectonic evolution of the Paradox Basin, Utah & Colorado: Geology of the Paradox Basin, Rocky Mountain Association of Geologists, p. 23-31.

Barbeau, D. L., 2003, A flexural model for the Paradox Basin: implications for the tectonics of the Ancestral Rocky Mountains: Basin Research, v. 15, p. 97-115.

Campbell, J.A., and Ritzma, H.R., 1979, Geology and Petroleum Resources of the Major Oil-impregnated Sandstone Deposits of Utah: Utah Geological and Mineralogical Survey Special Studies 50, p. 24.

Case, J.E., 1966, Geophysical anomalies over Precambrian rock, northwestern Uncompahgre Plateau, Utah and Colorado: AAPG Bulletin v. 50, no. 7, p. 1423-1443.

Case, J.E., and Joesting, H.R., 1973, Aeromagnetic Map of the Central Colorado Plateau, Utah, Colorado, and Arizona, US Department of the Interior Geological Survey Professional Paper 736 Plates 2 & 3.

Cater, F.W., 1955, Geology of the Naturita NW Quadrangle, Colorado: Geologic Quadrangle Maps of the United States, U.S. Geological Survey Map GQ-65, scale 1:24,000.

Cater, F.W., 1970, Geology of the Salt Anticline Region in Southwestern Colorado: Geological Survey Professional Paper 63, p. 1-66.

Deatrick, K., Giles, K.A., and Langford, R., 2014, Sequence stratigraphy, geometry, and formation of an exposed megaflap: Pennsylvanian Honaker Trail Formation, Gypsum Valley salt wall, Paradox Basin, Colorado: Geological Society of America Annual Meeting.

Doelling, H.H., 2001, Geologic map of the Moab and eastern part of the San Rafael Desert 30'x 60' Quadrangles, Grand and Emery Counties, Utah and Mesa County, Colorado: Utah Geological Survey Map 180.

Doelling , H.H., 2002, Geologic Map of the Fisher Towers Quadrangle, Grand County, Utah: Utah Geological Survey Map 183, plate 1, scale 1:24,000.

Doelling, H.H., and Ross, M.L., 1998, Geologic Map of the Big Bend Quadrangle, Grand County, Utah: Utah Geological Survey Map 171, scale 1:24,000.

DuChene, H.R., Cole, S.L., and Greenberg, N., 2009, Geology of the Double Eagle Unit, Andy's Mesa Field, San Miguel County, Colorado in The Paradox Basin Revisited – New Developments in Petroleum Systems and Basin Analysis: RMAG 2009 Special Publication – The Paradox Basin, p. 519-533.

Fillmore, Robert, 2011, *Geological Evolution of the Colorado Plateau of Eastern Utah and Western Colorado*, The University of Utah Press.

Giles, K.A., and Rowan, M.G., 2012, Concepts in halokinetic-sequence deformation and stratigraphy: Geological Society, London, Special Publications, v. 363, p. 7-31.

Goldhammer, R.K., Oswald, E.J., and Dunn, P.A., 1991, Hierarchy of stratigraphic forcing: Example from Middle Pennsylvanian shelf carbonates of the Paradox Basin: Kansas Geological Survey Bulletin, v. 233, p. 361-413.

Goldsmith, L.H., 1969, Concentration of Potash Salts in Saline Basins: AAPG Bulletin, v. 53, No. 4, p. 790-797.

Hite, R.J., 1960, Stratigraphy of the saline facies of the Paradox Member of the Hermosa Formation of southeastern Utah and southwestern Colorado: Geology of the Paradox Basin fold and fault belt: Four Corners Geol. Soc. 3rd Annual Field Conference, p. 86-90.

Hite, R.J., 1970, Shelf carbonate sedimentation controlled by salinity in the Paradox basin, southeast Utah: Northern Ohio Geological Society, v.1, p.48-66.

Hite, R.J., 1975, An unusual northeast-trending fracture zone and its relations to basement wrench faulting in northern Paradox Basin, Utah and Colorado: Four Corners Geol. Soc. Guidebook, 8th Field Conference, Canyonlands, p. 217-223.

Hite, R.J., Anders, D.E., and Ging, T.G., 1984, Organic-rich source rocks of Pennsylvanian age in the Paradox Basin of Utah and Colorado: Rocky Mountain Association of Geologists, p. 255-274.

Hite, R.J., and Gere, W.C., 1958, Potash deposits of the Paradox Basin: Guidebook to the Geology of the Paradox Basin, Ninth Annual Field Conference, 1958, p. 221-225.

Hunt, C.B., 1958, Structural and igneous geology of the La Sal Mountains, Utah: U.S. Geological Survey Professional Paper 294-I, p. 305-364.

Joesting, H.R., and Case, J.E., 1962, Regional geophysical studies in the Salt Valley-Cisco area, Utah and Colorado: AAPG Bulletin, vol. 46, no. 10, p. 1879-1889.

Jones, R.W., 1959, Origin of salt anticlines of Paradox Basin: AAPG Bulletin, vol. 43, no. 8, p. 1869-1895.

Kamola, D.L., and Chan, M.A., 1988, Coastal dune facies, Permian Cutler Formation (White Rim Sandstone), Capitol Reef National Park area, southern Utah: Sedimentary Geology, vol. 56, p. 341-356.

Kelley, V.C., and Clinton, J.N., 1960, Fracture systems and tectonic elements of the Colorado Plateau: Univ. of New Mexico Pub. Geology, no. 5, p. 104.

Kluth, C.F., and Coney, P.G., 1981, Plate tectonics of the Ancestral Rocky Mountains: Geology, p. 10-15.

Kluth, C.F., and DuChene, H.R., 2009, Late Pennsylvanian and Early Permian structural geology and tectonic history of the Paradox Basin and Uncompahgre Uplift, Colorado and Utah: RMAG Special Publication, p. 178-197.

Lawton, T.F., and Buck, B.J., 2006, Implications of diapir-derived detritus and gypsic paleosols in Lower Triassic strata near the Castle Valley salt wall, Paradox Basin, Utah: Geology, vol. 34, no. 10, p. 885-888.

Mack, G.H., and Rasmussen, K.A., 1984, Alluvial-fan sedimentation of the Cutler Formation (Permo-Pennsylvanian), near Gateway, Colorado: GSA Bulletin, v. 95, p. 109-116.

Nuccio,V.F., and Condon, M., 1996, Burial and thermal history of the Paradox basin, Utah and Colorado, and petroleum potential of the Middle Pennsylvanian Paradox Formation, US Department of the Interior, US Geological Survey Bulletin, 2000-O, p. 41.

Paz, M., 2006, Restoration of mountain front and salt structures in the northern Paradox Basin: Colorado School of Mines thesis, p. 1-142.

Paz, M., Trudgill, B., and Kluth, C., 2009, Salt System Evolution of the Northern Paradox Basin: AAPG Search and Discovery Article no. 30078, p. 1-13.

Peterson, F., 1988, Pennsylvanian to Jurassic eolian transportation systems in the Western United States: Sedimentary Geology, v. 56, p. 207-260.

Peterson, J.A., and Hite, R.J., 1969, Pennsylvanian Evaporite-Carbonate Cycles and their Relation to Petroleum Occurrence, Southern Rocky Mountains: AAPG Bulletin, v. 53, no. 4, p. 884-908.

Peterson, J.A., 1992, Aneth Field – U.S.A. Paradox Basin, Utah: U.S. Geological Survey, p. 41-82.

Randles, T., Clarke, S., and Richards, P., 2012, Development of Crestal Collapse Structures above Dissolving Salt Anticlines: Application to Seismic Interpretation within Salt-Controlled Basins: AAPG Annual Convention and Exhibition, p. 1-14.

Rasmussen, D.L., 2014, Namakiers in Triassic and Permian Formations in the Paradox Basin (USA) with Comparisons to Modern Examples in the Zagros Fold Belt, Iran: *in*, MacLean, J.S., Biek, R.F., and Huntoon, J.E., editors, Geology of Utah's Far South: Utah Geological Association Publication 43, p. 689-756.

Rasmussen, L., and Rasmussen, D.L., 2009, Burial history analysis of the Pennsylvanian petroleum system in the deep Paradox Basin fold and fault belt, Colorado and Utah, *in* W.S. Houston, L.L. Wray, and P.G. Moreland, eds., The Paradox Basin Revisited – New Developments in Petroleum Systems and Basin Analysis: RMAG 2009 Special Publication – The Paradox Basin, p. 24-66.

Ross, Michael L., 1998, Geology of the Tertiary Intrusive Centers of the La Sal Mountains, Utah – Influence of Preexisting Structural Features on Emplacement and Morphology: Utah Geological Survey, p. 61-83.

Rowan, M.G., Lawton, T.F., Giles, K.A., and Ratliff, R.A., 2003, Near-salt deformation in La Popa basin, Mexico, and the northern Gulf of Mexico: A general model for passive diapirism: AAPG Bulletin, v. 87, no. 5, p. 733-756.

Sanford, R.F., 1995, Ground-water flow and migration of hydrocarbons to the Lower Permian White Rim Sandstone, Tar Sand Triangle southeastern Utah: U.S. Geological Survey Bulletin 200-J, p. 24.

Sarg J.F., Markello, J.R., and Weber, L.J., 1999, The second-order cycle, carbonate-platform growth, and reservoir, source, and trap prediction: SEPM Special Publications No. 63, p. 11-34.

Schmoker, J.W., and Schenk, C.J., 1994, Regional Porosity Trends of the Upper Jurassic Norphlet Formation in Southwestern Alabama and Vicinity, with Comparisons to Formations of Other Basins: AAPG Bulletin, v. 78, no. 2, p. 166-180.

Stevenson, G.M., and Baars, D.L., 1986, The Paradox: a pull-apart basin of Pennsylvanian age, *in* J.A. Peterson, ed., Paleotectonics and Sedimentation in the Rocky Mountain Region, United States: AAPG memoir 41, p. 513-539.

Stevenson, G.M., and Wray, L.L., 2009, History of Petroleum Exploration of Paleozoic Targets in the Paradox Basin, *in* W.S. Houston, L.L. Wray, and P.G. Moreland, eds., The Paradox Basin Revisited – New Developments in Petroleum Systems and Basin Analysis: RMAG 2009 Special Publication – The Paradox Basin, p. 1-23.

Stone, D.S., 1977, Tectonic history of the Uncompahgre uplift, in H.K. Veal, ed., Exploration frontiers of the central and southern Rockies: Denver, Colorado, Rocky Mountain Association of Geologists Guidebook, p. 23-30.

Trudgill, B.D., Rowan, M.G., Fiduk, J.C., Weimer, P., Gale, P.E., Korn, B.E., Phair, R.L., Gafford, W.T., Roberts, G.R., and Dobbs, S.W., 1999, The Perdido Fold Belt, Northwestern Deep Gulf of Mexico, Part 1: Structural Geometry, Evolution and Regional Implications: AAPG Bulletin, v. 83, no. 1, p. 88-113.

Trudgill, B.D., 2011, Evolution of salt structures in the northern Paradox Basin: controls on evaporite deposition, salt wall growth and supra-salt stratigraphic architecture: Basin Research, p. 1-31.

Trudgill, B.D., and Paz, M., 2009, Restoration of Mountain Front and Salt Structures in the Northern Paradox Basin, SE Utah, *in* W.S. Houston, L.L. Wray, and P.G. Moreland, eds., The Paradox Basin Revisited – New Developments in Petroleum Systems and Basin Analysis: RMAG 2009 Special Publication – The Paradox Basin, p. 132-177.

Venus, J., Mountney, N., and McCaffrey, B., 2013, Synsedimentary salt diapirism as a control on fluvial system evolution: an example from the Permian Cutler Group, SE Utah, U.S.A.: Basin Research, p. 1-74.

Vogel, J.D., 1960, Geology and Ore Deposits of the Klondike Ridge Area, Colorado: U.S. Geological Survey, p. 1-235.

Warner, L.A., 1978, The Colorado Lineament: A middle Precambrian wrench fault system: GSA Bulletin, vol. 89, p. 161-171.

Weber, L.J, Sarg, J.F., and Wright, F.M., 1995, Sequence stratigraphy and reservoir delineation of the middle Pennsylvanian (Desmoinesian), Paradox Basin and Aneth Field, southwestern USA: SEPM, p.1-16.